

POLITECNICO DI TORINO

Collegio di Ingegneria Chimica e dei Materiali

Corso di Laurea Magistrale in Ingegneria dei Materiali

Tesi di Laurea Magistrale

3D printing of self-healing materials



Relatore

prof. Marco Sangermano

Correlatore

dott. Ignazio Roppolo

Candidato

Davide Garnero

Dicembre 2020

Index

1. Introduction and aims of the work	4
2. Mechanisms and chemistries of self-healing	6
2.1. <i>Extrinsic self-healing systems</i>	7
2.1.1. Catalytic systems.....	9
2.1.1.1. Dicyclopentadiene + Grubbs' Catalyst.....	9
2.1.1.2. Siloxane-based healing system.....	11
2.1.1.3. Epoxy/hardener healing system.....	12
2.1.1.4. Thiol-Epoxy healing system.....	12
2.1.1.5. Thiol-Ene healing system.....	13
2.1.1.6. Thiol-Maleimide healing system.....	13
2.1.1.7. Azide-Alkyne healing system.....	13
2.1.2. Non-Catalytic systems.....	13
2.1.2.1. Amine-Epoxy healing system.....	13
2.1.2.2. Epoxy-Based healing system.....	14
2.1.2.3. Isocyanates-Based healing system.....	14
2.1.2.4. Vinyl Ester healing system.....	15
2.2. <i>Intrinsic self-healing systems</i>	15
2.2.1. Self-healing via supramolecular chemistry.....	16
2.2.1.1. Self-healing via hydrogen bonding.....	16
2.2.1.2. Self-healing via ionic interactions.....	19
2.2.1.3. Self-Healing via π - π stacking interactions.....	20
2.2.1.4. Self-healing via metal-ligand complexation.....	21
2.2.1.5. Self-healing via host-guest interaction.....	23
2.2.1.6. Self-healing via hydrophobic interactions.....	25
2.2.2. Self-healing via dynamic covalent bonds.....	26
2.2.2.1. Condensation reactions.....	27
2.2.2.2. Addition reactions.....	29
2.2.2.3. Exchange reactions and Metathesis.....	31
2.2.3. Molecular Interdiffusion.....	33
3. 3D printing of self-healing materials	36
3.1. <i>3D printing overview</i>	36
3.1.1. 3D material extrusion.....	38
3.1.1.1. Fused deposition modeling (FDM) (Fused filament fabrication (FFF)).....	38
3.1.1.2. 3D Dispensing.....	39
3.1.2. Vat Photopolymerization 3D printing.....	40
3.1.2.1. Stereolithography (SLA).....	41
3.1.2.2. Digital Light Processing (DLP).....	42
3.1.2.3. Continuous Liquid Interface Production (CLIP).....	42
3.2. <i>3D-printed self-healing systems</i>	44

3.2.1.	Inks printed via extrusion-based 3D printing.....	44
3.2.1.1.	Extrinsic self-healing (vascular).....	44
3.2.1.2.	3D-printed inks involving dynamic covalent chemistry.....	45
3.2.1.3.	3D-printed inks involving supramolecular interactions.....	51
3.2.2.	Inks printed via vat photopolymerization 3D printing.....	59
3.2.2.1.	Extrinsic self-healing (capsule).....	59
3.2.2.2.	3D printed inks involving dynamic covalent chemistry	59
3.2.2.3.	3D printed inks involving supramolecular interactions.....	61
4.	Experimental part	65
4.1.	<i>Self-healing requirements vs. DLP requirements</i>	<i>65</i>
4.2.	<i>Materials screening</i>	<i>66</i>
4.3.	<i>3D printed hydrogel with complex shape via DLP.....</i>	<i>69</i>
5.	Conclusions	72
	Bibliography	73
	Acknowledgements	83

1. Introduction and aims of the work

Over the past few years, there has been a great deal of interest in developing self-healing (SH) materials with tunable structural, mechanical, and rheological properties. Self-healing materials are capable of restoring their properties in response to damage whenever and wherever it occurs in the material. This unique feature makes them attractive for applications in biomedicine, sensors, soft robotics, and energy harvesting systems. Another emerging and promising research field is additive manufacturing (AM), also known as three-dimensional (3D) printing. AM enables fabricating structures with hierarchical architectures, a controlled spatial arrangement, and a high degree of complexity, such as hollow objects and graded or multi-material structures.

This work aims to show the combination of these two advanced research fields and describe the major results obtained so far in the literature. This evaluation can be done only by understanding the mechanisms involved in self-healing, as well as the peculiarities of different 3D-printing techniques, in order to open the possibility for future research in the field of 3D-printing of self-healing materials.

Therefore, in the first chapter, the different self-healing mechanisms and chemistries, extrinsic (capsule or vascular) and intrinsic (based on either supramolecular interactions or dynamic covalent bonds), are described, reporting relevant examples for each type of strategy. The cited studies have been used to assess the ability of materials to self-heal, specifying whether the system is autonomous or needs an external stimulus to trigger the repair process. Critical issues are highlighted to understand better how it is possible to improve a determinate system.

In the second and subsequent chapter, the description and fundamental basis of the main 3D-printing techniques adopted in 3D printing of self-healing materials are presented, emphasizing the key material requirements in each printing method. The second part of the chapter reports examples of 3D-printed self-healing materials to give a current state-of-the art in the field. The different results are sorted according to the 3D-printing method used and the mechanism of self-healing involved.

In the last chapter, the main results obtained from the experimental part, performed in collaboration with the Ph.D. student Matteo Caprioli, are described and discussed with a critical point of view. Unfortunately, because of the restriction related to the COVID-19 pandemic, it was not possible to develop an in-depth experimental analysis. However, a self-healing hydrogel was 3D printed with Digital Light Processing (DLP) technique, providing the first hydrogel system, to the best of our knowledge, with self-healing ability processed via vat photopolymerization techniques.

At the end of each chapter, the final remarks help the reader resume in a few lines the content of the entire chapter, highlighting the fundamental aspects and achievements.

Finally, the conclusion will resume all the topic cover in this work to entice the reader to explore the world of 3D-printable self-healing materials further.

2. Mechanisms and chemistries of self-healing

Damages and failure are natural consequences of materials usage, especially in structural applications. Therefore, to maximize the operational performance, there is a fundamental need to design and develop materials capable to autonomously repair without compromising the mechanical performance and without or with limited human intervention. This material property is commonly known as self-healing. Thus, self-healing materials are a class of materials that exhibit the ability to restore themselves and recover their functionality using only resources available in the material [1]. Such property can prolong the operational lifetime of the material before irreversible damage occurs even in the presence of microscopic cracks. Biological systems, such as skin tissue or bones, serve as a model for self-healing mechanisms. However, the complexity of nature is hard to achieve. Designing the self-healing mechanism in a material, even exploiting a well-established strategy or synthetic route, is not trivial as well [2].

According to literature, self-healing systems can be classified into autonomous and non-autonomous systems based on the constitutive mechanisms and external triggers. Autonomous self-healing polymers do not need any stimulus to promote the onset of self-healing. In contrast, non-autonomous self-healing polymers require triggers such as temperature, light, and pH [3]. Either the healing process is autonomic or externally assisted, the repair is triggered by the rupture. The system response to damage is threefold: triggering (induced by the damage), transport of material to the site of the crack, and chemical or physical repair process (e.g., polymerization, entanglement, reversible cross-linking) [1]. Mechanical damage of polymer networks may lead to chain cleavage or disentanglement among chains. If cleavage occurs, the stability of the reactive groups generated will determine the ability of the material to undergo repair. In the case of disentanglement among chains, repair relies on segmental rearrangements among the different chains. The groups' reactivity and the possibility of diffusion and rearrangement of the macromolecular segments determine the ability of the polymer to display self-healing. Moreover, the interplay between chemical reactions and physical network remodeling is fundamental to achieve an effective healing process [2].

The parameter used to define the ability of a determinate material to self-heal is the healing efficiency, η , defined as:

$$\eta = \frac{P^{Healed}}{P^{Virgin}} * 100$$

where P^{Virgin} is the value of a specific, measurable property of the virgin specimen and P^{Healed} is the same property measured after healing. However, the healing efficiency of two different self-healing systems is not always a reliable parameter to compare. This inconsistency can result from many factors such as the merged surfaces' geometry and dimensions (e.g., the healing ability of a cut strip changes if healing is performed by joining the two cut surfaces, which are very small, or by overlapping the lateral surfaces of the two parts, involving a more extensive surface), the time elapsed between breakage and re-join of the two surfaces, and the assessed parameters to calculate the healing efficiency. The latter factor is fundamental because many

mechanical properties can be measured before and after healing, such as tensile strength, fracture toughness, or strain. Therefore, all these considerations must be considered when comparing the results from different self-healing systems in the literature [4]. Self-healing materials can be further subdivided into two distinct classes based on the restoration mechanism triggered by damage: extrinsic self-healing (capsule-based or vascular-based) and intrinsic self-healing (figure 2.1) [1]. In extrinsic self-healing systems, the healing agents are confined in vesicles arranged in different configurations depending on the system's geometry: mono-, bi-, or three-dimensional. The restoring mechanism is triggered by the vesicles' rupture, after which the healing agent is released in the crack where it reacts, mending the damage [5]. In contrast to extrinsic systems that can perform self-healing in the same site only once, intrinsic self-healing polymers enable multiple repair processes [3]. Intrinsic mechanisms rely on reversible cross-links, either chemical cross-linking through dynamic covalent bonds or physical cross-linking through supramolecular interactions, that spontaneously reform with no external stimulus [6]. Supramolecular interactions induced in materials include hydrogen bonding, ionic interactions, π - π stacking, metal-ligand coordination, host-guest, and hydrophobic interactions. Dynamic covalent bonds are introduced into the polymer chains by exploiting the reversible nature of chemical groups like acylhydrazones, boronate ester, oxime, imine, thiol-ene, urea, disulfide, alkoxyamine, diarylbi-benzofuranone or groups involved in chemical reactions like Diels-Alder (DA) and cycloaddition [6]. Given their nature, dynamic covalent bond-based systems form self-healing materials with higher mechanical properties than the supramolecular-based ones [7]. Despite the soft nature of supramolecular polymers, they can be remodeled rapidly and reversibility, achieving self-healing with ease [2]. These two systems will be explained in detail in the following paragraphs.

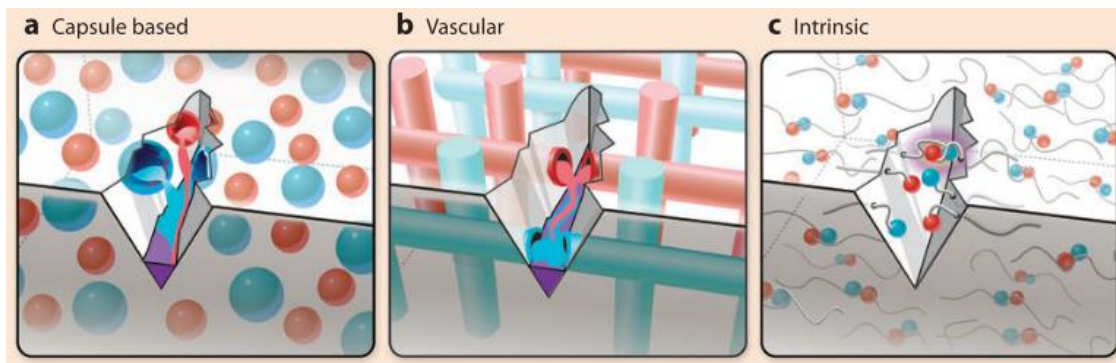


Figure 2-1 - Different approaches inducing self-healing in materials: a) capsule-based, b) vascular, and c) intrinsic [1].

2.1. Extrinsic self-healing systems

Extrinsic self-healing systems are based on reservoirs dispersed into the polymer matrix, containing external healing agents such as monomers, catalysts, or cross-linkers; those are designed to break when crack or damage occurs in the material. Consequently, the healing agents are released and can flow into cracks, healing the material through a designed chemical reaction. As previously mentioned, extrinsic self-healing materials can be divided into two topological arrangements: vascular and capsule. Although both systems exploit the same

principles, many differences arise when considering the design, manufacturing processes, and the number of healing events.

Vascular healing systems exploit a network in the form of capillaries or hollow channels, interconnected one-dimensionally (1D), two-dimensionally (2D), or three-dimensionally (3D), to confine the healing agent. Self-healing systems that rely on vesicles can achieve repeated healing if the vascular network is designed to enable the system to be refilled by an external source or a connected region of the vasculature [1]. Typically, clogging in the network can prevent any further flow of the healing agent towards the damaged zone. This problem limits the ability of the network to be replenished by healing agents. Vascular networks can be fabricated via many different manufacturing processes, such as subtractive manufacturing or sacrificial scaffold-based techniques. A new promising technique relies on Additive Manufacturing (AM) thanks to its ability to handle high degrees of complexity and reduce the total number of steps required to achieve the final component. Among the AM processes available, extrusion-based printing, direct ink writing, and stereolithography granted notable results [8].

On the other hand, capsule-based extrinsic self-healing systems sequester the healing agent in capsules evenly dispersed within the polymer matrix. Thus, because of the autonomous role of each capsule, the local repair of the damage can be performed only once [1]. Many parameters must be considered in the design and synthesis of microcapsules for effective self-healing. These parameters include the size (from micron to nano), distribution, mechanical strength, and the shells miscibility with the matrix. Moreover, the shell must be strong enough to be processable and, at the same time, weak enough to be breakable when a crack occurs in the material. The amount of healing agent delivered to the crack is critical and increases linearly with the capsule size. Therefore, the size of the capsules must match the required amount of healing agent to fill the cracks [3]. In the study of Keller and Sottos, the authors described the effect of the elastic modulus of the capsule on the crack propagation. If the capsule has a higher elastic modulus than the matrix material, a stress field is created, and it deflects cracks away from the capsule. On the other hand, lower elastic modulus capsules attract cracks towards the microcapsule, facilitating the rupture. This latter point ensures that the healing process will be triggered upon damage to the material [4].

In what follows, the description of the cross-linking chemistry in extrinsic self-healing systems will be divided into catalytic and non-catalytic systems. An overview of the different extrinsic self-healing systems that will be discussed is shown below in table 1.

Table 1 – Extrinsic catalytic (upper part) and non-catalytic (bottom part) self-healing systems [5].

Healing agent	Method of healing	Matrix material to be healed	Healing condition	Healing efficiency (η) [%]
DCPD/ENB	Microcapsules	Epoxy	Grubbs cat. [wax], 0-125°C, 1-2 d	10-93
			WCl ₆ cat., Room temperature (RT), 2 d	20
		Epoxy/vinyl ester	Grubbs cat., RT,	46-50

			2.5 min-2 d	
		PMMA	Grubbs cat., RT	80
		PS-block-PBD-block-PS	Grubbs cat., RT	Not mentioned
Siloxanes	Vascular Microcapsules	Epoxy	Grubbs cat., RT, 2 d	38-58
		Epoxy	Organotin cat., RT, 1 d	11-51
	Epoxy/vinyl ester	Organotin cat. [PU], 20-50°C, 1 d	24-46	
	PDMS	Pt cat., siloxane initiator, RT, 5 h-2 d	70-120	
Epoxy	Microcapsules	Epoxy	Organotin cat. [PU], RT, 1 d	33-100
			Imidazole init., 120-180°C, 30 min-1 h	68-111
			BF ₃ .OEt ₂ cat., 20-30°C, 30 min-2 h	76-89
Thiol-epoxy	Microcapsules	Epoxy	Amine cat., RT, 3 h-1 d	80-105
Thiol-ene	Microcapsules	Acrylates	Photoinitiator, UV, RT, 1 h	Not mentioned
Thiol-maleimide	Manual injection	Epoxy	m-cresol, RT, 3-5 d	50-121
Azide-alkyne	Microcapsules	Poly(isobutylene)	CuBr(PPh ₃) ₃ cat., 25-60°C, 5 d	91-107
Amine-epoxy	Microcapsules	Epoxy	RT, 2 d	77-91
	Fibers/vascular	Epoxy	(Acetone or chlorobenzene), RT-100°C, 2 h-5 d	82-100
GMA	Microcapsules	Epoxy	(Excess amine), RT, 3 d	75-90
Epoxy	Melttable	Epoxy	100°C, 10 min	100
			MWCNT, 150°C	55-70
Isocyanates	Microcapsules	Epoxy	H ₂ O	Not mentioned
Vinyl ester	Fibers	Epoxy/vinyl ester	➤	Not mentioned
PEMAA	Melttable	Epoxy	150°C, 30 min	85-121

2.1.1. Catalytic systems

2.1.1.1. Dicyclopentadiene + Grubbs' Catalyst

White et al. proposed one of the most common and studied extrinsic systems, based on dicyclopentadiene (DCPD) as the encapsulated healing agent, dispersed into an epoxy matrix, reacting by ring-opening metathesis polymerization mechanism (ROMP) with a ruthenium-based Grubbs' catalyst (figure 2.2). The healing efficiency of this system was tested by delamination, showing 38% healing efficiency on average under optimized conditions, increased to 66% if the specimens were heated to 80°C [9]. Brown, Sottos, and White looked more deeply into including microcapsules, stating that the maximum healing efficiency (90%) of this system could be achieved in a sample containing 2.5 wt% Grubbs' catalyst and 5 wt% microcapsules [10]. Many other works have been focused on using this self-healing system with other matrices such as PMMA-based bone cement, epoxy vinyl esters, and polystyrene-block-polybutadiene-block-polystyrene [5].

Aldridge et al. studied the curing kinetic as a function of network connectivity and chemical composition. They found out that the ROMP reaction rate is correlated with the square of Grubbs' catalyst concentration, and a

minimum amount of catalyst is always required [11]. Higher healing efficiency can be achieved by evaluating two crucial factors: the aggregation of the reservoirs and their compatibility with the surrounding matrix.

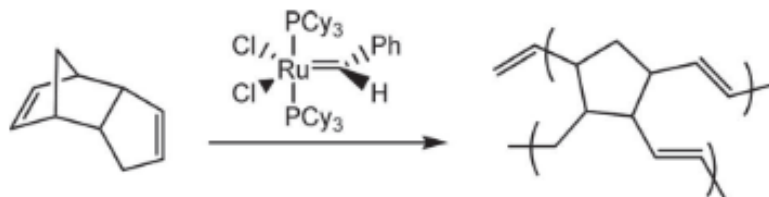


Figure 2-2 - Dicyclopentadiene-Grubbs catalyst ring-opening metathesis polymerization reaction (ROMP) [5].

Poly (styrene) (PS) or poly (methylmethacrylate) (PMMA) coatings are used to obtain better dispersion by preventing agglomeration. The functionalization of the surface of the reservoirs can enhance the interfacial bonding with the surrounding polymer matrix [5]. Wang et al. proposed the functionalization of poly (urea-formaldehyde) (PUF) microcapsules with 3-aminopropyltriethoxy silane or γ -glycidoxypropyltrimethoxysilane. Both hydrogen bonds and Si-O-C covalent bonds were responsible for the improvement of the strength of the composites. Drawbacks in using the Grubbs' catalyst in industrial self-healing applications are related to its high cost and low versatility [5]. Kamphaus et al. proposed a cost-effective alternative to the ruthenium catalyst based on WCl_6 as a catalyst precursor. The activation of the system is either by alkylation with phenylacetylene or by oxidation by contact with air. However, its application showed poor adhesion between the catalyst and the matrix and the catalyst's tendency to agglomerate. The highest healing efficiency obtained was 20% for a completely autonomous sample [12].

Liu and co-workers replaced DCPD with 5-Ethylidene-2-Norbornene (ENB) (figure 2.3) to face the low melting point of the DCPD, and the high cost of the Grubbs' catalyst, obtaining faster curing with a lower amount of catalyst required [13]. However, the mixture of 1:3 DCPD/ENB displayed the highest rigidity value after 120 min, even if the healing efficiency was not investigated. One drawback of using ENB as a monomer is that the resulting polymer is linear and has inferior mechanical properties than polyDCPD. Moreover, the blend does not show any melting temperature, consequently forming a high glass transition temperature resin, from $T_m=15^\circ\text{C}$ to T_g in the range from 120°C to 160°C , with a linear decrease increasing the EBN content [5] [4].

ethylidene norbornene

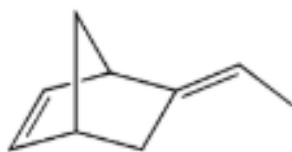


Figure 2-3 - Ethylidene norbornene (ENB) chemical structure [4].

2.1.1.2. Siloxane-based healing system

Although the dicyclopentadiene and Grubbs' catalyst has been the most studied and explored system, other solutions have been explored to tackle the limitations of the DCPD/Grubbs' system. Cho et al. proposed a new self-healing system based on the polycondensation of hydroxyl end-functionalized poly-dimethylsiloxane (HOPDMS) and poly-diethoxysiloxane (PDES) in the presence of a tin catalyst (di-n-butyltindilaurate or DBTL) (figure 2.4). In contrast with other systems, two different monomers, HOPDMS and PDES, were embedded as separate phases because of their low solubility in the polymer matrix (vinyl ester). Upon damage, the encapsulated and dispersed DBTL catalyzed the polycondensation between the two siloxane-based polymers (see the reaction in the figure). This low-cost system provides stability at high temperatures (>100°C), enabling healing in thermoset polymers and wet environments. Therefore, this system is more desirable for practical applications where moisture is always present [14].

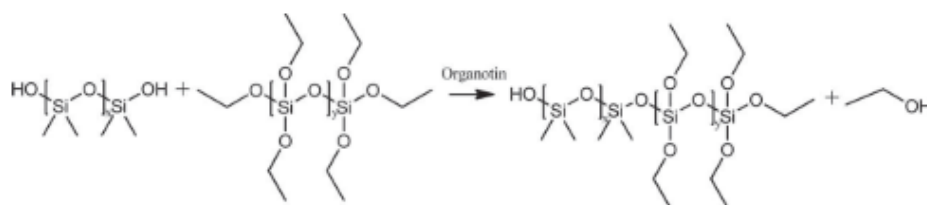


Figure 2-4 - Condensation reaction between silanol-terminated PDMS and PDES (cross-linker) catalyzed by organotin [5].

Later, Mangun and co-workers exploited the same system in an epoxy matrix. The two monomers were embedded in PUF microcapsules to prevent reactions with the polymer matrix. The reported healing efficiency ranged from 11 to 35% at 177°C. In order to improve the healing efficiency, two different silane-based adhesion promoters were tested. The first, the “amino silane”, with two primary amine groups that bond to the epoxy matrix and three methoxy groups on both sides reacting to the silanol-terminated PDMS. The second, called “mixed silane”, involved two coupling agents, one containing an equal number of amine/methoxy groups and the other with no amine functional groups. Using such adhesion promoters resulted in a higher healing efficiency, up to 45% and 52% for the “amino silane” and “mixed silane”, respectively. Moreover, this was the first self-healing system to repair at high temperatures (177°C) [15].

Sottos et al. explored the self-healing behavior of a PDMS healing agent in a PDMS matrix. Two different PUF microcapsule systems were dispersed within the polymer matrix. The first contained high molecular weight vinyl-functionalized PDMS and the platinum catalyst, whereas the second one contained a PDMS copolymer acting as a cross-linker to the functional PDMS. This approach benefits from using the same polymer nature in both the crack region and the host matrix. The strength of adhesion between the polymerized healing agent and the matrix tested under quasi-static conditions determined the healing efficiency. The material showed a recovery between 70% and 100% in the original tear strength. The highest healing efficiency value was obtained when the tear path deviated in a healed sample from the virgin tear path. This behavior was probably due to the same nature of the healing agent and the elastomeric matrix [16] [4].

2.1.1.3. Epoxy/hardener healing system

A different approach to self-healing involves the encapsulation of epoxy resins as the healing agent in an epoxy matrix. This system produces the same matrix constitutive material in the healed zone, ensuring good adhesion and mechanical properties. To accomplish the repair, a second component, a hardener, is solubilized within the matrix [5]. Yin and co-workers used uncured epoxy resin as the healing agent encapsulated in PUF microcapsules embedded into the matrix, and a dispersed latent hardener, CuBr_2 , with four 2-methylimidazole units. Upon damage, the healing agent came in contact with the latent hardener, but for the reaction to occur, imidazole had to be released from the latent hardener at 130-180°C. The need to heat the composite is the main limitation, making the self-healing of the material not fully autonomous. The resultant healing efficiency of this self-healing material reached the value of 111% after healing 1 h at 130°C (using 10 wt% epoxy microcapsules and 2 wt% latent hardener) [17]. As an alternative room-temperature healing system, Xiao et al. used $\text{BF}_3 \cdot \text{OEt}_2$ as a strong Lewis-acid catalyst responsible for the cationic ring-opening polymerization of the epoxy healing agent. Therefore, issues arise for the hardener's encapsulation because it is deactivated by contact with moisture since it is highly hygroscopic. The healing rate was very fast, resulting in a 76% impact strength recovery after 30 min at 20°C. The healing efficiency could be increased by either increasing the temperature up to 30°C or healing for 2 h (85% and 89% of healing efficiency, respectively) [18] [5].

2.1.1.4. Thiol-Epoxy healing system

Another possibility for a self-healing system derives from an epoxy healing agent's reaction with a hardener, such as thiols or amines. The latter can also react without catalyst, discussed in paragraph 1.2.1. Yuan et al. used Pentaerythritol tetrakis (3-mercaptopropionate) (PMP) (figure 2.5) as multifunctional thiol encapsulated with a tertiary amine, either benzyl dimethylamine (BDMA) or 2,4,6-tris (dimethylaminomethyl) phenol (DMP-30), to increase the thiol nucleophilicity in poly (melamine-formaldehyde) (PMF) microcapsules.

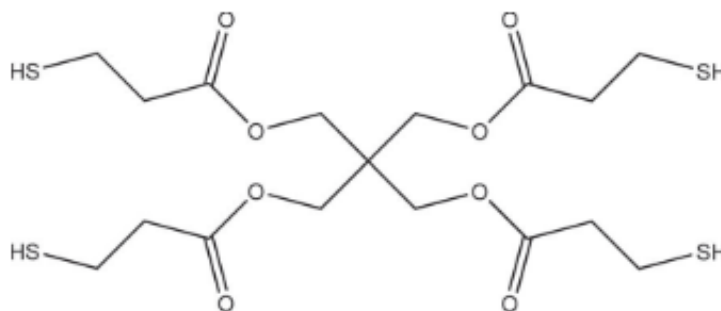


Figure 2-5 - Pentaerythritol tetrakis(3-mercaptopropionate) [5].

After healing for 1 d at room temperature, the healing efficiency, calculated measuring the fracture toughness, was 105%. A change in temperature affects the healing process: results showed a recovery of 86-88% for samples healed at -10°C for 36 h and 171% recovery at 55°C [19].

2.1.1.5. Thiol-Ene healing system

Van den Dungen et al. combined both a diacrylate (1,6-hexanediol diacrylate) and a dinorbornene (1,6-hexanediol di(norborn-2-ene-5-carboxylate)) with PMP in an acrylate matrix. Although this system does not require a catalyst, the network formation was accelerated by introducing a UV activated photoinitiator (2,2-dimethoxy-2-phenylacetophenone (DMPA)). The scanning electron microscope (SEM) observation showed that only partial recovery of the cut was achieved, probably due to aggregation between microcapsules. Moreover, this negative effect was more severe with nanocapsules, leading to the conclusion that the amount of healing agents delivered to the cut was not enough for the full recovery in both cases. However, no values of healing efficiency have been mentioned in their work [20].

2.1.1.6. Thiol-Maleimide healing system

Healing of epoxy polymers can also be achieved with this system, though only manual injection was experimented by Billiet et al. in 2013. The tertiary amine present in the epoxy matrix catalyzed the thiol-maleimide Michael addition. Moreover, the maleimides also react with the tertiary amines in the matrix, linking the healed part with the matrix material. The maleimide was dissolved into a solvent (m-cresol) to prevent the homopolymerization of the double bond. Recovery up to 92% was obtained after 3 d of healing at room temperature. The efficiency increased to 121%, prolonging the healing time [21].

2.1.1.7. Azide-Alkyne healing system

This system is based on the Cu(I)-catalyzed azide-alkyne cycloaddition reaction. This reaction was applied by Gragert and co-workers to poly(isobutylene) matrices using a trivalent polymeric azide and low molecular weight alkynes (figure 2.6), both encapsulated in PUF microcapsules. The catalyst, $\text{CuBr}(\text{PPH}_3)_3$, was dispersed into the polymer matrix. Healing was performed for 5 d at 25 and 60°C, resulting in a recovery of 91% and 107%, respectively [22].

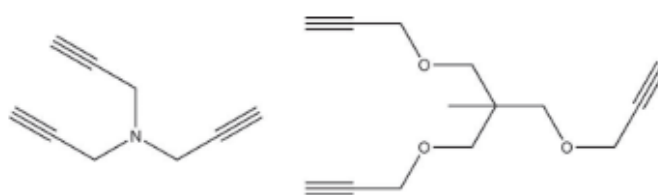


Figure 2-6 - Low-molecular-weight alkyne [5].

2.1.2. Non-Catalytic systems

2.1.2.1. Amine-Epoxy healing system

As mentioned before, self-healing can also be achieved using amines as hardeners for epoxy resins. For instance, Dry et al. used hollow glass fibers as a structure to deliver both reagents to the damaged zone. After healing (up to 8 months), the healed sample showed the ability to deflect the crack from the original crack path

[23]. Toohey et al. inserted the amine-epoxy healing system into a microvascular network similar to the DCPD system. Their results will be detailed in the section related to 3D printable systems. Williams et al. applied pressure to the network system, which showed an increase in recovery from 82% up to 114% due to increased mixing of the healing agents and delivery to the crack zone [24]. Later, this chemistry was also expanded to microcapsule-based systems by Kirk et al., who used nano-porous silica capsules, achieving only partial self-healing. Furthermore, Jin and co-workers encapsulated amine hardeners in PUF microcapsules using vacuum infiltration of a hollow polymeric capsule. This system could achieve healing efficiencies (77-91%) comparable with systems using fibers or microvascular networks by healing for 48 h [25].

Caruso et al. demonstrated that the repair could also be achieved using unreacted amino moieties present in the epoxy matrix. The presence of a solvent in the damaged area increased the chain mobility, promoting further curing of the unreacted functionalities. Chlorobenzene was used as a solvent, and it was encapsulated into the matrix with an additional amount of epoxy resin to optimize the system, obtaining a fracture toughness recovery of 82%. Furthermore, the addition of epoxy resins to the system increased the ability to form cross-linking with the residual amine functionalities, leading to an increase in the healing efficiency up to 100% [26].

Meng et al. used glycidyl methacrylate (GMA) to react with unreacted amines. This monomer, containing both an epoxide and an acrylate functional group susceptible to nucleophilic attack, was encapsulated in PMF microcapsules. The main effect on healing was not the solvent effect (due to the monomer solubility in the epoxy matrix) but due to the formation of hydrogen bonds and covalent bonds with amines. Different degrees of recovery were obtained depending on the stoichiometric matrix composition. After three days at 25°C, 75% of recovery was achieved with a matrix composition of 12:100 wt% DETA/epoxy, whereas over 90% of recovery was observed with 20:100 wt% DETA/epoxy. The healing efficiency could be increased by heating the sample above the T_g (160°C), achieving a value of 90% for the microcapsule system, most likely due to the increased chain mobility [27].

2.1.2.2. Epoxy-Based healing system

Zako and Takano introduced a 40% volume fraction of particles constituted of solid epoxy monomers in an epoxy matrix cured at low temperature. Upon heating at 100°C for 10 min, the particles melt, allowing the monomer to reach damaged sites, thus getting a full recovery. The heating of the material could be achieved with resistive heating of multi-walled carbon nanotubes (MWCNT) by applying a current to the MWCNT system. This strategy showed a healing efficiency of 55% and 70% with the incorporation of 25 wt% and 30 wt% of meltable particles, respectively [28].

2.1.2.3. Isocyanates-Based healing system

Self-healing can also be obtained using isocyanates, a very reactive compound, especially with water or air moisture [4]. A catalyst-free self-healing system was proposed by Huang encapsulating hexamethylenediisocyanate (HDI) in PU microcapsules through an interfacial polymerization between methylene

diphenyldiisocyanate (MDI) prepolymer and 1,4-butanediol in an oil-in-water emulsion. Healing was accomplished after 48 h in immersion in a salt solution [29]. Yang et al. have reported the microencapsulation of isophorone diisocyanate. Using these microcapsules in a composite can create a material capable of healing by reacting with air moisture [30].

2.1.2.4. Vinyl Ester healing system

Motuku and co-workers reported the use of vinyl ester resins inserted in hollow glass fibers to heal epoxy or vinyl ester matrices. However, they focused on the fibers' spatial resolution to obtain an even distribution of the healing agent, and no efficiencies were reported [31].

2.2. Intrinsic self-healing systems

This section will focus on materials and systems based on intrinsic self-healing chemistries. Intrinsic mechanisms rely on constitutional dynamic chemistry (CDC), the material's ability to undergo repair by dynamic/reversible bond breaking-reformation reactions without requiring a healing agent, preventing problems like inhomogeneous mixtures or interfacial effects. This ability exploits the formation of reversible bonds, either covalent bonds or supramolecular interactions. These reversible linkages can reform across the damaged surfaces, repairing the material. To accomplish the full restoration of the material is fundamental to combine the chemical properties of the network with the physical rearrangements of the macromolecules within interfacial regions. The healing is triggered by damage and driven by the surface tension and elastic energy of the stress source or by an external stimulus such as heat, light, presence of a solvent, and others. Intrinsic self-healing systems can perform multiple healing cycles thanks to the embedded functionalities, not involving a separately stored healing agent, and so averting the impact of their high viscosity on the healing rate. High temperatures can be used to overcome this obstacle. Intrinsic approaches are restricted to thermoplastic polymers, thermosets conventionally cross-linked with low T_g or based on dynamic covalent chemistries [32]. As previously mentioned, intrinsic self-healing can repair only small localized damage zones, therefore limiting its range of applications [32].

Intrinsic self-healing systems can be subdivided into two classes: reversible covalent bonds and supramolecular interactions (figure 2.7). Reversible covalent bonds are characterized by higher bonding energies, allowing the material to regain similar pristine properties. On the other hand, self-healing using supramolecular chemistry offers faster recovery under ambient conditions. In the latter class, mechanical integrity is achieved by incorporating extensive non-covalent interactions between groups covalently attached to the polymer side chain or chain ends of macromolecules [33]. The mechanisms involved in the repair of an intrinsic self-healing system differ from the extrinsic ones. Upon mechanically stressing, weaker linkages (e.g., secondary bonds, entanglements) fail first, then permanent bonds break (i.e., homolytic break), resulting in a sharp separation and material failure. The newly formed surfaces expose many available functional groups that can recombine upon re-joining to restore the material in a new state, close to the original. However, the process could be limited by several factors, such as the mobility of the moieties influenced by the high viscosity of the

system, chemical modifications (e.g., oxidation) of the functional units present onto the damaged surface, that limit the moieties available to repair the damage, as well as the reactivity of the functional groups to reform the original bond [34]. In the following sections, different approaches used to achieve intrinsic self-healing will be described, especially focusing on the chemistry and design of such systems (figure 2.7).



Figure 2-7 - Different available approaches to achieve self-healing in polymers. Upper part: via supramolecular interactions, bottom part: via dynamic covalent bonds [35].

2.2.1. Self-healing via supramolecular chemistry

2.2.1.1. Self-healing via hydrogen bonding

A hydrogen atom bonded to a highly electronegative atom, such as Oxygen or Nitrogen, hosts a partial positive charge counterbalanced by a negative charge on the hydrogen acceptor. This charge displacement establishes a physical electrostatic interaction between moieties located on different polymer chains. Multiple hydrogen bondings (H-bonds) formed directionally can significantly affect bulk properties and the degree of crystallinity, establishing a reversible cross-linking able to effect self-healing, even though being weaker than ionic bonding and covalent dynamic bonds [33]. The hydrogen bonding strategy requires hydrogen bonding donors and acceptors as side-chain groups, along the backbone, or at end chains. Moreover, since a single H-bond is not sufficient to form supramolecular assemblies, it is necessary to have a sufficient concentration of bonds to reach a strong binding affinity, thus facilitated by a suited rigidity of the polymer backbone. Therefore, typical associative functional groups are thymine (Thy) and 2,6-diamino triazine (DAT), able to form three interactions per group, and ureidopyrimidinone (UPy), that establishes quadruple H-bonds. Polymers end-functionalized with such motifs can assemble into clusters, resulting in phase segregation and robust structures [3] [33] [34].

Self-healing was first reported for a network comprising fatty acid oligomeric building blocks containing nitrogen-rich H-bonding moieties [36]. UPy motifs (figure 2.8) can be grafted to the main chain of a supramolecular bio-elastomer, poly(glycerol sebacate), that showed a scratch healing response within 1 h, and the cut samples healed within 12 h at 55°C achieving healing efficiencies up to 85%. Furthermore, by replacing poly(glycerol sebacate) with poly(sebacoyl diglyceride), the scratch healing was obtained within 30 min at 60°C [37]. Copolymers composed of synthetic monomers, such as n-butyl acrylate (nBA), methyl methacrylate (MMA) functionalized with UPy monomer displayed self-healing response at 100°C. The best results in terms of self-healing ability were achieved with 2 wt% of UPy end groups and an optimum chain interdiffusion showing 94% recovery in tensile strength and 84% in tensile strain within 1 h [34]. UPy-functionalized polymers exhibit temperature-dependent mechanical strength. UPy units incorporated into flexible poly(ethylene-co-butylene) and polydimethylsiloxane (PDMS) tend to form aggregates made of multiple UPy-dimers. They are responsible for the mechanical strength of the resulting hydrogel and thermally activated dissociation and reassociation processes, leading to repeatable self-healing. On the other hand, soft polymer chains provide sufficient mobility to the system when aggregates are dissociated. Thus, the healing temperature is related to the melting temperature of UPy dimers, and no self-healing occurs at lower temperatures [33].

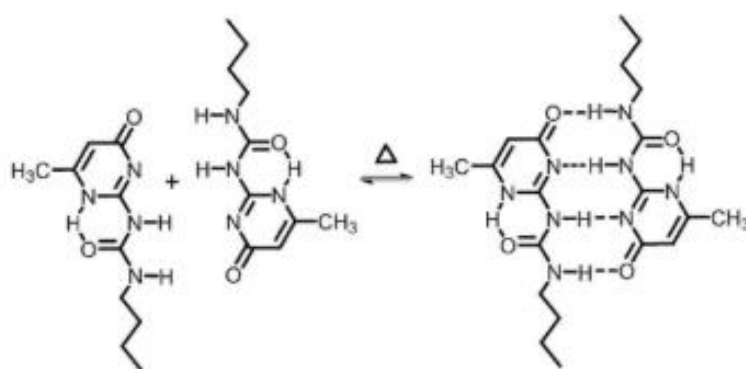


Figure 2-8 - Reversible dimerization of urea isopyrimidone (UPy) [33].

Microphase-separated structures were developed with UPy end-functionalized triblock oligomers composed of different hard poly(lactic acid) (PLA) and soft poly(ethylene-co-butylene) (PEB) blocks. The strong association between UPy functionalization increased the phase separation of the PLA segments from the PEB matrix. Complete scratch healing was observed under UV light within 20 min, which corresponded to an increase in temperature from room temperature to 76°C [38]. Another triblock copolymer was designed by replacing the previous UPy-functionalized PLA hard block with a rigid UPy-functionalized poly(norbornene) block. Although the dissociation temperature of UPy aggregates is around 90-100°C, scratch healing was observed already at 50°C. Moreover, upon applying a strain close to the fracture strain, 83% of strain recovery was shown within 24 h at room temperature [39]. UPy-bonding and bis-urea systems often lead to crystallization or clustering, making the material brittle, difficult to process, and limiting the dynamic

mechanisms of the associative groups. Therefore, zig-zag hydrogen-bonded arrays are formed by using thiourea moieties. These materials can heal at room temperature by compression without heating [33] [34].

The separation between hard and soft segments was also observed in block copolymer poly(urea) with poly(propylene glycol) (PPG) as the soft segment which provides sufficient mobility upon dissociation to the rigid block to reinstate the interaction. This system showed 82% of tensile strength recovery within 3 h at room temperature, and it further increased up to 98% within 24 h [40]. Another study showed that poly(urethane) (PUs) composed of 2,4-toluene diisocyanate as the hard segment and polyether polyol as soft segment achieved 82% recovery in stress and 55% recovery in the strain at room temperature [41]. Self-healing could also be obtained in an environmentally friendly and non-cytotoxic supramolecular elastomer deriving from urea, diethylenetriamine, and small carboxylic acids as sebacic acid and citric acid. The restoration was given by the interactions between amide alkyl-urea and imidazolidone groups, achieving self-healing efficiency at room temperature of 31% within 8h, increased to 99% after 72 h [42]. The presence of water typically causes dissociation of H-bonds among the chains because it tends to interact with the polymer's binding sites, replacing their mutual interactions with strong associations. In dry supramolecular polymers, H-bonding competes with air moisture and is sensitive to pH and temperature changes. In hydrogels, multivalent motifs containing both H-bond donor and acceptor groups, such as UPy, must be shielded by hydrophobic species from the aqueous environment to reduce water's competitive effect and achieve effective self-healing [33]. Cui and Del Campo and co-workers demonstrated self-healing in a hydrogel based on a copolymer composed of a monomer containing a pendant UPy units and a pH-sensitive monomer, dimethyl amino ethyl methacrylate (DMAEMA). The copolymer's aqueous solution gelled upon increasing the pH above 8 because the DMAEMA undergoes phase transition, forming hydrophobic regions within which the self-complementary H-bonding of UPy takes place, resulting in the gel formation. Self-healing occurred in 5 min in a humid environment at fixed pH and room temperature [43]. UPy motifs in a sufficiently high concentration have also been successfully used to impart rapid self-healing ability at room temperature to hydrogels based on polyurethane [44], polyethylene glycol (PEG) hydrogel [45], and dextran [46].

Strong H-bonds among adjacent chains can also arise from extensive interaction among moieties directly located along the polymer's backbone, such as hydroxyl moieties. Poly(vinyl alcohol) (PVA) is a hydroxyl-rich polymer that can form physically cross-linked hydrogels prepared by freezing-thawing method. When a PVA hydrogel is severed, and the cut surfaces brought back into contact, the self-healing results from the polymer chains interdiffusion to re-form the hydrogen bonds with the disappearance of the interface. The healing efficiency was 72% after 12h in contact, limited by the formation of H-bonds among water and the polymeric chains, with the predominant recovery happening in less than 1 hour due to the rearrangement of the hydroxyl moieties in the formation of intra- and inter-chain hydrogen bonds [47].

By plotting the H-bonding strength, the tensile strength of the material, and the self-healing efficiency of the previously described systems in the same graph, it is possible to state that no clear and direct correlation between these parameters exists (figure 2.9) [34].

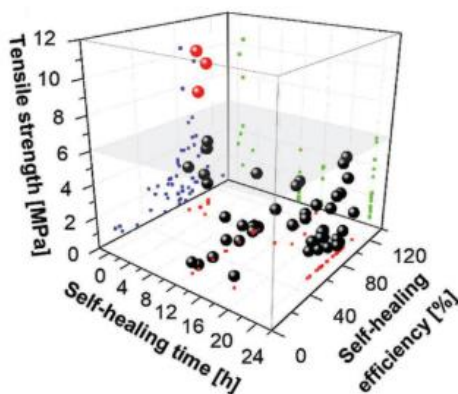


Figure 2-9 - Correlation of the tensile strength and the self-healing efficiency versus self-healing time of some supramolecular polymers with hydrogen bonding interactions [34].

2.2.1.2. Self-healing via ionic interactions

Ionic interactions arise when two oppositely charged ions electrostatically interact together. However, an ion can also interact with a polar molecule to form an ion-dipole interaction or induce a dipole in a non-polar molecule to establish a non-induced dipole interaction [33]. The strength of these interactions is tightly correlated with the electrostatic charge density, dielectric constant, and temperature. Experimental conditions must have the right value and sign of the electrostatic charge on the polymer chains, avoiding the formation of repulsive forces that would hinder the self-healing process from occurring correctly [26]. The main ionic systems are ionomers, polyelectrolytes, polyelectrolyte complexes, ionic liquids, and zwitterionic polymers [33].

Ionomers are polymers in which a small fraction of the monomeric units is made by ionic or ionizable groups (<10 wt%). The most common ionic groups include sulfonate ($-\text{SO}_3^-$), phosphonate ($-\text{PO}_3^{2-}$), and carboxylate ($-\text{COO}^-$). From their interactions, ionic clusters are formed and act as physical cross-links responsible for the self-healing process. Increased ionic content in ionomers produces systems with higher cross-link density but less chain mobility. These systems are more suitable for high-temperature healing since, at lower temperatures, the healing rate becomes too low to achieve an optimum repair of the material [33]. Self-healing was observed in the system composed of poly(ethylene-co-methacrylic acid) copolymers (EMAA) and sodium ionomers. However, the healing occurred only in specific temperature ranges (from -50 to 140°C) according to the number of ionic interactions induced in the system [48]. Moreover, as regards the neutralizing ions, sodium neutralized polymers show the slowest self-healing response, followed by zinc and cobalt neutralized specimens [33] [34]. Russell and co-workers showed the effect of carboxylic acid modifiers, such as oxalic acid, succinic acid, adipic acid, citric acid, and sebacic acid succinimide, sodium succinate, and sodium citrate, to EMAA ionomers. Overall, the addition of modifiers reduced the elastic properties, the impact stiffness, and the linear failure strength resulting in increased elastomeric behavior and enhanced elastic healing [49].

Polyelectrolytes are polymers in which substantial portions of the monomeric units bear ionic or ionizable groups. Self-healing occurred in polyelectrolyte complexes obtained from poly(acrylic acid) (PAA)/poly(allylamine hydrochloride) (PAH) pairs in the presence of NaCl salt (CoPECs). Using salt or even water (polar solvent) induced the interruption of the dynamic interactions between ionic groups, which increases the chain mobility leading to self-healing [50]. Polyelectrolytes complexes used to form self-healing hydrogels can also be synthesized from polycation with four ammonium groups and polyanions with a sulfonate group. Self-healing was achieved by pressing the two cut surfaces together in hot water (50°C) or dipping the surfaces in a saline solution before pressing them together [33]. Stiff and self-healing hydrogels can also be produced from the complexation of polyamines with phosphate-bearing multivalent anions. These hydrogels, healing for 10-30 min at RT, can regain the initial mechanical properties after deformation in strain amplitude sweep up to 200% [51].

Zwitterionic polymers have an equal number of anionic and cationic groups on each chain; thus, no charge is present if the overall chain structure is considered. Common zwitterionic groups are sulfobetaine (SB), carboxybetaine (CB), phosphorylcholine (PC) as anions, and commonly quaternary ammoniums are used as cations [33]. Self-healing systems were prepared by UV-initiated copolymerization of zwitterionic carboxybetaine methacrylamide (CBMAA-3) and 2-hydroxyethyl methacrylate (HEMA) in the presence of uniformly dispersed clay nanoparticles. Self-healing occurred by pressing the cut surfaces together for 5 min [52]. Another approach exploiting the zwitterionic behavior is the carboxybetaine acrylamide (AAZ) hydrogel (figure 2.10), which can repair even when the two surfaces are not readily re-joined after being damage. The stated healing efficiency was 90% (tensile strength and modulus) after healing for 24 h at RT [53].

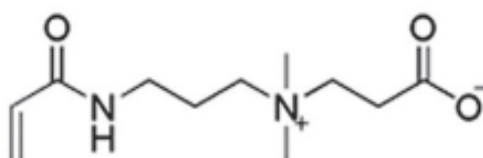


Figure 2-10 - Zwitterionic nature of carboxybetaine acrylamide (AAZ) [7].

Ionic liquids are a new class of ionic interactions that may offer many novel opportunities in self-healing materials. The main advantage derives from the non-volatile nature of the ionic liquids, which allows a wide range of processing conditions and application methodologies to be adopted. However, self-healing systems using ionic liquids have not been studied deeply so far, but they offer great potential for future researches and approaches to induce self-healing in polymers [33].

2.2.1.3. Self-Healing via π - π stacking interactions

π - π stackings are attractive interactions between π orbitals in aromatic rings, which form non-covalent bonds. These thermally triggered reversible supramolecular interactions were obtained by interacting end-capped π electron-deficient groups with π electron-rich aromatic backbone molecules. Upon heating, π - π stacking units

are broken, enabling the chain to flow. Thus, upon the reformation of the π - π stacking interactions, repair of damage will take place, leading the material to recover its initial mechanical properties [33].

Self-healing systems based on π - π stackings have been first reported by Burattini et al., who synthesized a polyimide with π electron-deficient naphthalene-diimide units and a pyrenil end-capped polyamide with π electron-rich pyrene groups [54]. Other following approaches showed the possibility to form networks with enhanced mechanical properties by using tweezer-type bis-pyrenyl end groups instead of monopyrenyl groups (figure 2.11). The tweezer-type blend displayed higher modulus and elongation, although requiring a higher healing temperature and longer time for healing [55].

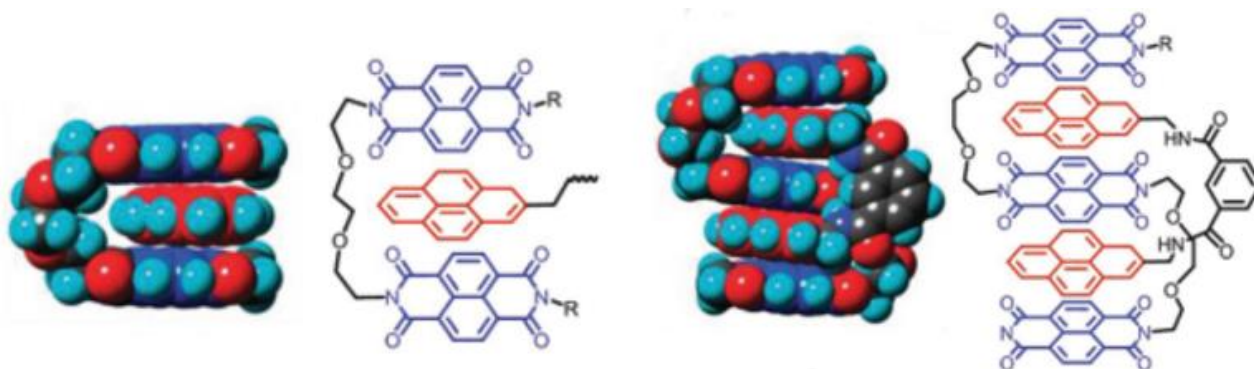


Figure 2-11 - Left: Polyamide end-capped with pyrenyl groups and the formations of two face-to-face π - π stacking interactions. Right: polyamide end-capped with tweezer type bis-pyrenyl groups and the formations of four face-to-face π - π stacking interactions [33].

Developed systems exploiting π - π stacking as reversible supramolecular interactions in highly cross-linked polymers were composed of di- or trivalent PEG-based polymers with pyrenil end-groups. The trivalent blend showed a higher self-healing temperature (160°C) because of the higher degree of cross-linking than the divalent blend (100°C). The self-healing efficiency addressed over three breaking/healing cycles was 95% for the trivalent system and 90% for the divalent one. By changing the π electron-rich end group of the PEG from pyrene to perylene, the healing occurred at 125°C, showing 97% recovery in toughness within 30 min [56]. Another approach utilized π - π interactions combined with metal-ligand interactions by incorporating a cyclometalated platinum (II) complex Pt(6-phenyl-2,2'-bipyridyl)Cl into a PDMS. Full recovery was achieved at room temperature in 12 h. The self-healing process was faster if the temperature was raised to 50°C or 80°C, observing recovery within 2 h and 1 h, respectively. Moreover, no aging was observed; therefore, even after keeping apart the cut surfaces for 24 h, full recovery was achieved [57].

2.2.1.4. Self-healing via metal-ligand complexation

Metallo-supramolecular polymers are formed by the coordination of metal atoms with covalently attached ligands to the side chains either as chain ends within the polymeric backbone or as pendant groups [33]. Their interaction, called chelation, arises when two electrons from one atom are supplied to one of the empty d-orbitals of a metal ion [58]. The non-covalent bonds between ligands and metal atoms can vary from strong covalent-like to highly dynamic depending on the two groups involved. One significant advantage of these

systems when dealing with self-healing is the possibility to tune binding kinetics and thermodynamics by selecting different metal-ligand pairs. Furthermore, the coordination strength can also be tuned via the ligand synthesis by forming linear, star-shaped, highly branched, or dendritic moieties according to the number of binding sites of the chelate molecule (figure 2.12) [33]. Essential for the formation of self-healing hydrogels exploiting the metal-ligand coordination is the equilibrium constant (K_{eq}) of the coordination bond formed between the selected pair of metal ion and ligand. Besides the concentration of the ligand moieties, the value of the K_{eq} affects the degree of metal-ligand association. Therefore, if the value of the K_{eq} is too low, the cross-link density will be insufficient to form a strong enough structure. By contrast, if the K_{eq} is too large, the networks will be too rigid to show dynamic behavior [59].

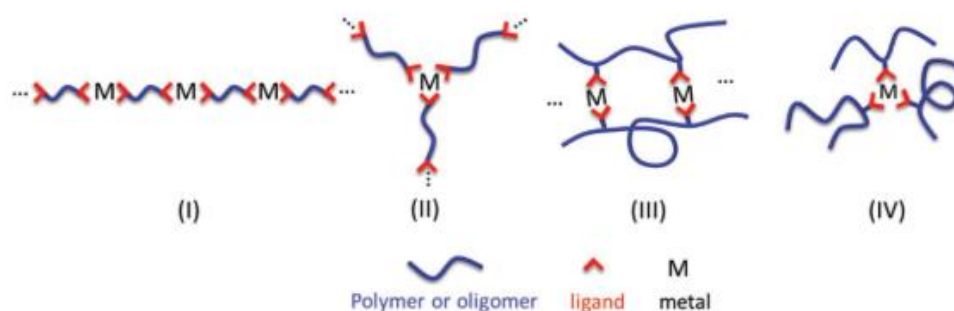


Figure 2-12 - Possible chelating geometries depending on the number of binding sites available on the metal-ligand [33].

Chelating ligands can be conjugated to the polymer backbones or introduced into the polymeric network by co-polymerization with hydrogel precursor monomers. The most common ligands include bisphosphonate (BP), catechol, histidine (His), pyridine (Py), thiolates, carboxylates (figure 2.13) [59].

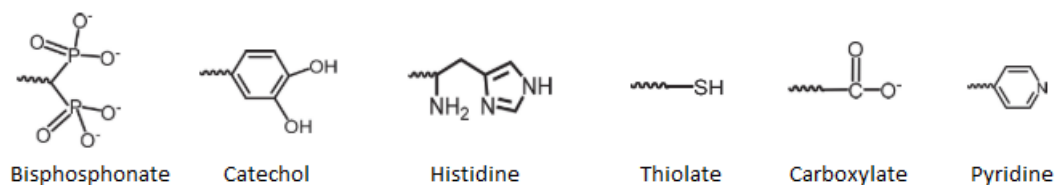


Figure 2-13 - Chemical structures of the most common ligands [4].

Shi et al. developed a self-healable hydrogel by introducing Ca^{2+} ions into a polymeric solution composed of hydroxyapatite modified with bisphosphonate groups (HA-BP). The interactions between Ca^{2+} and BP groups led to hydrogel formation with a fully reversible and dynamic nature. Furthermore, this system showed the ability to flow under shear stress (shear thinning behavior), which is a necessary request when dealing with inks for extrusion-based 3D printing. The autonomous self-healing was stated after macroscopic observation and rheological analysis. Upon strain decrease from 400% to 1%, the complete and immediate recovery of the storage modulus (G') was observed. Lopez-Perez et al. followed a different approach by conjugating BP to PEG to form a reversible network with Ca^{2+} ions. The produced hydrogel could be cut and then self-recovered after 2 min without leaving a visible interface. Moreover, $\text{PEG-BP}\cdot\text{Ca}^{2+}$ showed a liquid-like behavior at low

shear stresses and solid-like behavior at high shear stresses [59]. Zheng et al. reported the possibility of producing a printable self-healing material by using a poly(acrylamide-co-acrylic acid) (P(AAm-co-AAc)) based self-healing hydrogel cross-linked by carboxylate-Fe³⁺ coordination complexes [60]. Different ligands can be found in nature, namely catechol, which contains amino acid 3,4-dihydroxyphenyl-L-alanine (DOPA). DOPA has two different chemical forms: an oxidized catechol form and a non-oxidized quinone form (under slightly alkaline or oxidizing conditions). The coordination between catechol and various metal ions generates reversible interactions, whereas quinone can react with amines or thiols to form covalent bonds [59]. Holten-Andersen et al. first reported how self-healing could be obtained by using catechol functionalized PEG (PEG-cat) with the addition of Fe³⁺ ions [61]. Later, other research groups developed other self-healing hydrogels based on the same principles by modifying with catechol polymers like dopamine methacrylamide, poly(acrylic acid) (PAA) [62]. Fullenkamp et al. described the possibility of using histidine (His) as a ligand in a star PEG polymer. Dynamic bonds were observed upon coordination with Zn²⁺, Cu²⁺, Co²⁺, and Ni²⁺ ions [63]. Self-healing behavior can also be obtained by coordinating thiolates present along the chains and Au nanoparticles (NPs). For example, Qin et al. fabricated a self-healing hydrogel by polymerizing N-isopropylacrylamide with N,N'-cystamine bisacrylamide in the presence of Au NPs. Upon laser-assisted healing for 1 min, 96% of recovery was observed [64]. Besides this system, thiolates can also be grafted to other polymers, such as HA, gelatin, and PEG, to form self-healing hydrogels [59]. Finally, carboxylates-metal chelation can be exploited as reversible interactions to develop self-healing hydrogels. Wei et al. reported a hydrogel capable of displaying autonomous self-healing obtained from the polymerization of acrylic acid monomer in the presence of N,N'-methylene bisacrylamide cross-linker. Two types of cross-linkages were established: covalent cross-links between the poly(acrylic acid) (PAA) chains, which contributed to the high mechanical strength of the hydrogel, and the dynamic bonds deriving from the coordination between the carboxylate ligands of (PAA) chains and Fe³⁺ ions which give to the system the self-healing behavior [65].

2.2.1.5. *Self-healing via host-guest interaction*

The development of host-guest interactions dates back to the 80s, thanks to Lehn, Cram, and Pedersen's discoveries, who won the Nobel prize in 1987 [66]. Host-guest interactions are based on the transient association between a macrocyclic containing a cavity (the host) and a suitable molecular guest, leading to non-covalent bonds formation. The two molecules must be selected carefully to have the guest fit perfectly in the host cavity among the different possible structures available. H-bonding, π - π , van der Waals, or hydrophobic interactions can drive the association/dissociation processes. Commonly exploited macrocyclic hosts include either natural molecules, such as cyclodextrins (CDs), or synthetic molecules, such as cucurbiturils (CBs), crown ethers, calixarenes (CAs), and pillararenes (figure 2.14). They must interact with the suitable guest molecules, ranging from small molecules to cumbersome bio macromolecules or synthetic polymers. Hydrogels can be prepared by exploiting this chemistry: mixing host and guest polymers, copolymerization of a host-guest complex monomer and a cross-linker, copolymerization of a host-guest complex monomer and the main monomer, and mixing a host polymer and a guest cross-linker [33] [67] [68].

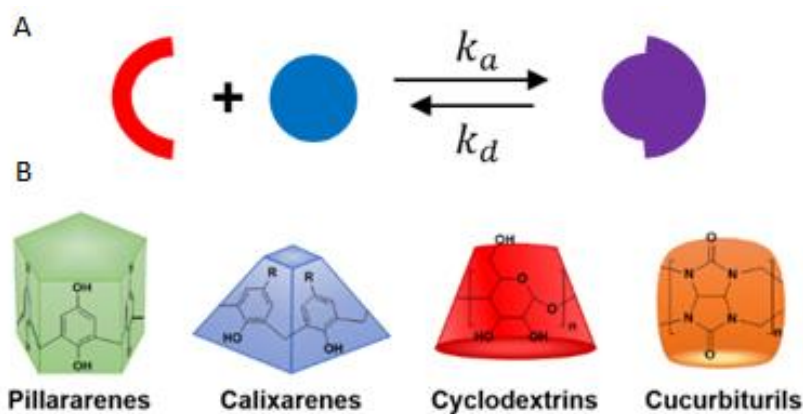


Figure 2-14 - A) Schematic representation of assembly between a host (red) with the corresponding guest (blue) to form a host-guest interaction. The stability of the host-guest complex is governed by the equilibrium constants (K_a and K_d). B) Schematic representation of the chemical structure and geometry of the commonly used host units [68].

CDs can form host-guest interactions with various types of molecules thanks to their amphiphilic nature, deriving from the hydrophilic outer surface and hydrophobic inner cavity. Polymers modified with CDs offer great potential in self-healing due to their water solubility, low cost, multi-stimuli responsiveness, and biocompatibility [33]. Harada and co-workers developed a self-healing hydrogel by copolymerizing a complex β -CD and Ad-based monomers in an aqueous solution. This system showed 99% recovery of the initial strength after standing for 24 h. Besides, they showed that the elastic modulus and self-healing ability of the CD-guest hydrogels increase with the increase in the association constant between a determinate CD-guest pair [69]. In a similar study, Tong et al. utilized polycyclodextrin (PCD) instead of a monofunctional CD to improve the self-healing properties. The hydrogel was synthesized via in situ copolymerization of the Ad-containing monomer N-adamantylacrylamide (Ad-AAm) and acrylic acid (AAc) in a polycyclodextrin (PCD) aqueous solution. A self-healing efficiency of 73% after healing for 120 min at 70°C under humid conditions was observed [70]. Another approach employed Ferrocene (Fc) as a guest molecule with α -, β -, and γ -CDs to build redox-responsive self-healing systems. The reduced form of Fc can be included in the CD cavity, whereas the oxidized form cannot be contained, constitutes the mechanism used for self-healing [67]. Nakahata et al. used poly(acrylic acid) modified with cyclodextrins (pAA-CDs) as a host polymer and pAA with ferrocene (pAA-Fc) as a guest polymer. Upon cut, the two surfaces showed 84% recovery of the initial strength after re-joining for 24 h. However, the measured storage modulus was only 176 Pa showing the soft nature of the hydrogel, which may limit its application. They also studied a system including two different types of host-guest interactions in the same hydrogel. Besides the self-healing behavior, also the shape memory effect by redox stimuli was observed [71]. Another approach adopted azobenzene (Azo) as guest molecules of α - and β -CD. Azo molecules can be triggered by UV light, which inducing the transformation of the Azo units from the trans configuration to the cis configuration. The lower association constant of the system in the cis configuration enables the dissociation between the two species allowing self-healing to occur [67]. Sun et al. synthesized a hydrogel through the copolymerization of acrylamide (AAm), β -CD AAm, and SP-Azo AAm monomers. Self-healing was observed within 10 s, and 77% of tensile strength recovery was obtained after 2 h at RT [67].

Cucurbiturils (CBs) are another utilized host that contains a hydrophobic cavity and polar carbonyl groups in the outer part, which enables strong binding with guests [67]. Scherman et al. reported a high viscosity three-component supramolecular hydrogel using CBs as host and methyl-viologen (MV) side chains of the modified poly(vinyl alcohol) (PVA-MV) and the naphthalene attached to hydroxyethyl-cellulose (HEC-Np) as guests. Such a system showed 100% healing efficiency (storage modulus, step strain measurement) after the samples were cut and then re-joined for 6 s. The presence of cellulose nanocrystals reinforced the hydrogel that displayed a storage modulus higher than 10 KPa [72]. Later, Kim and co-workers reported a self-healable hydrogel obtained by mixing solutions of nor-seco-cucurbituril (NS-CB) and adamantylamine-terminated 4-armed polyethylene glycol (Ad-4-arm-PEG). This hydrogel showed rapid self-healing within 1 min at room temperature. The recovered hydrogel regained its original physical properties even after multiple breaks and self-healing cycles [73].

A different approach comprises using double cross-linked networks to form self-healing hydrogels by combining host-guest interactions with stronger covalent cross-links. These hydrogels were developed to overcome issues related to the weak mechanical properties of the supramolecular hydrogels [67]. As later described, Burdick et al. reported a strategy using guest-host pair CD and Ad attached as pendant groups on the hyaluronic acid polymer chain (HA) [74]. Miao et al. developed a self-healing alginate-based (Alg) hydrogel exploiting the intermolecular entanglements of guest polymers (e.g., PPG) and Alg-g-CD host molecules to create a structure which showed shear-thinning and self-healing behaviors. Furthermore, thanks to the Pluronic F108 functionality, a dual cross-linked hydrogel is generated after increasing temperature, allowing self-healing to occur [75].

2.2.1.6. *Self-healing via hydrophobic interactions*

Supramolecular hydrophobic hydrogels are typically obtained by micellar copolymerization, described by Candau, between macromolecular chains containing hydrophilic blocks with small amounts of hydrophobic units [76]. To get self-healing following this strategy, many different parameters are crucial: the balance of hydrophobic and hydrophilic moieties, the strength of the hydrophilic units, and the presence of surfactants the number and stability of physical cross-links. The presence of the surfactant makes the association/dissociation of hydrophobic cross-links reversible [33]. Jiang and co-workers developed the first pioneering work via copolymerization of hydrophilic acrylamide with octyl phenol polyethoxy ether acrylate hydrophobic monomers. Micelles were formed by associations between acrylates and sodium dodecyl sulfate (SDS). After cutting the specimen into two parts, the SDS micelles dissociate and form a monolayer on the cut surfaces. These micelles contain the hydrophobic parts of polymer chains; thus, when the two parts are rejoined, SDS molecules can arrange in cylindrical micelles at the contact surface, allowing the polyacrylamide modified with hydrophobic groups to bind such hydrophobic micelles. This process led to the healing of the sample, reaching a healing efficiency of 70% in 3 days [77] [7]. Later, Okay et al. developed a system obtained via micellar copolymerization of hydrophobic monomer, stearyl methacrylate (C18), with the hydrophilic monomer acrylamide (AAm) in an aqueous solution of SDS/NaCl. Upon cutting the samples and placing them

back together, self-healing was observed after 10 min at 24°C achieving 100% of healing efficiency calculated from the elongation at break. In addition, this system was able to repair even after long separation times due to the orientation of the hydrophobic groups towards the air-gel interface. Moreover, the self-healing ability of this system can be tuned by utilizing n-alkyl (meth)acrylates of various lengths and concentrations. For example, the healing efficiency increased from 29 to 34% when using an alkyl with 18 carbons instead of 16 [78]. Recently, a self-healing system was developed using a mixture of an anionic surfactant SDS and a cationic surfactant cetyl- trimethylammonium bromide (CTAB) to form wormlike micelles, inducing increased lifetime of the hydrophobic interactions and enhanced mechanical properties [7].

2.2.2. Self-healing via dynamic covalent bonds

The concept of dynamic covalent chemistry was first introduced by Rowan et al., and it includes all the covalent bonds able to break and re-form under equilibrium [79]. To overcome the problem related to the weakness of the supramolecular bonds leading to soft, weak materials, dynamic reversible covalent bonds have been used to obtain more robust self-healing materials. Determinate bonding energy corresponds to each type of bond, which defines not only the stability of the material but also the amount of energy required to cleave the bond enabling self-healing to occur. The reversibility of the cross-linking points in polymers can be reached mainly in three different ways. The first widespread approach is implementing side groups in a linear copolymer backbone with functional moieties (figure 2.15a). A second approach involves the incorporation of reversible bonds in a linear polymer main chain (figure 2.15b). In this case, upon bonds cleavage, the absence of a proper network leads to low mechanical properties. This problem is not present in the last system, which exploited two functional groups with multiple binding sites, which can form a reversible network without requiring a permanent copolymer backbone (figure 2.15c).

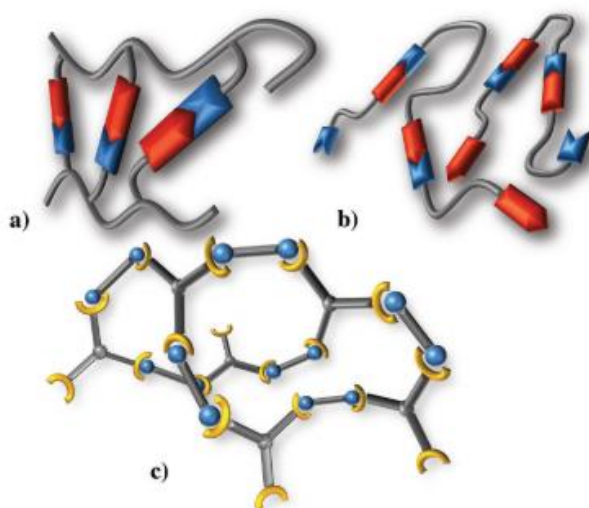


Figure 2-15 - Schematic representation of the three concepts for reversible covalent polymer formation: a) Reversible bonds in the main chain, b) side chain, and c) network with multifunctional linker [6].

Self-healing processes belonging to this category are often triggered by external stimuli such as temperature, light, or pH. These stimuli enable the polymer chains to rearrange at the damaged surface by activating the dynamic behavior. Upon the removal of the trigger, dynamic covalent bonds are reformed, repairing the crack. The amount of functionality within a copolymer can strongly impact thermal (T_g) and mechanical properties of the polymer. Therefore, the ability of temperature triggered intrinsic self-healing systems to repair will be affected by the T_g of the system since it will determine the temperature range required for increased mobility, which allows self-healing to take place [6] [80].

During the last years, a large variety of self-healing polymers with dynamic covalent nature has been proposed. In the following sections, an overview of these systems will be provided, dividing them according to the main reaction type, which takes place during healing (figure 2.16) [6].

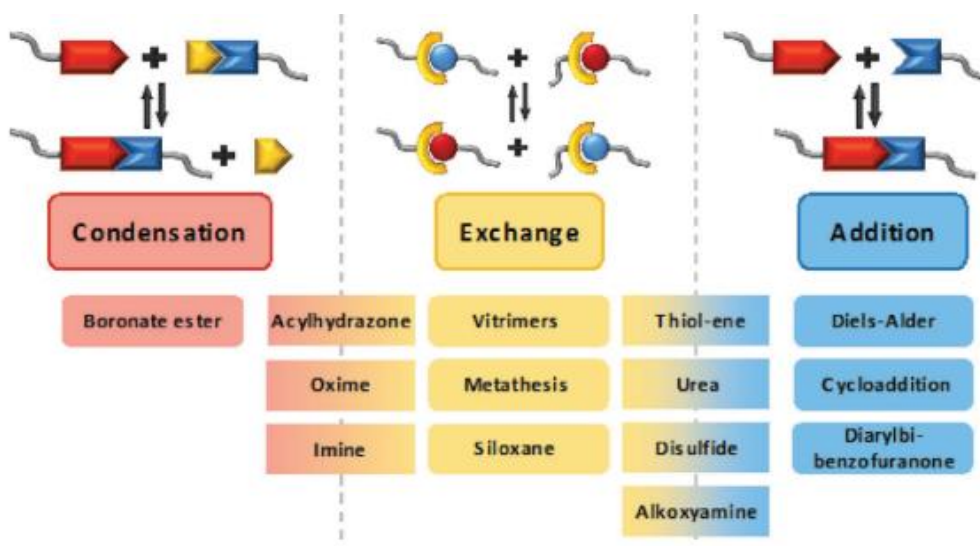


Figure 2-16 - Overview of the different reversible bonding types for application in intrinsic self-healing systems [6].

2.2.2.1. Condensation reactions

Condensation reactions occur when two different molecules react together to form a new chemical bond, and a small molecule is released, most of the time, water. The reversible nature of the reaction can be triggered by the addition of byproducts, which leads to the formation of the two initial functional groups. For instance, the condensation reaction of acylhydrazones can be exploited to reach self-healing in polymers (figure 2.17a). Such bonds can form either covalent and reversible bonds or hydrogen bonds between the free electron pair of the nitrogen atom, and the partial positively charged hydrogen atom makes them unique [6]. These double types of bond formation can be advantageous when high mechanical properties are needed. At the same time, it can diminish the mobility of the networks necessary for healing to occur. The reversible acylhydrazone reaction can be triggered either by a thermal stimulus or by a pH variation [6] [81]. Deng and co-workers developed one of the first self-healing systems based on acylhydrazones produced via condensation of acylhydrazines at the two ends of a poly(ethylene oxide) (PEO) with aldehyde groups in tris[4-

formylphenoxy)methyl] ethane (figure 2.17b). The cleavage and regeneration of acylhydrazone bonds were reversible with glacial acetic as catalyst [82].

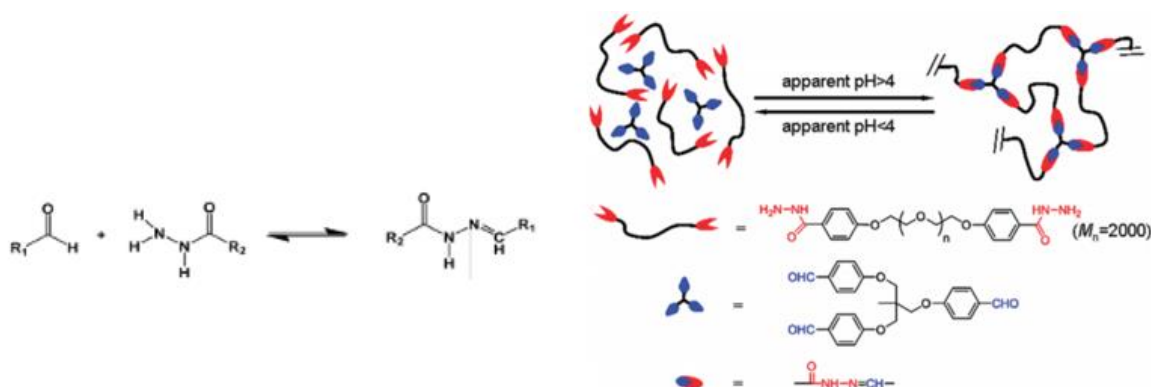


Figure 2-17 - a) Reversible reaction of acylhydrazones. b) The reversible polymer networks cross-linked by acylhydrazone bonds through condensation of acylhydrazines at the two ends of PEO with aldehyde groups [3] [82].

Later, the same research group developed a self-healing hydrogel named HG1G2 containing both acylhydrazone and disulfide bonds as multi-dynamic bonds. Self-healing occurred within 48 h by keeping in contact the cut surfaces under acidic conditions (pH=6). However, healing occurred also under basic conditions due to the reversible nature of disulfide bonds at pH=9. These results provided the idea to expand the study of self-healing hydrogels by incorporating multi-dynamic bonds into one system. A thermal trigger can also activate the reversibility of acylhydrazone bonds, as demonstrated by Kuhl and co-workers [83].

A second common bonding type that belongs to condensation reactions is boronic acid-based interactions (figure 2.18). They are obtained by complexation of diols and boronic acid in acid solution, and their self-healing behavior can be triggered either by pH, water, or temperature. Many boronates are available, and the pK_a values can be tuned by selecting the proper substituents of the phenylboronic acid linkers. However, the long-term stability of these linkages can be an issue; therefore, they usually are used in coordination with more permanent and rigid bonds [6] [84]. Kiser and co-workers designed a hydrogel based on the reversible boronate ester complexation of polymer-bounded phenylboronic acid (PBA) and salicylhydroxamic acid (SHA) (PBA–SHA), which self-healed in an acidic environment [81]. Later, Messersmith et al. designed a self-healing system exploiting the complexation of a catechol modified tetra-arm PEG (cPEG) with 1,3-benzenediboronic acid (BDDBA) in phosphate buffer saline (PBS) at 20 under alkaline pH. The hydrogel showed almost full recovery of G' in 100 s when the strain was reverted to 5% after a large amplitude deformation was applied (1000% strain). Moreover, the self-healing of the hydrogel was confirmed under neutral or acidic conditions [85].

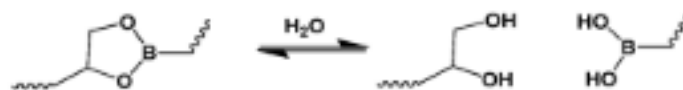


Figure 2-18 - Reversible formation and degradation of the boronate ester [3].

2.2.2.2. Addition reactions

The second type of reaction exploited in self-healing of polymers is the addition reaction, which differs from the condensation because no additional molecule is formed in the reaction step. The most common addition reaction used to induce intrinsic self-healing in polymer networks is the Diels-Alder (DA) reaction (figure 2.19) [6]. This thermally triggered [4+2] cycloaddition reaction is not a recent discovery since this technology was first reported in 1969 by Craven et al. [86]. Later, this concept was expanded to obtain reversible structures capable of showing self-healing behavior: systems containing furan-based components as diene and maleimide-based ones as dienophiles were developed. Polymers containing this type of bond show decross-linking at elevated temperatures due to the retro-DA reactions, which leads to increased mobility and self-healing ability. Then, upon cooling, the functional units can reconnect to restore the network regaining higher mechanical properties. Furthermore, by adjusting the chemical structure, the temperature for the healing process can be finely tuned. Most of the reactions reported in the literature need elevated temperatures beyond 100°C to initiate the rDA reaction [80].

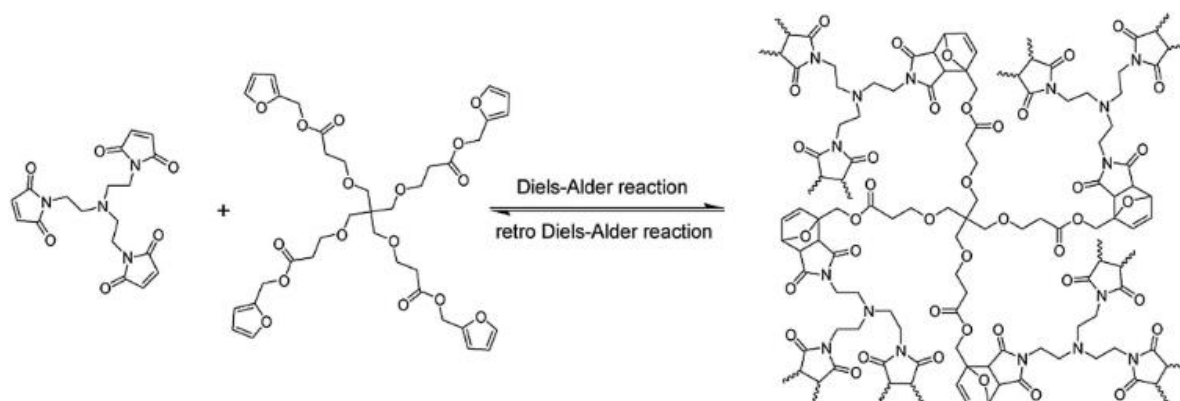


Figure 2-19 - Thermally reversible Diels-Alder reaction between furan and maleimide exploited to form healable polymer networks [80].

One of the first works, based on the thermal reversibility of furan-maleimide-based benzyl aryl ether dendrons and dendrimers, showed a 40% dissociation in DA links after 1 h at 110°C, and the reassembly of 82% of such bonds was obtained in 5 days [87]. Afterward, the maleimide-furan system was applied in epoxy resins, where the reversibility was achieved at temperatures above 90°C. This reversible chemistry was also applied to polyamides, which exhibited self-repair when the temperature was raised to 150°C [6] [80]. In addition, Feng et al. incorporated the Diels-Alder chemistry in polyurethanes via the reaction between furan-terminated prepolymer (MPF) and bismaleimide (BMI). A healing efficiency of 71% was obtained by healing the sample at 120°C for 15 min [88]. However, such high temperatures can be a drawback, especially for specific applications of self-healing materials. Thus, self-healing systems based on the DA reactions capable of healing at room temperature gained lots of interest. Roy et al. reported three different self-healing polymer systems able to repair at room temperature. The first was based on the reaction of 6,6'-substituted fulvenes with dicyano- and tricyano-ethylene carboxyesters in an organic solvent under ambient conditions. By monitoring

the H-NMR signal, they stated that the reversible DA reaction occurred at 25°C [89]. Later, two other systems were developed using anthracene derivatives as dienes and cyanofumarates and N-phenyltriazolinedione as dienophiles [90] [91].

Besides the well-known DA reactions, an alternative approach to build reversible systems may be found in the [2+2] cycloaddition. The peculiarity of this reaction is the photochemical activation of the reaction, which can be achieved with UV light or even with sunlight, making this system highly interesting for potential outdoor applications. One major drawback related to the use of irradiations as a trigger is the low penetration depth of the light, which might result in incomplete healing of the material. Typical chemical structures used to achieve reversible [2+2] cycloadditions are coumarin and cinnamoyl derivatives [6]. Ling and co-workers demonstrated self-healing in a polyurethane network with coumarin side-chains using UV light at 254 nm for cleavage of the bonds and at 350 nm to reform cross-links [92]. Moreover, isomerization can be a problem when only one of the isomers is reactive toward addition; therefore, in this case, thermally or UV light triggered [4+4] cycloaddition is used [6].

A well-investigated and economically attractive self-healing approach relies on thiol-ene click reactions (figure 2.20), which showed healing ability under mild thermal treatment of the networks. Upon heating, the thiol-ene bonds are broken, and the polymer chains are free to rearrange themselves. Afterward, the bonds are reformed, leading to the repair of the damage by cooling down the system. However, this chemical functionality suffers from instability at high temperatures, limiting the applications of such materials [6]. For instance, Kuhl et al. developed a thermally reversible network by involving the Michael addition reaction of multifunctional thiol linkers to cyanoacetamide molecules, which showed repair at 60°C [93].

Although most of the dynamic covalent systems show self-healing upon temperature changes, some systems do not require any external trigger to show the self-healing behavior. As previously described, temperature enhances the chain mobility, thus impacting the healing rate of the system; therefore, sufficient chain mobility must be present at room temperature [6]. Imato et al. proposed a system based on a network of terminal functionalized poly(propylene glycol) and a bifunctional linker containing diarylbibenzofuranone (DABBF). The gel showed self-healing when the damaged surfaces were wetted with the solvent (DMF), providing sufficient mobility to the polymer chains [94].

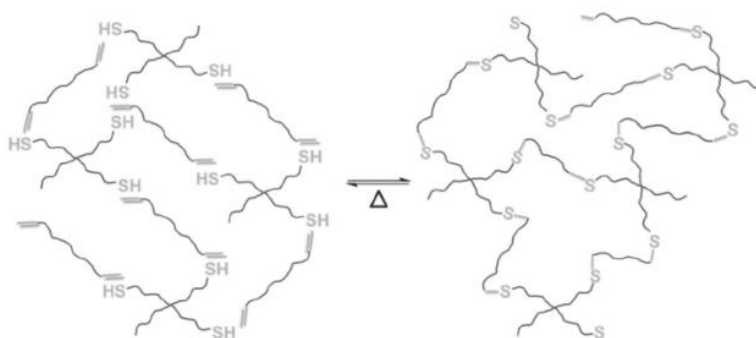


Figure 2-20 - Schematic representation of the reversible thiol-ene click reaction exploited to form self-healing polymers [6].

2.2.2.3. Exchange reactions and Metathesis

As shown in (figure 2.16), most reactions do not belong to a distinct category because it is often defined precisely by the type of reaction involved. Thus, in this paragraph, alternative chemistries used to achieve self-healing and hard to categorize will be described.

Imine bonds, commonly called Schiff bases, are very strong covalent bonds which are intrinsically labile towards water. The reaction of the imine with water can form aldehydes, which can be deleterious in certain applications. Due to their high stability in the physiological environment, they have attracted much attention as reversible bond structures in self-healing materials. The imine exchange reactions, and hence their healing ability, can be controlled when coupled to a photochromic moiety, allowing the possibility to tune the healing rate of the material [6]. Zhang et al. obtained a dynamic self-healing chitosan–PEG hydrogel using aromatic Schiff base linkages. Imine bonds are rapidly formed from the reaction between the aldehyde groups of benzaldehyde difunctionalized PEG and the amine groups present on the chitosan backbone. The recovery of the mechanical properties and thus the self-healing ability was demonstrated with repeated step strain rheological measurements, which showed a recovery of the G' to its original value after decreasing the amplitude to 20%. After inducing a hole with a diameter of 0.9 cm in the hydrogel disc, the system could self-heal within 2 h [7] [58]. Schiff base reactions with imine bonds were also used by Ding et al. in a hydrogel composed of acrylamide-modified chitin and oxidized alginate. Self-healing was pH-dependent, showing repair only in a neutral or basic environment at RT after 3 h [95].

Another approach exploited oximes to achieve self-healing. Oximes show high bond strength and stability against hydrolytic cleavage. However, Kuhl et al. showed that the higher stability of oximes compared to imines or acylhydrazones led to a decrease in the network mobility, thus inhibiting the self-healing behavior of the polymer [96]. Mukherjee and coworkers developed a self-healing hydrogel bearing oxime as functionality and obtained via the copolymerization of N, N-dimethylacrylamide (DMA), and diacetone acrylamide (DAA), and subsequent crosslinking with the difunctional alkoxyamine O,O'-1,3-propanediylbishydroxylamine dihydrochloride. Self-healing was observed by putting in contact the two cut surfaces for 2 h at RT [97].

The previously described issue related to oximes can be overcome by using disulfide bonds (figure 2.21). Those are weaker and enable healing at lower temperatures. Moreover, the reversibility can also be controlled by irradiation or additives like additional thiols or by pH changes. One of the first systems was developed by Klumperman et al. using disulfide bonds in epoxy resin, which showed restored mechanical properties after healing for 1 h at 60°C [98].



Figure 2-21 - Schematic reaction taking place during healing in disulfide systems [3].

Later, in 2012, Matyjaszewskii et al. presented a novel approach to construct a self-healing organogel based on a thiol/disulfide redox reversible exchange reaction. The atomic force microscope (AFM) test showed that the cut gel film, with a thickness of 1.5 μm and width $<2.5 \mu\text{m}$, could heal within 20 min. However, they observed that the healing efficiency was tightly correlated with the width of the damaged area resulting in incomplete healing in larger cuts [6] [99].

Recently, Chang et al. reported a self-healing polyurethane based on disulfide bonds. The shape memory effect of the polyurethane allowed the closure of the crack, and the healing was achieved through exchange reactions of the disulfide bonds. The obtained healing efficiency, calculated measuring the tensile strength, was 93% with healing at 80°C for 24 h [100]. Furthermore, Grande et al. investigated the effect of the cross-link density of disulfide bonds in a poly(urea-urethane) network on the mechanical properties and the self-healing ability. It was observed that a higher self-healing ability corresponded to lower values of tensile strength. This is still one of the main challenges in self-healing systems, where both mechanical properties and self-healing ability should be maximized. In order to increase the mechanical properties, Zechel et al. designed a system using methacrylate-based copolymers cross-linked by hindered urea moieties (figure 2.22). [2].

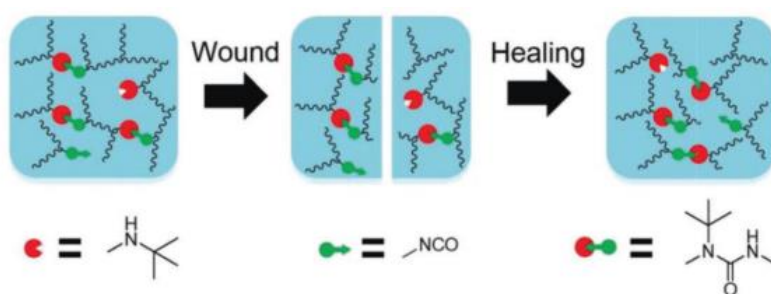


Figure 2-22 - Healing mechanism in self-healing hydrogels based on reversible urea bonds [2].

Urea bonds induce additional hydrogen bond interactions leading to higher stability and mechanical properties. Furthermore, the reversibility of urea bonds is thermally triggered, inducing the formation of isocyanates and amines if a sterically hindered amine has been utilized for the synthesis. The strength of the urea bonds can be tuned via the steric hindrance of the amine groups, thus affecting the self-healing ability of the system [6].

Another very promising class of dynamic covalent bonds used in self-healing hydrogels is alkoxyamines (figure 2.23), which can be triggered by either UV irradiation or temperature. The homolytic cleavage of the C-O-N bond forms two radicals, which can later recombine or exchange with other functional units in the network to reform the cross-link [6]. Yuan et al. were the first to design self-healing polymers based on alkoxyamines introducing bifunctional monomers into styrene copolymers. The healing system could be applied in a wide range of temperatures, and the network showed high mechanical and thermal stability [101]. The alkoxyamine concept was also extended to polyurethane copolymers and epoxy-based systems [102] [103].

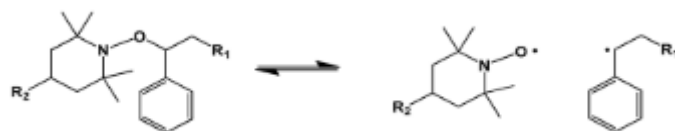


Figure 2-23 - Alkoxyamine reaction generating radical species which later react to induce healing of the material [3].

The last important type of bond used in self-healing materials is the olefin metathesis. This system is transition-metal catalyzed and can exchange double bonds. Lu and Guan have shown how these bonds can be incorporated into polymer networks to form self-healing polymers. They used a polybutadiene network, and a ruthenium catalyst was used to provide self-healing at room temperature and even sub-ambient temperatures. Different healing efficiency degrees were obtained depending on the temperature, amount of catalyst, and applied compression pressure [104]. However, this system is quite limited for real-life applications because of drawbacks like the complicated synthesis, which makes them expensive.

2.2.3. Molecular Interdiffusion

Molecular interdiffusion is a system which can belong to both types of self-healing mechanisms, extrinsic and intrinsic. In extrinsic systems, the healing agent is a thermoplastic polymer, considered an additive because it is composed of a different material than the matrix in which is distributed. Increasing the temperature above the T_g in thermoplastic activates the flowing of the polymer chains, restoring the damage, contrarily to thermoset materials, where the cross-linking prevents the free motion [5].

Meure et al. proposed a system fabricated by blending thermoplastic polyethylene-co-methacrylic acid (PEMAA) additives into a thermosetting epoxy matrix. The damaged area was heated at 150°C for 30 min, inducing the melting of the thermoplastic part, which repaired the crack by diffusion. The filling action was pressure-driven due to bubble formation within the composite, deriving from the reaction between PEMAA and the epoxy matrix. After cooling, 100% of recovery was achieved, mainly attributed to hydrogen bond formation between the two polymer materials. Similarly, Hayes et al. selected poly(bisphenol-A-co-epichlorohydrin) as a thermoplastic polymer to provide self-healing ability combined with an epoxy thermoset [105].

Molecular interdiffusion is more suited for applications in intrinsic self-healing systems made by a thermoplastic material. The healing mechanism differs from the one described for the extrinsic systems: O'Connor and Wool stated that the healing phenomena occurred via void closure, surface interaction, and molecular entanglement between the damaged surfaces [1]. Repairs in such systems can be obtained by increasing the temperature above the T_g of the material, enabling the polymer chains' flow. The main process that enables healing is the possibility of forming entanglements between the polymer that flows into the damaged zone and the polymer present in damaged surfaces. Solvents (ethanol, methanol, or a combination of both for PMMA and CCl₄ for PC) can be used to lower the T_g thanks to their plasticizing effect to perform healing at a lower temperature, reducing the energy consumption. Thermoplastic materials used for self-

healing are poly (methacrylate) (PMMA) and polycarbonate (PC) [5] [1]. Yamaguchi et al. demonstrated self-healing via molecular diffusion and entanglement of dangling chains in a weak PU gel. The repair was carried out at room temperature, requiring a short time for healing to occur. This gel reached healing efficiencies up to 80% due to strong interactions between dangling chains [106].

Final remarks:

In this chapter, an overview of self-healing mechanisms, analyzing both extrinsic and intrinsic strategies, was presented. To sum up, extrinsic systems are more suited for applications in rigid structures, where chain mobility is limited. Thus, it is necessary to add a healing agent (monomer, catalyst, and hardener) with high mobility to enable the self-healing process. By contrast, intrinsic self-healing strategies are more versatile, being able to adapt to a lot of matrices and many conditions. They are particularly suited for application in soft systems such as hydrogels or soft elastomer in which the chain mobility is significantly higher. Due to their soft nature and the absence of foreign structures (capsules or vasculatures), intrinsic systems are more suitable as inks for 3D-printing. Therefore, in the next chapter, an overview of the different 3D-printed self-healing materials will be detailed.

3.3D printing of self-healing materials


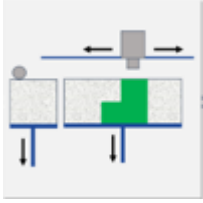

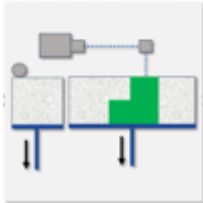
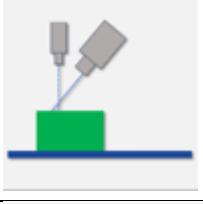
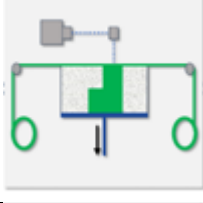

Despite the multitude of successful synthesis and applications, the existing self-healing materials are still facing a critical bottleneck-deficiency in 3D shaping. In addition, several potential applications of self-healing polymers require complex 2D/3D architectures, such as structural composites, soft robotics, and architected electronics. However, 3D-printing of self-healing systems is not always trivial because ink specific properties such as shear thinning behavior, viscosity, post-printing stability, and robustness are required for a successful printing process. In the last years, researchers have been developed numerous printable self-healing systems exploiting different restoration mechanisms as well as different printing techniques. In what follows, there is first a description of the different 3D printing methods, followed by an overview of the developed inks, focusing on the printability and self-healing ability of each of them.

3.1. 3D printing overview

Additive manufacturing (AM), also called 3D printing, is one of the most promising fabrication technologies nowadays, currently gaining momentum in large-scale parts production. AM enables complex 3D structures such as hollow objects, lattice framework, and graded or multi-material structures starting from a three-dimensional computer-aided design (3D CAD). These models are created by the selective and successive addition of material, layer by layer, until completion. The different layer fashions derive from converting the 3D CAD into a computer-readable format (STL file), which allows the machine to produce the object. 3D printing offers many advantages over traditional production methods such as subtractive manufacturing, forming, or casting methods. It permits on-demand fabrication of customized products with shapes and features unattainable with traditional processes. Besides the various advantages in terms of complexity achieved, AM also entails environmental benefits because it enables the production of final objects with more efficient material usage, allowing the reuse of feeding material and requiring less energy if compared to subtractive processes for small-batch production. Furthermore, being a near-net-shape process reduces the number of processing and post-processing steps required to achieve the final component [107] [108].

Nowadays, several different AM fabrication technologies are established, which can be grouped according to how the layers are created and bonded, and the kind of material used. These techniques result in variable object resolution and different production speed, mostly related to the intrinsic characteristic of the printer, the fabrication parameters, but also the model design and topological optimization. Following the ASTM International Committee F42 on Additive Manufacturing in 2009, AM technologies can be classified as follows: material extrusion, material jetting, binder jetting, sheet lamination, vat photopolymerization, powder bed fusion, and direct energy deposition [107]. In the table below (table 2), all these AM techniques are reported with advantages and disadvantages. Since 3D printed self-healing materials reported in the literature have been fabricated only by material extrusion or vat photopolymerization, only techniques belonging to these two categories will be explained and detailed in the next sections.

Table 2 - Categorized AM techniques for polymers, along with Advantages and Disadvantages [107].

Categorized techniques	Name	Scheme	Process	Typical feature resolution	Advantages	Disadvantages
Material Extrusion	FDM (FFF) 3DD		Thermo-softening material selectively dispensed through a nozzle.	100-150 μm	- Inexpensive machines and materials; - Biocompatible materials; - Allows multi-material AM.	- Limited mechanical properties; - Z-direction anisotropy.
Binder Jetting	BJ		A liquid bonding agent is selectively deposited to fuse powder materials.	100 μm	- Fast; - Allows multi-material AM.	- Low viscosity ink required; - Limited mechanical properties.
Material Jetting	DOD MJ		Droplets of build material (such as photopolymer or thermoplastic materials) are selectively deposited.	25 μm	- Good accuracy and surface finish; - Allows multi-material AM.	- Only works with wax-like materials; - Materials not durable in time.
Powder Bed Fusion	SLS SLM EBM		Thermal energy (provided by a laser or an electron beam) selectively melts a powder bed region.	50-100 μm	- Best mechanical properties; - Less anisotropy. - No support material is required.	- Rough surfaces; - Poor reusability of unsintered powder.
Direct Energy Deposition	LENS EBAM		Focused thermal energy (e.g., laser or plasma arc) is used to fuse materials by melting as they are being deposited	Low resolution	- Uses powder or wire product; - High deposition rate.	- Low dimensional accuracy; - May require post-processing steps.
Sheet Lamination	LOC UC		Sheets of material are bonded together to form an object.	200-300 μm	- Compact desktop 3D printer; - Fast and accurate.	- Limited materials; - Low resolution; - High anisotropy.
Vat Photopolymerization	SLA DLP CLIP 2PP		Liquid photopolymer (resin) in a vat is selectively cured by light-activated polymerization.	0.1-100 μm	- Excellent surface quality and precision; - High build speed (no for 2PP).	- Low-viscosity resin required; - Limited mechanical properties;

3.1.1. 3D material extrusion

Extrusion-based 3D printing consists of a computer-controlled layer-by-layer deposition of molten and semi-molten polymers, polymer solutions, and dispersions through a nozzle which acts as the print head. After the deposition of one layer is completed, either the build platform moves downward, or the printing head moves upward to continue with the deposition of the next layer. Extrusion-based AM includes many different techniques such as fused deposition modeling (FDM) (also called fused filament fabrication (FFF)), 3D dispensing, 3D micro-extrusion, and 3D bio-plotting, differing mainly by the nature and consistency of the feeding material used to produce the final construct [107].

3.1.1.1. Fused deposition modeling (FDM) (Fused filament fabrication (FFF))

Fused deposition modeling (FDM) comprises 3D extrusion of thermoplastic polymers in the melted state through the heated print head. The print head is heated to the appropriate temperature according to the material used: above the melting temperature for semicrystalline polymers and above the glass transition temperature for amorphous polymers. Both the model and support materials are fed as thin strands from a spool into the heated print head by mechanisms involving either a screw or a pressure-driven system, enabling the deposition of the highly viscous polymer melts (figure 3.1) [107].

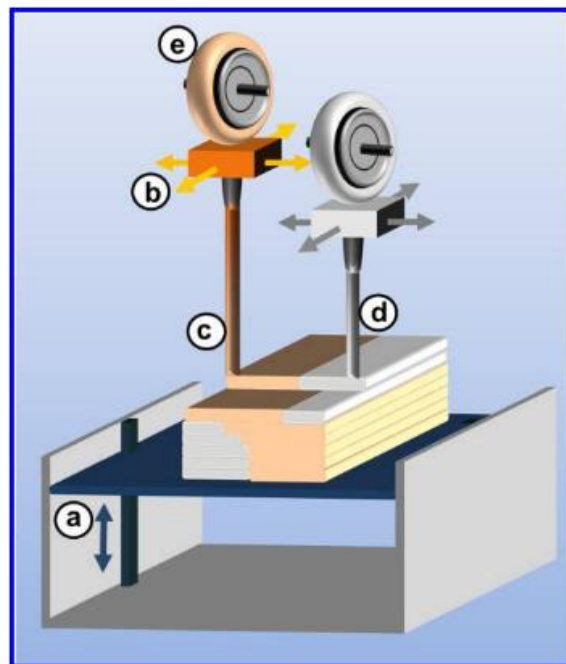


Figure 3-1 - Schematic illustration of the fused deposition modeling process with a) a vertically movable building platform, and b) heated print heads for deposition of both c) model and d) support materials wound on e) spools [107].

In order to achieve a successful build process, an optimal balance among several parameters such as polymer melt rheology, build speed, processing temperature, and CAD model is essential. However, the main disadvantage of this method is the lack of adhesion at the interface between two subsequent deposited layers, resulting in non-uniform mechanical properties within the printed structure (mechanical anisotropy). This

effect is further pronounced when an incomplete fusion of the filament is observed (layering effect). Layering always results in high surface roughness and porosity within the final constructs [107] [109].

3.1.1.2. 3D Dispensing

3D dispensing, which comprises 3D Plotting, 3D Micro Extrusion, 3D Fiber Deposition, comprises a print head with a nozzle and a cartridge which can move vertically and horizontally, enabling the fabrication of 3D parts (figure 3.2). The material is extruded through the print head by a pneumatically controlled system, thus varying the air pressure. The fundamental difference compared to FDM can be found in the exploited method to induce the solidification of the extruded material. In 3D dispensing, various strategies can be applied without requiring the melting of the material. Besides using thermoplastic materials, a large variety of thermoset resins such as polyfunctional epoxides, acrylics, polyurethanes, and silicones can be processed. In this case, the crosslinking of the material to form the covalent network must be performed immediately after the deposition to allow the 3D construct to self-withstand without collapsing [107].

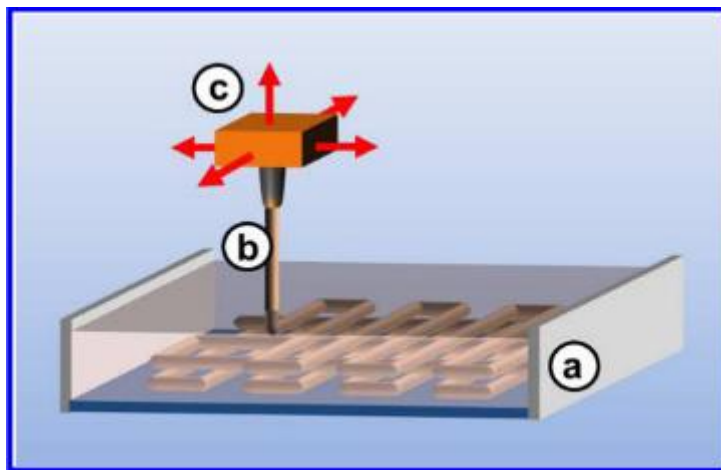


Figure 3-2 - 3D dispensing comprising a) a building platform immersed in the air or a liquid, b) a nozzle, and the c) movable print head [107].

Furthermore, the direct ink writing (DIW) technique allows processing polymers mixed with a liquid to form inks (hydrogels or, more rarely, colloids). By carefully mixing and selecting the proper concentration of each element present in the ink, the material should easily flow under shear, thus showing shear thinning behavior, and quickly recover upon deposition to be able to self-support its weight. Therefore, printable formulations are non-Newtonian fluids that present yield stress. After the yielding point, the material has a shear thinning behavior with minimal flow index values; thus, the material behaves like a liquid allowing a facile deposition. Then, upon removal of the shear stress, the material should be capable of regaining its initial mechanical strength. Moreover, to quantify and evaluate the printability of these formulations, shear tests like amplitude sweep or frequency sweep must be carried out. Resultant graphs will provide the storage modulus (G') and loss modulus (G''), as well as the crossover point (stress at which $G' = G''$), which usually represents the gelation point of the formulation. Specifically, the crossover point must be high enough for the material to

self-withstand in the absence of stress when the material is deposited, but not too high (< 2500 Pa) because this could easily hinder the extrusion process by clogging formation into the nozzle [110].

However, very often, polymers do not show the shear thinning behavior; hence they would not be processable with the DIW method. This obstacle is usually overcome by adding to polymers functionalities that permit dynamic covalent bonds or reversible supramolecular interactions within the material. These reversible bonds can be easily broken under certain conditions (shear stress, temperature, pH) to allow printing of the material and then reformed after the deposition onto the build platform to form self-supporting objects (figure 3.3). Moreover, reversible bonds are also formed between two adjacent layers, increasing the mechanical strength in the z-direction, thus enhancing the isotropy of the final component. All these strategies will be more deeply described in the next sections because they are also responsible for the self-healing ability of those polymers [111].

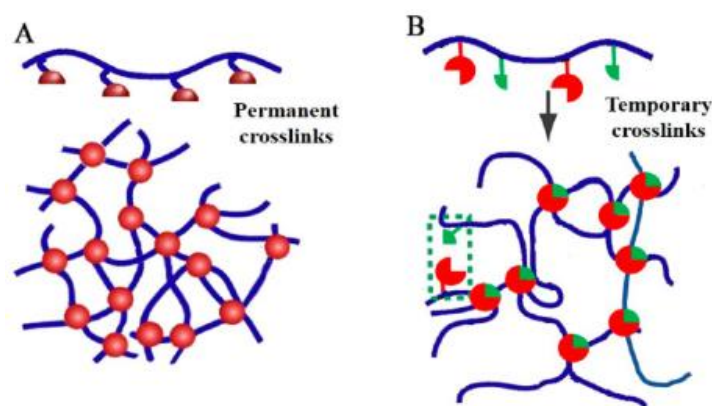


Figure 3-3 - Schematic illustration of cleavage of bonds induced by shear forces. If dynamic reversible bonds (B) are present, they can be reformed after the material has been deposited [111].

3.1.2. Vat Photopolymerization 3D printing

The first reported use of vat photopolymerization was dated in the mid-1980s with the Hull's patented system where a laser was scanned over a photopolymer vat layer by layer to fabricate solid objects from liquid photopolymer resins [112]. However, the scientific and industrial interest in this technology is still growing year after year. This technique involves using a vat containing a photopolymerizable liquid polymer that is selectively cured upon light irradiation. Thus, the object is built on a platform that moves according to the layer fashion, without requiring complex machines and supporting material. During the 3D printing process, small monomers are linked together into chain-like polymers, forming a cross-linked structure. A photoinitiator is required to initiate the reaction upon absorption of the incident light, thus generating reactive species or radicals that interact with monomers, enabling the photopolymerization process. Photopolymerization reactions can be divided into two classes according to the initiation mechanism: free-radical polymerization systems and ionic polymerization systems. Notably, the polymers must be sufficiently cross-linked to avoid the solubilization of the part into the liquid monomer during fabrication. Through vat photopolymerization 3D printing, customized and complex shape structures can be fabricated with excellent

printing resolution (compared to extrusion-based 3D printing techniques), and without the necessity to use any support materials. In addition, the 3D cross-linked structure possesses good mechanical properties, therefore not requiring any post-processing operation, as often is required when using extrusion-based 3D printing [113] [114]. Vat photopolymerization technologies mainly comprise three different and well-established methods: Stereolithography technique (SLA), Digital Light Processing (DLP), and Continuous Liquid Interface Production (CLIP) [107].

3.1.2.1. Stereolithography (SLA)

Stereolithography techniques rely on the selective polymerization of liquid resins using a coherent light source (usually lasers emitting in the UV-range). The laser exposure of each photosensitive layer is performed sequentially, point-by-point, following the pre-designed CAD model geometry. The key feature of this method is the high spatial resolution, which is proportional to the spot size of the focused laser beam, around $1\ \mu\text{m}$ [115]. Both the spot size and the speed with which the laser beam is scanned determine the time necessary to produce one final construct layer. After the production of one layer is completed, the building platform moves along the Z-axis according to the thickness of the next layer. In this way, a fresh layer of uncured liquid resin is located on top of the printed object, ready to be photopolymerized. However, this is the foremost time-consuming step in SLA, and the viscosity of the formulation plays an important role. So often, additives or solvents have to be used to decrease the viscosity of the resin. Sometimes, dyes and light-absorbers are added to the liquid resin to limit the penetration depth of the light, enabling higher precision of the 3D printing process. SLA machines can be configured either in a top-down or in a bottom-up configuration (figure 3.4).

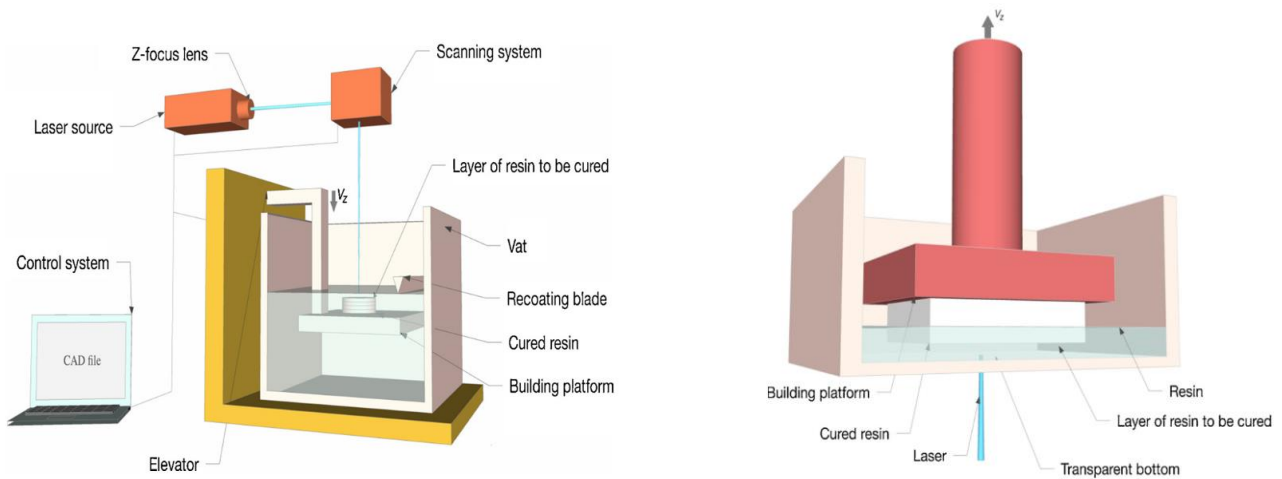


Figure 3-4 - Schematic representation of Stereolithography (SLA) 3D printing machines: top-down orientation (left) and bottom-up orientation (right) [116].

While in the top-down configuration, the platform is submerged in the liquid resin as the part is created, in the bottom-up approach, the object remains attached to the platform, and it is raised after each polymerized layer. In this case, the laser beam hits the resin from below the vat through a transparent window. The bottom-up approach is preferred over the top-down for many reasons. It is independent of the depth of the vat container,

it requires less printable material (since it is not necessary to fill the entire vat to print), and most importantly, it avoids the direct contact of the resin undergoing photopolymerization with the ambient, reducing the oxygen inhibition. A derivative SLA 3D printing technology is provided by the micro-stereolithography, with which lateral resolution in the range of a few micrometers can be achieved. However, this technique is slower, thus used to produce small objects [107].

3.1.2.2. Digital Light Processing (DLP)

Digital light processing (DLP) is similar to SLA because both techniques use light to cure a photoresin in a layer-by-layer fashion. However, in the DLP method, the entire surface of the resin is selectively exposed to the light all-at-once. The information for the specific slice of the object is transferred in the form of light ON/OFF via a digital micro-mirroring device (DMD) to each layer (figure 3.5). Each micro-mirror on the DMD represents one pixel in the digital image, providing printing resolutions between 10-200 μm in the X-Y plane according to the optical setup. This method allows for considerably shorter building time compared to SLA, where the surface of each layer is exposed point-by-point, but with a lower in-plane resolution. Additionally, DLP suffers less from oxygen inhibition because the layer of resin being polymerized is on the bottom of the vat and not in contact with air, as in SLA. The vertical resolution of the system depends mainly on the light penetration depth that can be adjusted, as previously mentioned, with light-absorbing additives or dyes. However, also other factors, such as the printer's mechanical elements, the precision of the engine, and the accuracy of the step-by-step screw, influence the resolution in the Z-axis [107].

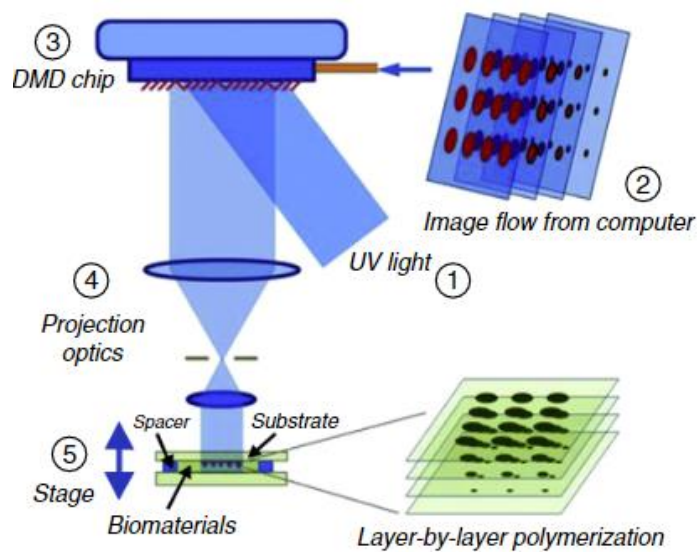


Figure 3-5 - Schematic illustration of the Digital Light Processing (DLP) 3D printing setup [117].

3.1.2.3. Continuous Liquid Interface Production (CLIP)

Unlike the layer-by-layer strategy of DLP and SLA approaches, CLIP-3D printing allows the continuous fabrication of objects by creating a thin interfacial film of oxygen through an oxygen-permeable window. The oxygen film forms a “dead zone” at the bottom of the vat, which inhibits free-radical polymerization at the

surface close to the UV source, enabling 3D printing to be performed with no intermediate re-coating step for each layer (figure 3.6). Generally, a dead zone with thicknesses in the range of 20-30 μm is suitable for a fast and precise CLIP process. As earlier described, the resin re-coating step is the most time-consuming operation for SLA and DLP, thus CLIP results in a much faster 3D printing process. Features resolution in the Z-axis can be increased by adding light adsorbers. However, decreasing their concentration allows the light to penetrate more in-depth, enabling a faster production [107].

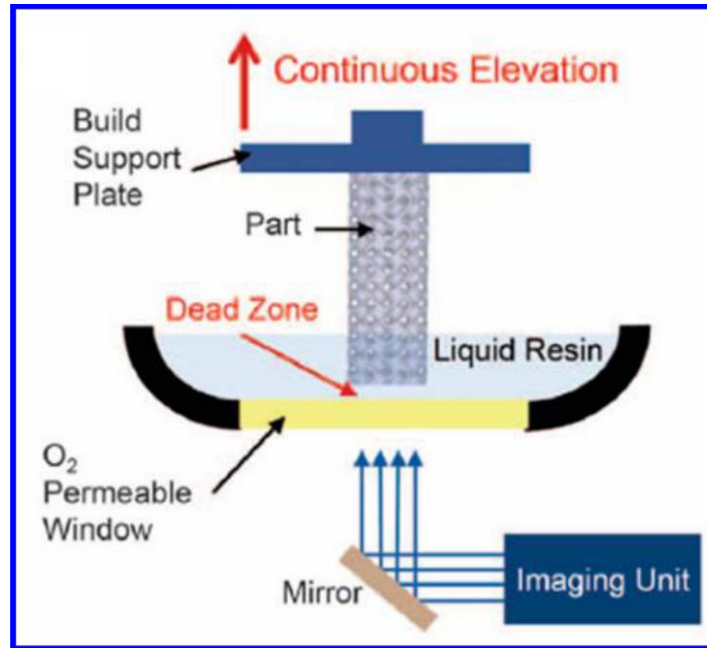


Figure 3-6 - Schematic illustration of the Continuous Liquid Interface Production (CLIP) 3D printing process [107].

To sum up, table 3 reports and compares the main characteristics of the two 3D printing systems: material extrusion and vat photopolymerization.

Table 3 - Characteristics comparison of extrusion printing and vat photopolymerization.

Process	Material	Material deposition [118]	X-Y resolution [119]	Z-resolution [120]	Model surface [120]	Fabrication speed [121]	RTM ratio* [122]	Viscosity [111]
Material extrusion (FDM, FFF, DIW, Bioplotter)	Viscous liquids, thermosoftening materials	Continuous line	100-200 μm	100-200 μm	Very rough	Slow ($\mu\text{m/s}$)	0.5-1 m^2/min	10^6 - 10^8 $\text{mPa}\cdot\text{s}$
Vat Photopolymerization (SLA, DLP, CLIP)	Liquid photocurable resins	SLA – line rastering DLP – layer exposure	SLA – 1-10 μm DLP - 20-200 μm	> 1 μm	Smooth	SLA – medium (mm^2/s) DLP – fast (mm^2/s)	0.5-2 m^2/min	10^2 - 10^4 $\text{mPa}\cdot\text{s}$

*RTM ratio is defined as the spatial resolution/time for manufacturing ratio.

3.2. 3D-printed self-healing systems

In this section, a description of the different 3D printed self-healing formulations can be found, dividing them according to the printing method used and the self-healing mechanism involved.

3.2.1. Inks printed via extrusion-based 3D printing

3.2.1.1. Extrinsic self-healing (vascular)

Toohey et al. developed a self-healing system capable of autonomously repairing multiple damage events mimicking the human skin. A 3D microvascular network was embedded into the substrate via direct-write assembly of a fugitive organic ink. The layer-by-layer build sequence was followed by infiltration of the 3D structure with an epoxy resin. After curing the resin, the fugitive ink was removed upon heating under a mild vacuum forming the 3D microvascular structure (figure 3.7) [123]. Self-healing of this system was demonstrated via ring-opening metathesis polymerization of dicyclopentadiene (DCPD) monomer, embedded into the 3D microvascular network, by Grubbs' catalyst particles, which were incorporated within the epoxy coating. This system allows self-healing to occur due to multiple factors. The low viscosity of the healing agent facilitates the flow of the DCPD into the cracks, and the Grubbs' catalyst particles remain reactive even during and after the curing process. Finally, the rapid dissolution of the Grubbs' particles when in contact with the monomer led to the polymerization under ambient conditions, repairing the damage. The healing efficiency was assessed by calculating the ability of the coating to recover its fracture toughness upon crack generation by a four-point bending test. The crack formation was monitored via an acoustic-emission sensor. After testing, the two surfaces were brought in contact without external pressure, and healing occurred at room temperature after 12 h. The healing efficiency was studied over multiple crack/repairing cycles for different systems containing 2-5-10 wt% of Grubbs' catalyst, respectively. The best result in terms of healing efficiency was obtained with the largest amount of Grubbs' catalyst, showing 70% recovery after the second healing cycle. Furthermore, they stated that the amount of catalyst did not significantly affect the healing efficiency for a given cycle. Instead, the number of successful healing cycles achieved was two, three, and four for samples with 2 wt%, 5 wt% and 10 wt%, respectively [123].

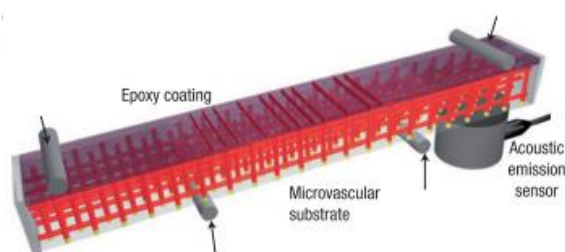


Figure 3-7 - Schematic diagram of the self-healing structure composed of a microvascular substrate and a brittle epoxy coating containing embedded catalyst [123].

3.2.1.2. 3D-printed inks involving dynamic covalent chemistry

Shi et al. overcame issues in printing self-healable thermosetting polymers by designing a new thermosetting vitrimer epoxy ink that can be modeled in complicated geometries by direct ink writing and then recycled to be reprocessed. A vitrimer polymer shows the same behavior of a traditional thermoset at room temperature, whereas at higher temperatures, it can modify its structure through transesterification-type bond exchange reactions (BERs), which allow the material to be reshaped. In their work, they explained how to perform the curing step at high temperatures without causing the collapse of the structure because of the decreased viscosity of the ink. Despite the improvement in shape fixity for the addition of nanoclays as viscosity modifiers, the epoxy solution was pre-cross-linked at 130°C for 30 min under vacuum conditions. Due to the high viscosity of this system, a high temperature (70°C) was adopted because the only shear thinning was not enough to reach the optimal value of viscosity for printing. The recyclable ink was obtained by mixing epoxy precursors such as bisphenol A diglycidyl ether (DGEBA), fatty acid, and a Zn(Ac)₂ catalyst, with the modifier nanoclay (18 wt%). The printed structure (a twisted vase) was then cured at 60°C for 20 h, and the fully curing was obtained with a second curing step under vacuum for 6 h at 130°C.

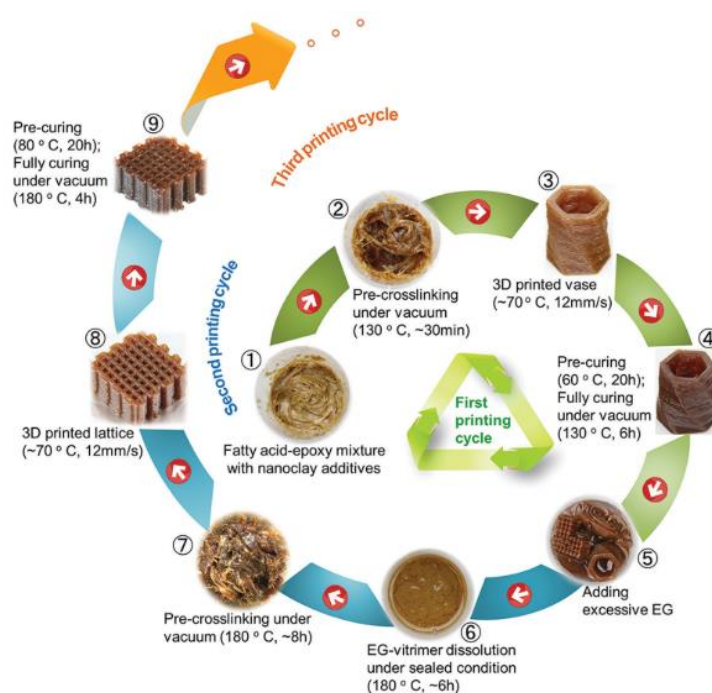


Figure 3-8 – Schematic representation of the crosslinking/dissolution/recrosslinking cycle of recyclable 3D printing of nanoclay-reinforced vitrimer epoxy [124].

Finally, complete recycling of the ink is possible by dissolving the printed part within ethylene glycol (EG) (figure 3.8). The printed polymer parts darkened after a few printing cycles, most likely due to the intrinsic brown color of the nanoclays and thermo-oxidation of the epoxy chains. In addition, temperature-dependent stress relaxation tests revealed that the presence of nanoclays did not affect the transesterification type BER kinetics. Furthermore, the network adaptability was also maintained for the recycled nanoclay-vitrimers. Based

on their work, self-healing can be achieved by filling the damaged area with a solution of vitrimer epoxy soaked in EG and heated at 100°C in order to increase the fluidity. Finally, the full curing was carried out in an oven at 180°C for 4 h. However, they used such a system to get a glossy coating onto the surface of the part; thus, no healing efficiency was reported in this work [124].

Later, Wu and coworkers designed a self-healing, adaptive, and conductive polymer composite for extrusion-based 3D printing based on the polyborosiloxane (PBS) dynamic chemistry. The ink was obtained by mixing PBS with 5 wt% of electrochemically exfoliated graphene (PBS/G5), and its 3D printing was performed onto polydimethylsiloxane (PDMS) substrates. The presence of the graphene network provides higher mechanical properties as well as a continuous conductive channel. The dynamic behavior of the boron/oxygen dative bond was activated by methanol, giving to the material chemical-activated mechanically adaptive properties (MAPs). The effect of the addition of methanol was assessed by rheological analysis and Fourier-transform infrared spectroscopy (FTIR). The former revealed that the storage modulus (G'), loss modulus (G''), and the value of complex viscosity ($|\eta^*|$) of the liquefied PBS in methanol were lower than those of the virgin PBS. Furthermore, the viscosity decreased with increasing frequency, showing a shear thinning behavior. FTIR analysis was performed to confirm the chemistry involved in the dynamic behavior, the methanol-induced alcoholysis of the boron/oxygen dative bond in the Si-O-B moiety. Finally, self-healing of this ink can occur at room temperature or can be electrically activated by the conductive graphene network. By bringing the two damaged surfaces in contact and monitoring the electrical conductivity of PBS/G5, they stated that the conductive healing efficiency was 99.4% [125].

Boronate esters mediated self-healing was also used by Biswas and coworkers to produce three hydrogels composed of phenylboronic acid (PBA), 4-nitrophenyl boronic acid (4-NPBA), and 4-methoxyphenyl boronic acid (4-MPBA) with guanosine (G). The first two gels were strong, whereas the latter formed a weak gel. Gels were not formed under acidic pH because of the instability of the boronate ester linkages. On the other hand, basic conditions resulted in deprotonation of the guanosine, thus a loss in hydrogen bond formation, leading to weaker hydrogels. Therefore, the suitable pH value for 3D printing was 7.6. Shear-thinning and self-healing behavior of gels was demonstrated by cyclic dynamic strain sweep experiments. Besides, three pieces of the GPBA gel were joined with each other, and after 30 min, an integral piece was obtained without the application of external stimuli [126].

Another approach to achieve self-healing ink was proposed by Appuhamillage et al., exploiting Diels-Alder dynamic reactions. Furan-maleimide-based polymers were used as mending agent (MA) (25 wt%) for polylactic acid (PLA) (figure 3.9). Partially cross-linked polymers with furan-maleimide Diels-Alder (fmDA) functionality enabled fused filament fabrication (FFF). The 3D printing was feasible because the system undergoes depolymerization (retroDA reactions) during the printing process at high temperatures (205°C), thus lowering the molecular weight and enabling a decrease in melt viscosity. Then, upon cooling at low temperatures (<60°C), by re-polymerization and fmDA adduct formation, the material regains its mechanical strength, producing a self-withstanding structure. Moreover, introducing cross-links between printed layers

can mitigate anisotropy within printed parts. The self-healing efficiency was evaluated via tensile tests on dogbones prepared in the Z-print direction. After the dogbone failure, the two surfaces were first heated at 120°C for 5 s and then stuck together. After curing at 65°C for 15 min, tensile tests were carried out to assess the recovery in ultimate strength. These tests showed that the MA-PLA-100 sample was able to recover 77% of its ultimate strength (figure 3.3) [109].

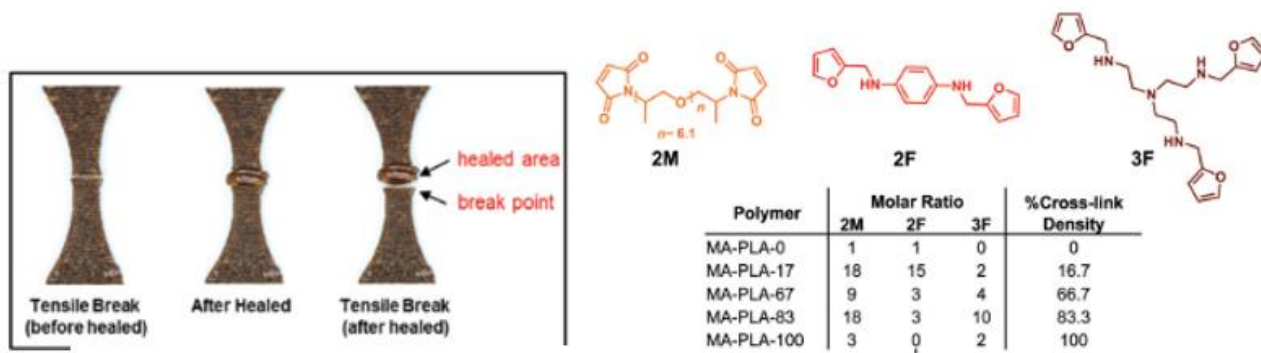


Figure 3-9 - Left: Breakage and healing of a 3d-printed dogbone; Right: mending agents used with a different number of functional moieties [109].

The same principle was followed by Yang and coworkers, who developed three new fmDA cross-linked polymers printable with the FFF method. The monomers utilized in this study were: a bismaleimide (2M), two trifunctional furan monomers (ICN3F and 3F), and a tetra-functional furan monomer (4F). DMA analysis revealed that the moduli dramatically dropped when the temperature reached 80°C due to retroDA reactions, exhibiting thermoplastic behavior (figure 3.10). This statement was also confirmed by the endothermic transition starting around 90°C showed in differential scanning calorimetry (DSC) measurements. By contrast, thermoset behavior was showed by polymers at room temperature because both molded and printed samples swelled during the solvent test. In addition, printed parts showed low values of surface roughness ranging from 23 μm to 36 μm .

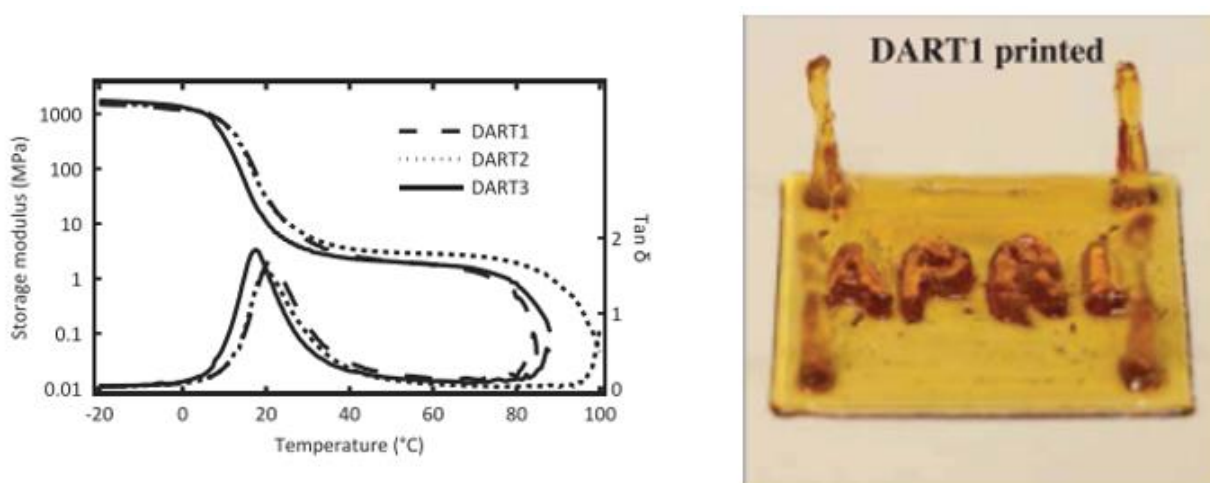


Figure 3-10 - DMA curves of the three tested inks; Right: Printed structure with DART 1 [127].

The main result obtained with this study was the ability to print structure with no or low values of anisotropy, measured in toughness, within the printed part (0.6% and 4% anisotropic behavior for 45° and 90° respectively, both relative to 0°). The isotropy resulted from the improved layer adhesion enhanced by the Diels-Alder reactions, which occurs upon cooling, after the deposition, during the thickening and solidification of the printed part. However, although the high isotropy in printed components, those inks cannot be employed to print arbitrary 3D structures due to the slow formation of the fmDA adducts, which makes challenging to print tall structures or components with large overhanging parts without the aid of supports (figure 3.10) [127].

In a different approach, Wei et al. designed a printable hydrogel based on the oxidation of benzylamine (BA) catalyzed by horseradish peroxidase (HRP) to benzaldehyde by carrying out a monoamine oxidase B (MAO B) on the BA-functionalized polyethylene glycol (PEG-BA). The obtained aldehyde-functionalized moieties were then cross-linked with glycol chitosan (GC) or gelatine (collagen) via Schiff bonds, giving hydrogel the dynamic behavior. Time sweep tests revealed that gelation occurred after 1430 s, leading to an increase of the viscosity. Thus, 3D printing was performed when the hydrogel possessed shear thinning properties before the gelation occurs. Although only simple structures were printed (with the shape of letter T and J), cells can be mixed in the hydrogel retaining high viability after 48 h, resulting in potential applications in biocompatible and printable scaffolds. Self-healing was demonstrated by making a hole (diameter of 5 mm) into the printed part, which disappeared after 6 h thanks to the dynamic nature of the hydrogel. Self-healing was also observed when two discs are mended together for 12 h at room temperature (figure 3.11), obtaining a much higher value of G' after healing [128].

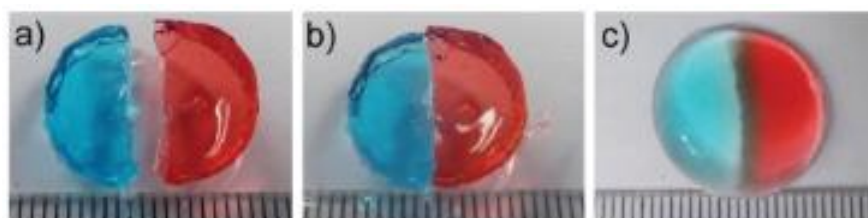


Figure 3-11 - Self-healing observed in merged discs [128].

Based on the same dynamic chemistry, Nadgorny's research group reported 3D printing of gels obtained from benzaldehyde functionalized poly (2-hydroxyethyl methacrylate) (PHEMA). A small functional diamine molecule, ethylenediamine (EDA), was used to form dynamic and reversible imine bonds reacting with aldehyde groups present in the polymer chains. In order to achieve an optimal 3D printing process, the amount of cross-link density in the gel and the polymer concentration have to be tuned to avoid the formation of a stiff gel or a spreadable gel (figure 3.12). An optimal formulation for extrusion-based 3D printing was achieved when using 6.5% PHEMA_{0.35}-co-P4FBA_{0.65} and maintaining the molar ratio of aldehyde unit to EDA at 1:0.08. The self-healing ability of the gel was evaluated with rheological tests. With the decrease in strain values, 97% of recovery of the moduli to initial values occurred immediately. Furthermore, the gel could also recover after prolonged exposures (2 min) to high strains (1000%). They stated that 98% of recovery was showed after 12 min. The gel could also withstand multiple healing cycles, even though the time required for self-healing

increased after each cycle. Besides, to further assess the self-healing ability in a macroscopic 3D printed object, a star-shaped structure was 3D printed and cross-linked with EDA. Mechanical damage induced with a scalpel self-healed autonomously at room temperature after 30 min (figure 3.12). Finally, they showed the ability of this gel to form self-rolling objects [129].

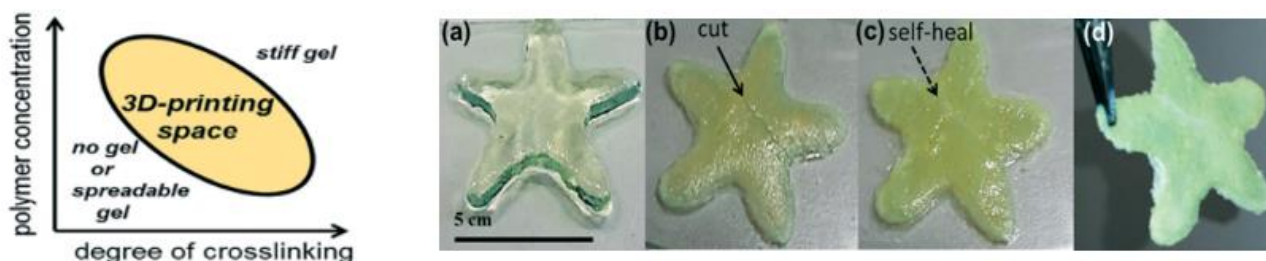


Figure 3-12 - Left: Influence of the polymer concentration and degree of crosslinks on the printability of the gel; Right: star-shaped 3D-printed structure used to test the healing ability [129].

Later, the same research group developed a doubly dynamic self-healing network using poly(*n*-hydroxyethyl acrylamide-co-methyl vinyl ketone) (PHEAA-co-PMVK) to fabricate microporous 3D-printed objects. The double dynamic behavior of the gel derived first from the formation of dynamic and reversible oxime bonds between ketone groups and bifunctional hydroxylamine cross-linkers. Second, the amide and the hydroxyl groups of HEAA units can form hydrogen bonds, which enabled physical cross-links during a post-printing reinforcement technique, namely thermally induced phase separation (TIPS). The printing process was conducted at 80°C using a stainless-steel cartridge to enhance the gel flowability, thus requiring lower shear stress values than room temperature 3D printing. The macroscopic self-healing ability was demonstrated by inducing a scalpel cut into a printed part. After 3 h at room temperature with no external additives and the gels were able to support themselves under gravity, self-recovery was observed. Moreover, it was shown how the TIPS treatment, involving subsequent freeze-thaw cycles, was an efficient method to increase the gel strength after printing. After TIPS was performed, the gel became too stiff to be printable. More important, the rheological characterization of the cryogel indicated that the self-healing properties of the gel were not affected by TIPS [130].

Wang et al. explored self-healing in hydrogels based on hydrazone dynamic chemistry applied to hydroxyapatite (HA) for applications as bioink. Hydrazone bonds were induced by mixing two synthesized macromers: HA modified with hydrazides (HA-HYD) and HA modified with aldehydes (HA-ALD). Oscillatory rheometry revealed the shear-thinning behavior of the hydrogel, demonstrating its ability to be extruded through a syringe. The self-healing ability of this system was assessed by forming cylindrical discs. Upon cutting the disc in half, self-healing was observed after 10 min and the two parts cannot be separated manually. Furthermore, the healing efficiency was calculated by the ratio between the failure stress of hydrogel discs after cutting in half and re-healing for 30 min and virgin hydrogel discs. The best result was obtained with 1.5 wt% of macromer concentration achieving almost 100% of repair. Higher concentrations (3 wt% and 5%) were also tested, resulting in lower healing efficiency values (around 50%). They hypothesized that 1.5

wt% possessed lower cross-link density, thus fewer bonds have to be reformed after breaking. Moreover, the hydrolytic nature of the hydrazone bond breakage may facilitate bond rearrangements, hindered by dense entanglements in the network present with higher macromer concentration. Finally, the influence of the 3D printing process on cell viability was evaluated, showing around 90% of viability, achieved using the 1.5 wt% hydrogels with the largest needle (18 G), suggesting the potential for future applications in fabricating 3D scaffolds. Additional long-term stability could be conferred to the hydrogel by introducing norbornene-functionalized HA and the cross-linker (pentaerythritol tetramercaptoacetate (PETMA)) within the HA-HYD/HA/ALD hydrogel. By exploiting UV light-activated thiol-ene click reactions, a secondary network is formed within the hydrogel, increasing the mechanical properties and adding heterogeneity to 3D-printed architectures [131].

Kim et al. designed a bio-printable hydrogel prepared from partially oxidized hyaluronate (OHA) and glycol chitosan (GC) in the presence of adipic acid dihydrazide (ADH). The self-healing ability was attributed to the double dynamic behavior of the hydrogel, including imine bonds obtained via Schiff base reaction between OHA and GC and acylhydrazone bonds deriving from the reaction between OHA and ADH. The degree of oxidation induced in the HA and the amount of GC and ADH added to the system impacted the practical application of the gel in 3D bioprinting. A high degree of oxidation led to the formation of gels with high mechanical stiffness, but gelation was almost instantaneous. The addition of ADH resulted in a decreased

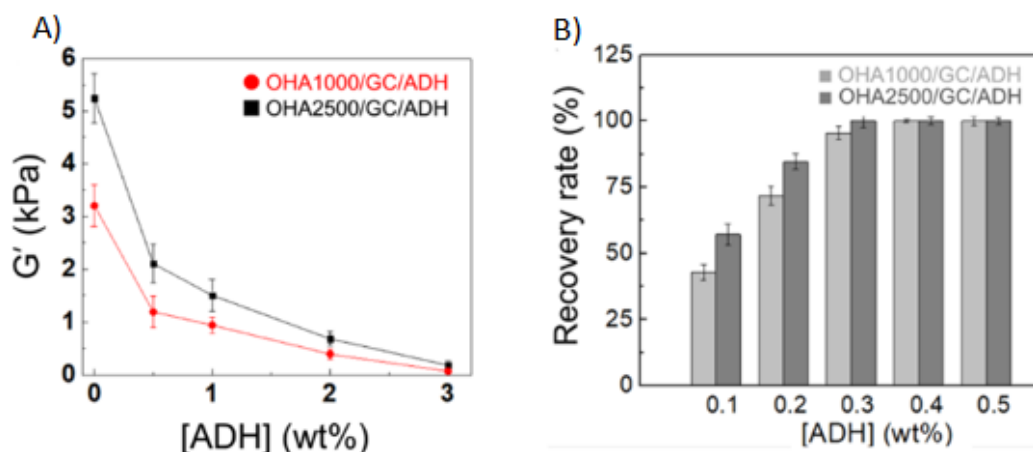


Figure 3-13 - Effect of the increase in ADH content in the two types of gels differing by the molecular weight of OHA, 1000, and 2500 kDa, respectively. A) Mechanical stiffness; B) Recovery rate [132].

mechanical stiffness because the hydrazone bonds do not participate in the formation of the proper cross-linked structure (figure 3.13A). In the study, 34% of oxidation was induced in the HA, and 0.3 wt% of ADH was added to the gel. Extrusion-based 3D printing of objects with different shapes was performed without requiring any post-gelation or additional cross-linking process (figure 3.14). The self-healing ability of the hydrogel was evaluated by cutting hydrogel discs in two pieces with a razor blade. The two pieces were then placed back in contact, and autonomous and complete integration was observed in less than 10 min. Interestingly, the recovery rate in the hydrogel stiffness increased with the ADH content (figure 3.13B) [132].

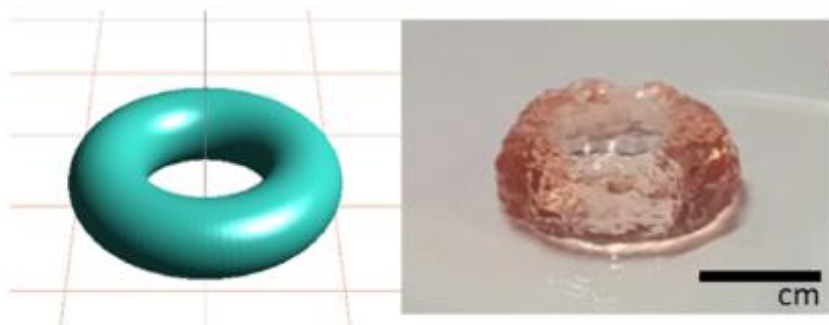


Figure 3-14 - Example of a 3D-printed donut-shaped part [132].

Another extrudable self-healing hydrogel was designed by Kabb and coworkers based on the photoreversible behavior ([2+2] cycloaddition reactions) of coumarin derivatives. They synthesized the hydrogel by direct copolymerization of coumarin containing monomers (7-acryloyloxyethoxy)-4-methylcoumarin (CoumAc), and 7-(2-acrylamidoethoxy)-4-methylcoumarin (CoumAAm)) with a hydrophilic comonomer (N,N-dimethylacrylamide (DMA)) to form water-soluble copolymers with coumarin pendent units. They printed very sophisticated hollow structures such as tubes or spheres by printing and curing the degradable coumarin-based copolymer core inside a non-degradable polymer shell (poly-vinyl alcohol (PVA)) (figure 3.15). Upon photoinduced de-cross-linking and removal of the interior gel, the hollow PVA tube was formed [133].

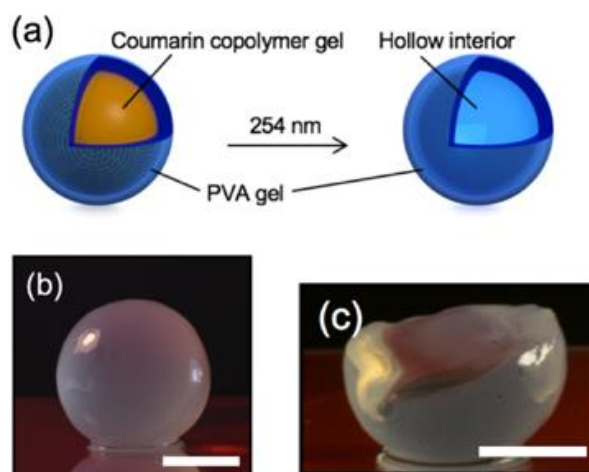


Figure 3-15 - a) Schematic representation of the process for the formation of a hollow semi-sphere. b) and c) show the correlated photos obtained by 3D-printing and the followed photo-induced decross-linking of the coumarin gel [133].

3.2.1.3. 3D-printed inks involving supramolecular interactions

Application of shear forces to induce the disruption of reversible bonds, enabling extrusion-based 3D printing, can also be exploited in self-healing hydrogels based on supramolecular interactions instead of the previously described dynamic covalent bond-based hydrogels. Higley et al. reported 3D printing by direct writing of a hydrogel based on guest-host interactions as reversible cross-links. The supramolecular hydrogels used were based on hyaluronic acid (HA), which was modified with either adamantane (Ad) or β -cyclodextrin (β -CD). The supramolecular hydrogel was formed as soon as Ad-HA and CD-HA were mixed. With a larger amount

of modification in the HA repeated units, the same ink was suitable to print the support structure, which accommodated the extruded material avoiding the collapse of the printed part. For the support gel, 40% of the repeated HA units were modified by Ad and CD, respectively, and then mixed with the ratio 1:1 and a total concentration of 4 wt/v%. Instead, the extruded ink had a 25% modification of the repeated HA units with the same mixing ratio and a total concentration of 5 wt/v%. Thanks to the presence of the support matrix, and not air around the extruded material, continuous 3D printing in any direction was possible. Although supramolecular interactions gave the material shear thinning, shear yielding, and self-healing properties, their weak nature may be an issue for long-term stability applications. To accomplish this problem, 20% of repeat units of HA were functionalized with methacrylates, which formed covalent crosslinking upon UV irradiation [134]. This dual-cross-linking system was later studied by Ouyang et al., evaluating the rheological behavior of the ink and the stability of 3D-printed structures [135].

Later, Song and coworkers demonstrated the possibility to 3D print complex microchannels within a hydrogel using the same chemistry of the previously described supramolecular hydrogels. The shear-thinning and self-healing properties of such hydrogels allowed the printing of the ink within the support hydrogel. Then, for the support gel, Ad-HA was modified with 20% of norbornene (Nor) to permit covalent crosslinking with di-thiol cross-linkers via thiol-ene click reactions resulting in increased stability. Therefore, the 3D printed material can be washed away from the support hydrogel to retain microchannels [136].

More recently, Wang et al. proposed a new self-healing biocompatible hydrogel based on a novel host-guest supramolecule (HGSM) obtained from the inclusion reaction between isocyanatoethyl acrylate-modified β -cyclodextrin (β -CD-AOI2) and acryloylated tetra-ethylene glycol-modified adamantane (A-TEG-Ad) (figure 3.16). HGSMs were then used as multifunctional cross-linkers to cross-link gelatin methacryloyl (GelMa), providing the covalent network to the hydrogel. The hydrogel printability was demonstrated by rheological analysis that revealed the shear-thinning behavior of the hydrogel. In order to reach a sufficient strength of the extruded filament, the temperature of the printing ink was lowered down to 24°C. Self-healing of the hydrogel was possible because of the presence of guest-host interactions. To assess the healing process, a sample of the gel was cut into two halves, and then the two halves were placed back in contact together. After keeping them in close contact for 1 h, the gel could withstand a force applied by tweezers. Finally, the self-healing behavior of the hydrogel could be demonstrated even by a continuous cyclic deformation of oscillatory strain between 1000% and 0.5% at a constant frequency of 10 rad s⁻¹. The gel was capable to show liquid-like behavior at higher shear strain, whereas at low shear strain, the gel recovered nearly immediately its solid-like behavior through the reformation of host-guest interactions [137]. Still exploiting guest-host interactions, Shim's research group was the first that studied the 3D printing of multi-layered construct comprising two different extracellular matrix (ECM) materials (atelocollagen and hyaluronic acid), which may be effectively used for applications in the regeneration of heterogeneous tissues and osteochondral tissues. The printable and cytocompatible hydrogel was successfully obtained by simply mixing monofunctionalized CB [6]-conjugated HA with 1,6-diaminohexane (DAH)-conjugated HA, forming host-guest interactions. The multi-layered

structure consisted of mono CB[6]/DAH-HA and pepsin-treated collagen (atelocollagen) with human turbinate-derived mesenchymal stromal cells (hTMSCs) [138].

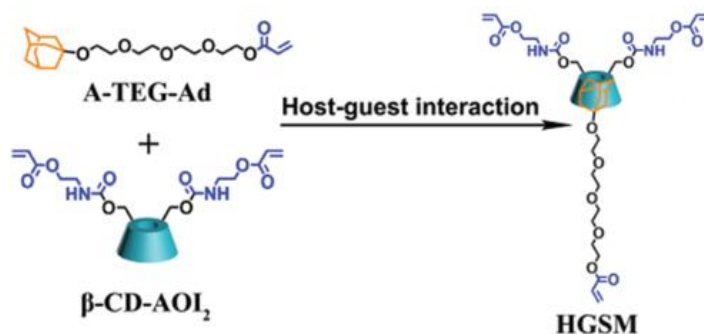


Figure 3-16 - Schematic representation of the HGSM synthesis [137].

Wang et al. designed mechanically strong supramolecular hydrogels synthesized by copolymerizing N-acryloyl glycinamide (NAGA) and 1-vinyl-1,2,4-triazole (VTZ) without adding any chemical cross-linker. The reversible nature of the hydrogel is derived from the dual amide inside the chain of NAGA, which form stable multiple hydrogen bonds. Dynamic temperature sweep rheological tests showed a decrease in G' and an increase of G'' , which intersect at the crossover point at 82°C triggering the thermoreversible gel-sol transition. This demonstrated the ability of the hydrogel to be processed by extrusion-based 3D printing techniques. To assess the healing ability of the hydrogel, a cylindrical part was cut into two parts. Then, the two freshly surfaces were brought into contact within a plastic syringe under a little pressure. After the syringe immersion in water at 55°C for 45 min, the gel self-healed completely. By measuring the tensile strength of the pristine hydrogel and the healed hydrogel, a healing efficiency of 90% was achieved. They attributed the great self-healing ability to the dissociation/reassociation of hydrogen bonds at the cut surfaces [139]. The NAGA monomer was also copolymerized with hydrophilic 2-acrylamide-2-methylpropanesulfonic acid (AMPS) to form 3D printable conductive self-healing hydrogels (the conductive behavior was obtained with the addition of an aqueous dispersion of poly (3,4-ethylenedioxythiophene)-poly (styrenesulfonate) (PEDOT/PSS)) (figure 3.17). By following the same self-healing test and raising the water bath temperature to 90°C for 3 h, the observed healing efficiency was 85% [140].



Figure 3-17 - 3D -printed patterns of T, J, U with PNGA-PAMPS/PEDOT/PSS [140].

Recently, Zhang and coworkers came up with a novel strategy to form self-healing bioinks capable of being extruded. The hydrogel was produced by photopolymerization of chitosan methacrylate (CHMA) and polyvinyl alcohol (PVA). The hydrogel did not flow and was not suitable for 3D printing, being chemically cross-linked. Therefore, the hydrogels were divided into microparticles with an average size of 197 μm . Such particles could associate and form the hydrogels establishing hydrogen bonds between chitosan and PVA chains. The microparticles gel showed the common gel-fluid transition under the application of shear and self-healing, proving the possibility of applying the gel in extrusion-based 3D printing. Moreover, multiple cycles of high and low strain can be performed many times without impacting the hydrogel modulus. Interestingly, the concentration of CHMA was found to be critical for both viscosity of the system during printing and the printing fidelity. With increasing CHMA concentration, the number of hydrogen bonds, thus the adhesion forces between particles increased, leading to higher viscosity and fidelity of 3D printed hydrogels. The authors showed the possibility to produce precise tubular structures without using any support or post-printing treatments. Moreover, their printed scaffolds remained stable in shape and dimension for months at room temperature. Finally, they reported more complex 3D printed structures like a rat tight bone and a human ear, printed with high shape fidelity (figure 3.18) [141].

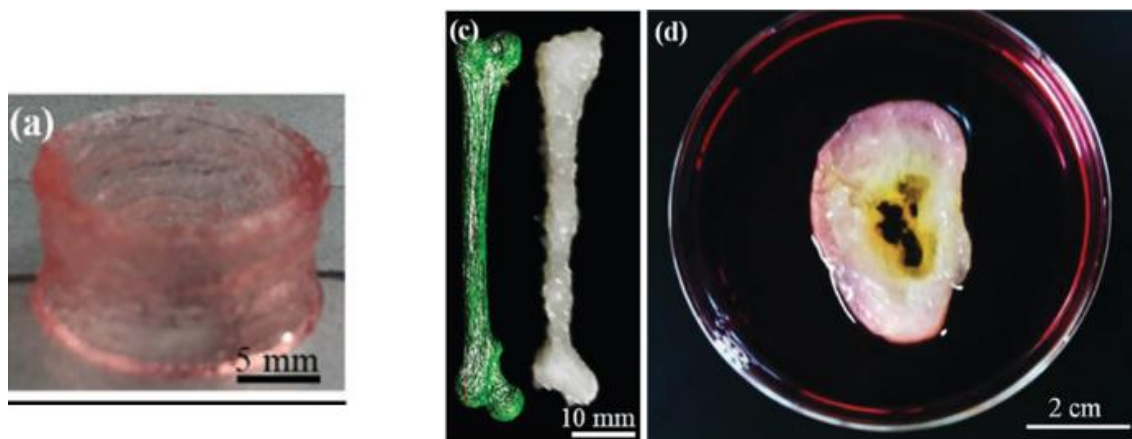


Figure 3-18 - Complex biomimetic structures 3D printed with microparticle-based bioinks. a) cylinder with 35 layers, c) rat tight bone, and d) human ear model [141].

Zhu et al. exploited electrostatic forces to achieve extrusion-based 3D printing of tough hydrogels into complex structures. Polyion complex (PIC) were obtained by precipitation from mixed poly(3-(methacryloylamino)-propyl-trimethylammonium chloride) and poly(sodium p-styrenesulfonate) (PMPTC and PNaSS). The precipitate was then plasticized in saline water to form printable inks. This raw material could be extruded out of a nozzle into a deionized water bath. The viscous PIC solution rapidly gelled by dialyzing out the salt and counterions of PIC, generating a tough solid gel. Although 3D printing could be performed at room temperature, the temperature used was 60°C in order to minimize the gel viscosity, thus lowering the extrusion pressure required. The strength of the interfacial bonding between layers was measured by tensile tests, showing values of breaking strain very close to that of a printed single fiber. This result showed the strong interfacial bonding between connected layers, which led to good mechanical properties of the printed

components [142]. Still exploiting the formation of PIC, 3D printing of alginate-based inks resulted in high printing fidelity, which was very difficult to guarantee in the previous systems because of the low viscosity of the ink. With this aim, Liu and coworkers added chitosan particles into the alginate solution. Upon treatment with a hydrochloric acid solution, chitosan particles reacted with alginate to form the final tough three-dimensional structure (AlCh PIC). In order to demonstrate the ability of the ink to print complex structures, they printed a nose model with Al1Ch1.2 (1:1.2 mol/mol) printing ink, which resulted in high printing fidelity without collapsing (figure 3.119) [143].

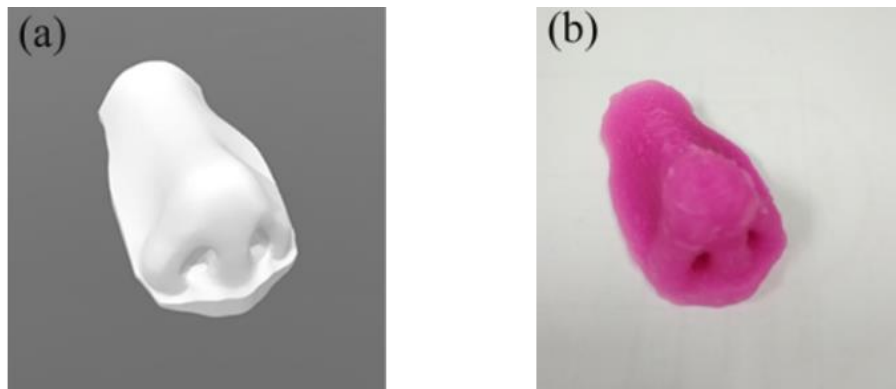


Figure 3-19 – a) 3D model of the nose, b) 3D printed nose prepared with 3D printing ink Al1Ch1.2 [143].

Chang et al. designed hydrogels from natural egg white with excellent stretchability, direct-writing 3D printability, and self-healing properties. The protein chains were denatured upon NaOH addition, leading to the formation of reversible interactions between chains, such as electrostatic interactions, hydrogen bonding, and hydrophobic interactions. Electrostatic repulsions were necessary to process by decreasing the viscosity of the ink through extrusion printing, whereas hydrogen bonding resulted in the formation of the three-dimensional network upon gelation. The shear-thinning and self-healing behavior of the gel enabled 3D printing. For example, they printed a multilayer cube (15mm x 15 mm), which did not collapse under its weight, showing good self-supporting ability. The self-healing performances of the gel were evaluated by rheological tests and macroscopic tests. After the hydrogel was cut into two parts and then brought together, they spontaneously merged without the application of any external stimulus. Finally, the strength of the resultant hydrogel could be further increased by inducing a secondary crosslinking with cations [144].

Liu and coworkers fabricated a double-network hydrogel based on an ionically cross-linked k-carrageenan network combined with a covalently cross-linked polyacrylamide (PAAm). However, the self-healing behavior was observed only when the hydrogel was heated above the gel-sol transition for the temperature-activated dissociation of the double helices of k-carrageenan. Then, upon cooling, the reassociation of the double helices takes place, enabling the ionic gelation to occur. Self-healing performance was assessed by cutting a cylinder sample into eight parts. Later, the cut surfaces were brought in contact and sealed into a polyethylene bag and then immersed for 20 min in a hot water bath (90°C). Upon cooling, the samples showed a well self-healing (figure 3.20). Furthermore, due to the conductive nature of the gel, self-healing was also tested by measuring the conductivity of the virgin gel and the conductivity of the healed gel, resulting in 99.2%

self-healing efficiency. The k-carrageenan/AAm gel could be printed into multiple shapes, such as a mesh patten with five layers, a hollow cube and a hollow triangular prism, a cone, and a dumbbell shape.

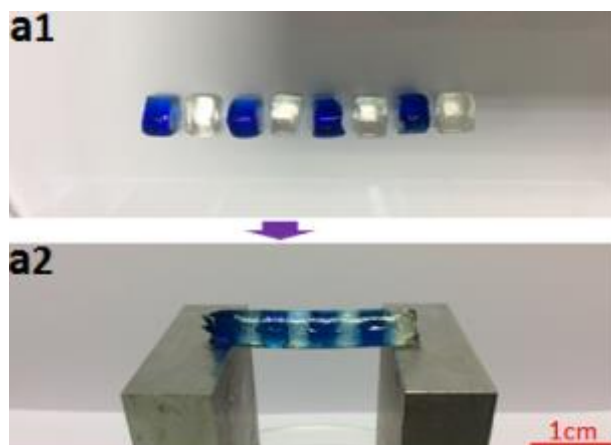


Figure 3-20 - Self-healing test conducted on k-carrageenan/AAm gel, showing that the gel can withstand its weight after healing [145].

The successful printing of the hollow parts showed that the gel could be printed with relatively high strength and self-supporting properties. The mechanical properties of the gel could be further enhanced by the addition of a physical cross-linker (KCl) or chemical cross-linker (N,N'-methylene bisacrylamide (MBA)) [145]. In another approach, Wilson et al. proposed the incorporation of nanosilicates (nSi) within k-carrageenan hydrogel to achieve high fidelity in printed objects. The introduction of nanoparticles into the hydrogel induced physical interaction (hydrogen bonds) between them, enhancing the mechanical properties of the polymeric network. This is important in bioprinting, where the deposition of bioinks is requested only in a specific area, and consequently, the filament can be quickly extruded or held at rest. Furthermore, the addition of nSi to the hydrogel decreased the gelation point, enabling printing the k-carrageenan gel. To demonstrate the effective printability of the gel, structures with large overhangs and multiple layers were printed. They revealed high shape-retention, even when many successive layers were deposited (around 30 layers) [146]. Moreover, Shi and coworkers designed an ink based on ionic interactions deriving from the interactions between Ca^{2+} ions and bisphosphonate ligands attached to the macromolecular backbone of hyaluronic acid (HA). However, this ink (HA-BP/ Ca^{2+}) showed low mechanical properties, which prevented the 3D printing of real 3D objects. To overcome this issue, as previously described for many other inks, acrylamide (Am) groups were introduced as a modification within the HA chains to induce a secondary cross-linked network within the final construct. Interestingly, this gel was tested with the “free-form reversible embedding of suspended hydrogels” (FRESH) 3D printing method. A tube-like structure with Am-HA-BP/ Ca^{2+} gel was printed into an HA-BP/ Ca^{2+} support bath. After exposure to UV light, the separation of the object from the support gel was possible by inducing cleavage of the reversible ionic interactions present in the hydrogel upon immersion in an acidic solution pH = 5.0 PBS for 1 h [147].

A different approach involved a dual ionic cross-linking between the carboxyls present on both the sodium alginate (SA) molecules and poly(acrylamide-co-acrylic acid) (P(AAm-co-AAc) chains with iron ions,

forming a sodium alginate/poly(acrylamide-co-acrylic acid)/Fe³⁺ double network hydrogel. Mechanical tests showed good mechanical properties of the gel with 3.24 MPa tensile strength and 1228% strain. Self-healing was observed in the hydrogel after the cyclic loading test with the maximum strain of $\lambda_{\max} = 6$, showing 40% and 64% recovery after 15 min and 4 h, respectively. Furthermore, the healing process could be triggered by pH changes, inducing dissociation in acidic conditions, and association at pH 12-14. This hydrogel responsiveness to pH was exploited to produce a soft printable hydrogel at pH 1 [148]. Alginate-based hydrogels were also used together with poly(ethylene glycol) (PEG) to form an interpenetrating network. The resultant hydrogel with covalently cross-linked PEG and ionically cross-linked alginate (with Ca²⁺ ions) could recover partially and readily the mechanical properties after being stretched, thanks to the chemical cross-linked network. Further recovery was stated after leaving samples at 37°C for 24 h, resulting in the restoration of the reversible ionic interactions. The hydrogel printability was achieved by introducing nanoclay particles, which physically cross-linked both with themselves and with PEG and alginate polymer networks to increase the system viscosity (figure 3.21) [149].



Figure 3-21 - 3D- Printed structures with alginate-PEG-nanoclay hydrogels (hollow cube, hemisphere, pyramid, twisted bundle, the shape of an ear, and a nose) [149].

Zheng et al. reported another type of tough physical hydrogel obtained by swelling a cast film of poly(acrylamide-co-acrylic acid) (P(AAm-co-AAc)) in FeCl₃ aqueous solution. Supramolecular interactions were formed between carboxyl groups coordination with Fe³⁺ ions, giving the material a combination of self-recovery, stimuli-triggered healing, and shape memories properties. As previously described, the pH-mediated stability of such hydrogels resulted in reversible sol-gel transition, which enabled the use of hydrogels in extrusion-based 3D printing. The printability of the gel was also influenced by the amount of copolymer dissolved within the ferric solution, as well as the concentration of Fe³⁺ ions. Decreasing the concentration of both of them resulted in weak hydrogels that collapsed after 3D printing because of insufficient ionic interactions. Moreover, the fracture gels can be healed only under precise conditions. The two cut surfaces were softened and thus activated in acidic conditions, followed by re-swelling in FeCl₃ solution and water to regain almost the initial mechanical properties [150]. Hydrogels based on ionic interactions between carboxylic groups of PAA and ferric ions found large applications in extrusion-based 3D printing of artificial skin devices [151] [152]. Finally, 3D printing inks based on ionic interactions were also formed by weak but abundant thermally reversible cross-links between carboxylates groups present within a poly(dimethylsiloxane) (PDMS)

polymer backbone with Zn (II). The reversible nature of the coordination was activated at 120°C inducing the dissociation of carboxylates-Zn (II) bonds, showing shear-thinning and self-healing properties. Precisely, almost 100% self-healing efficiency was observed after keeping the two cut surfaces in contact for 4 h at 80°C. Upon cooling, the system could be printed in rigid, self-supporting parts, with high fidelity (figure 3.22) [153].



Figure 3-22 - Irregular object obtained by 3D printing with PDMS/Zn inks, followed by healing [153].

Kuang et al. used direct ink writing (DIW) approach to print semi-interpenetrating polymer network (IPN) elastomer composites composed of a photocurable resin, made of aliphatic urethane diacrylate (AUD) and n-butyl acrylate (BA), containing semi-crystalline poly(caprolactone) (PCL), which acted as the thermoplastic component. In addition, fumed silica nanoparticles (4 wt%) were added to the system to increase the viscosity, imparting the shear-thinning effect to the uncured ink. The polymer could be easily extruded, increasing the temperature of the syringe at 70°C. The followed UV-assisted crosslinking enabled printing a large variety of 3D architectures, such as Archimedean spiral, honeycomb, hollow vase, and Gumby toy (figure 3.23).

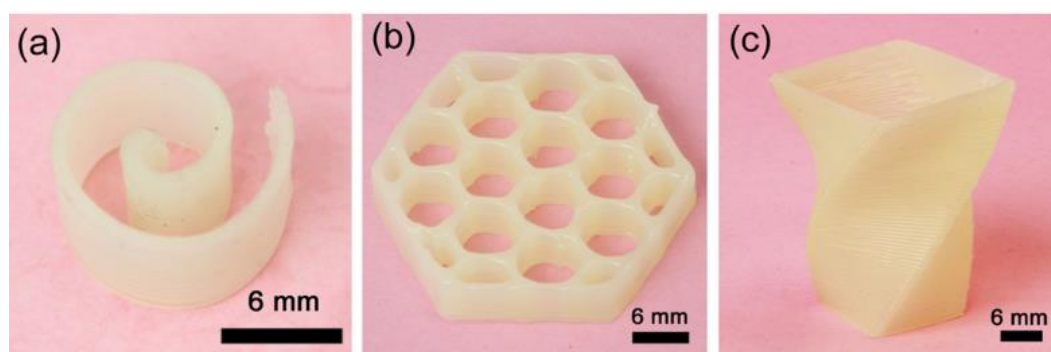


Figure 3-23 - 3D printed structures obtained via direct ink writing with semi-IPN elastomer composites based on urethane and PCL. a) An Archimedean spiral, b) a honeycomb, and c) a hollow vase [154].

The post-printing curing process induced an excellent inter-filament adhesion, resulting in a high degree of isotropy in the final object. Moreover, shape memory effect and self-healing could be achieved with these elastomers. Self-healing of an induced scratch on the surface was observed after treating the sample in an oven at 80°C for 20 min, activating diffusion and entanglements formation between PCL chains at the broken interface. Besides the analysis of self-healing at the surface, healing was also performed with a notched strip. However, the healing efficiency, evaluated from the fracture strain, was relatively low, 30% [154]. Thermoplastic PCL was also blended with thermoplastic poly(urethane) to develop multifunctional magnetorheological plastomer with 3D printability, shape memory, and self-healing ability [155].

3.2.2. Inks printed via vat photopolymerization 3D printing

3.2.2.1. Extrinsic self-healing (capsule)

Wallin et al. used thiol-ene click chemistry with the resin composed of a blend of poly(mercaptopropyl)methylsiloxane-co-dimethylsiloxane (M.S.: Mw B 6000–8000) and bifunctional vinyl terminated PDMS (V.S.) to achieve 3D printing of soft robots. When dealing with stereolithography techniques, it is challenging to detach printed parts from the bottom of the transparent vat, typically made of siloxane-based polymer. Thus, to achieve a successful separation step, a high transparency poly-4-methylpentene-1 (PMP) build window was used. In addition, the molecular weight of the M.S. was in the range 6000-8000, enabling the resin to flow perfectly onto the building platform. Compared to the common photopolymerized acrylate-based resin, in this system, gelation was achieved at a much lower light dose, enabling a more rapid build speed. This system was adopted to print fluidic elastomer actuators successfully. Moreover, self-healing of the reticulated resin was possible thanks to the embedded capsules containing unreacted low viscosity prepolymer resin. Upon capsule breakage, the system rapidly provided newly exposed thiol-ene fluid which could polymerize within 30 s under ambient sunlight (figure 3.24) [156].

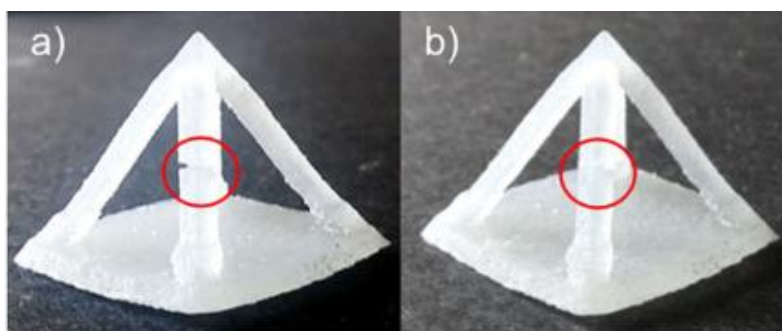


Figure 3-24 - 3D printed sample containing 5 wt% anisole with PMMA capsules. a) Crack is generated, b) and allowed to heal for 72 h at RT [157].

Other researchers combined stereolithography with a UV-curable resin embedded with anisole/PMMA containing PUF microcapsules. The self-healing system was based on the solvent welding mechanism. Upon damage and capsules rupture, the solvent is released, promoting polymer diffusion and entanglement formation across cracks. The system self-healing ability was investigated with mode I fracture testing, achieving a maximum healing efficiency of 87% after 72 h at room temperature, at a capsule concentration of 10 wt% (figure 3.18). Moreover, the effect of microcapsule presence within the resin did not impact the print quality due to light scattering by capsules [157].

3.2.2.2. 3D printed inks involving dynamic covalent chemistry

As previously mentioned, inks relying on intrinsic self-healing are more suited to be processed with 3D printing techniques due to the absence of external particles within the material. Li et al. developed a self-healing polyurethane elastomer fabricated through DLP 3D printing. The polyurethane chains were modified with both acrylate and disulfide functional units to get a photopolymerizable and self-healable resin. The elastomer self-

healing efficiency, attributed solely to the metathesis of disulfide bonds, was assessed via tensile tests. Three cycles of breakage and healing into an oven at 80°C for 12 h were performed, revealing self-healing efficiency of 95%, 87%, and 60%, respectively. The decrease of the healing efficiency was attributed to the defects present onto the surfaces, which did not afford a perfect connection between the two broken parts. However, this system allowed printing complex structures with high shape-retention, such as a honeycomb, a hollow cube, a Maya Pyramid, and a circular cone [158]. Similar chemistry was recently adopted by the same group to build structures capable of autonomous self-healing due to the shape memory effect, which permits the alignment of the two broken surfaces without manual contact with the material [159].

Instead of exploiting acrylate groups, Yu and coworkers reported a strategy for photopolymerization-based 3D printing relying on a photo-elastomer ink with both thiol and disulfide groups ([4–6% (mercaptopropyl)methylsiloxane]-dimethylsiloxane copolymer (MMDS) and vinyl-terminated polydimethylsiloxane (V-PDMS)). The former was responsible for the thiol-ene photopolymerization, and the latter enabled a disulfide methatesis reaction, thus self-healing. When dealing with the thiol-ene photopolymerization, the adhesion between the printed part and the window cannot be quenched by oxygen. Therefore, a PTFE membrane with a low surface tension was used. To evaluate the self-healing performance of 3D printed parts, dogbone-shaped samples were produced and cut into two parts (figure 3.25). Self-healing efficiency was found to be 100% of the original strength after 60 min at 60°C. Furthermore, they stated that the healing efficiency remained in the range of 90-100% even after over 10 cycles. This system did not request any solvent as a plasticizer to induce healing, and it did not show water-sensitivity. Despite the many advantages, this elastomer displayed a low Young's modulus (17.4 kPa), which may limit its range of applications [160].

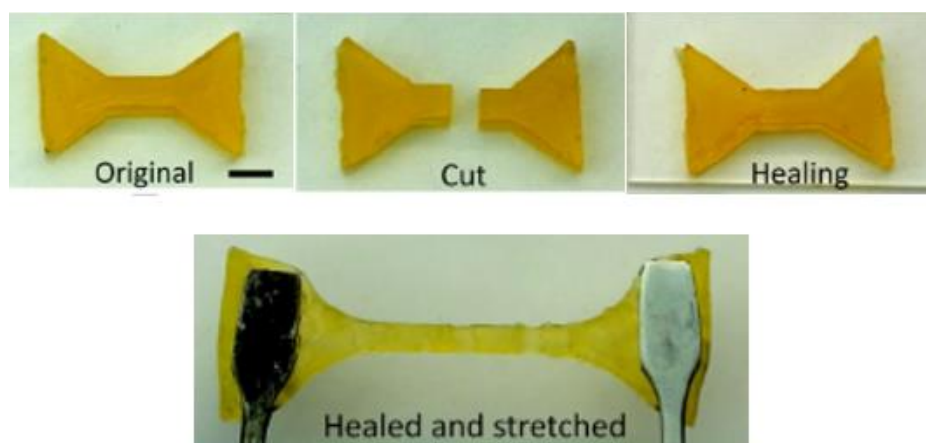


Figure 3-25 - Self-healing test with a dogbone elastomer sample [160].

Furthermore, the low mechanical properties also limited another self-healing thermosetting polymer based on a photocurable resin, obtained by mixing 2-hydroxy-3-phenoxypropyl acrylate as monomer and bisphenol A glycerolate (1 glycerol/phenol) diacrylate as cross-linker. Self-healing abilities of the polymer were attributed to the heat-triggered bond exchange reactions (BERs), which involved hydroxyl functional groups and adjacent

ester functional groups of the two damaged surfaces. The studied system achieved self-healing by deposition of virgin material into the damaged area, followed by healing at 180°C for few hours. This healing process resulted in 100% recovery of stiffness and 93% recovery of strength [161].

3.2.2.3. 3D printed inks involving supramolecular interactions

Invernizzi and coworkers designed a self-healing polymer with shape-memory behavior obtained by combining poly(caprolactone) dimethacrylate (PCLDMA) with methacrylates containing 2-ureido-4[1H]-pyrimidinone units (UPyMA) (4 wt%), which can be printed via DLP. Self-healing abilities were provided by the reversible formation of four hydrogen bonds between the two UPy moieties. Although a structure with ten layers was printed to show the ability to build 3D constructs with multiple levels, more complex 3D structures were not printed. Both surface and bulk self-healing performance were evaluated. An induced scratch and a sample cut in two parts showed perfect repair after 1 h at 80°C. The healing efficiency was calculated on tensile strength, and the value obtained was 54%. Besides, a higher degree of healing efficiency could be achieved with a longer healing time [162].

Light-direct 3D printing of double network hydrogels was demonstrated by Valentin et al. using UV light to cross-link poly (ethylene glycol) diacrylate (PEGDA) in the presence of dispersed high-molecular-weight poly (acrylic acid) (PAA). Additionally, the carboxyl units of the acrylic acid were used to form a reversible secondary network via ionic bonds with added Fe^{3+} ions. These established ionic interactions were reversed using EDTA to chelate Fe^{3+} , leading to carboxyl/ Fe^{3+} moieties dissociation. Self-healing was assessed by cutting a cylindrical specimen in half with a scalpel, and then both halves were brought back in contact into a solution of 0.1 M FeCl_3 in 1x PBS (figure 3.26). After 60 min, the structure was able to support itself against gravity. Furthermore, self-healing abilities were also tested using a three-point flexural test, conducted on both virgin hydrogel and healed hydrogel, that revealed that both samples' flexural modulus was ≈ 1 MPa. Although the material could not self-heal autonomously, without the addition of the ferritic solution in the broken zone, moderate cation concentration resulted in robust self-healing [163].

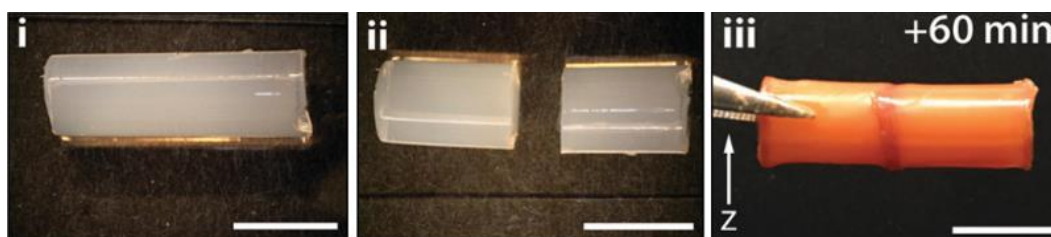


Figure 3-26 - PEGDA-PAA cylinder was used to assess the self-healing ability of the material after immersion in 0.1 M FeCl_3 in 1x PBS for 60 min [163].

Ionic interactions were also used by Liu's research group to design a self-healable, 3D printable silicone elastomer. Thiol-ene photopolymerization of a mixture of thiol-modified silicone oil (PDMS-SH), vinyl-terminated polysiloxane (PDMS-Vi), amino-modified silicone oil (PDMS-NH₂), carboxyl-modified silicone oil (PDMS-COOH) with ethyl (2,4,6-trimethylbenzoyl) phenylphosphinate as photoinitiator was adopted to

form the primary covalent cross-linked network. Additionally, a secondary reversible ionic cross-linked network was formed between the carboxyl and amino-functionalized polysiloxanes. The dynamic network could be destroyed at high temperatures ($\approx 120^{\circ}\text{C}$) and reversibly reformed when the temperature was lowered down, ensuring self-healing and reprocessing abilities of silicone elastomers. The self-healing performance of elastomers was analyzed by comparing the mechanical strength of the virgin and healed samples. Following the thermally-activated dissociation/reassociation of ionic cross-links, the highest self-healing ability of 98% on tensile strength was observed in samples containing 10% or more of ionic cross-links. Further analysis revealed the elastomer ability to maintain a high healing efficiency value even after triple healing cycles, with a recovery of 92% of the mechanical strength. However, the printed structures were not as complicated as in other studies, not allowing for complete analysis from this perspective [164].

Finally, Zhang and coworkers proposed a new ink printable with DLP, involving the incorporation of semi-crystalline poly(caprolactone) (PCL) acting as a self-healing agent within a photopolymerizable resin composed of benzyl methacrylate (BMA) and poly(ethylene glycol) dimethacrylate (PEGDMA) (figure 3.27). The printing solution was obtained by increasing the temperature above the melting temperature of the healing agent (about 60°C) to get a material with the ability to be spread onto the platform. As concerning the self-healing abilities, a broken 3D printed chess piece was repaired after keeping in contact the two separate surfaces for 5 min at 80°C . The self-healing process was driven by the diffusion, at temperatures above T_m of PCL, of PCL linear chains through the boundary between two separated surfaces. Upon cooling, the PCL chains formed crystalline domains, which connected the two damaged surfaces together. Self-healing efficiency was further evaluated with tensile tests on overlapped 3D printed strips, resulting in a recovery of almost 100% of the initial strength when the concentration of PCL was higher than 20 wt% [165].

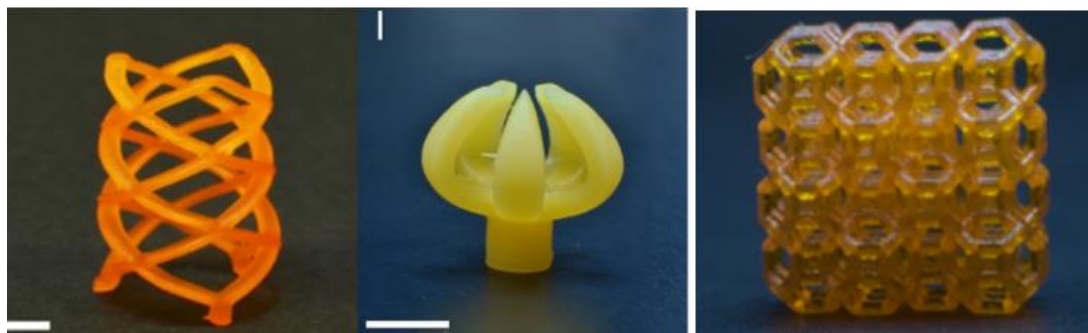


Figure 3-27 - 3D printed geometries using DLP-based 3D printing with the PCL-based solution. Structures of a) a gripper, b) a stent, and c) a foam [165].

At the end of this section, it might be interesting to compare the results of the two main 3D printing techniques so far explored to print components with self-healing abilities: material extrusion 3D printing and vat photopolymerization 3D printing. Overall, there is no quantitative comparison available on the complexity achievable by the different processes, but a visual comparison can still be performed. We can compare here images taken from different studies (figure 3.28, 3.29).

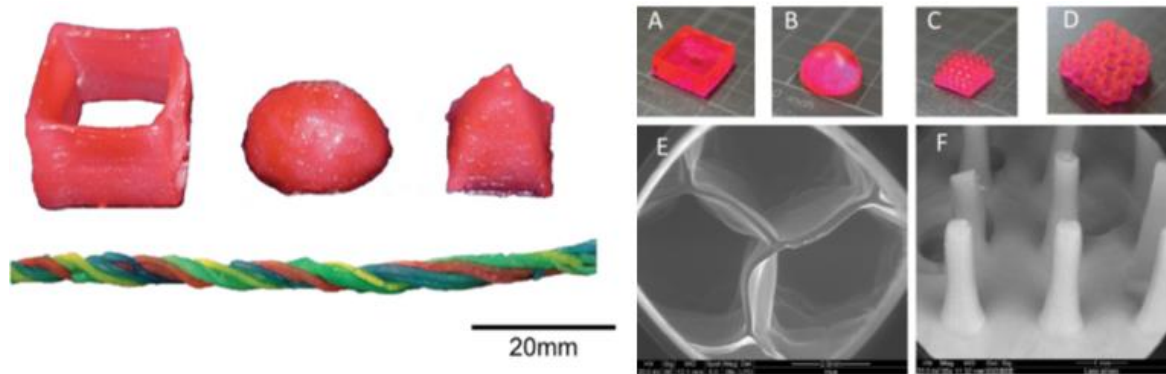


Figure 3-28 - Vertical structures with no overhanging features and cavities fabricated with extrusion printing (left) [149] and vat photopolymerization (right) [166].

As can be seen, vat photopolymerization (right image on both figures) allows achieving flat vertical surfaces with negligible distortion and great shape fidelity. Lattices, comprising overhanging features and through-holes, show clean and sharp edges that could easily approximate smooth rounded surfaces by decreasing the layer thickness. On the other hand, extrusion printing shows warped and slightly deformed planes due to the filament shape and behavior during extrusion.

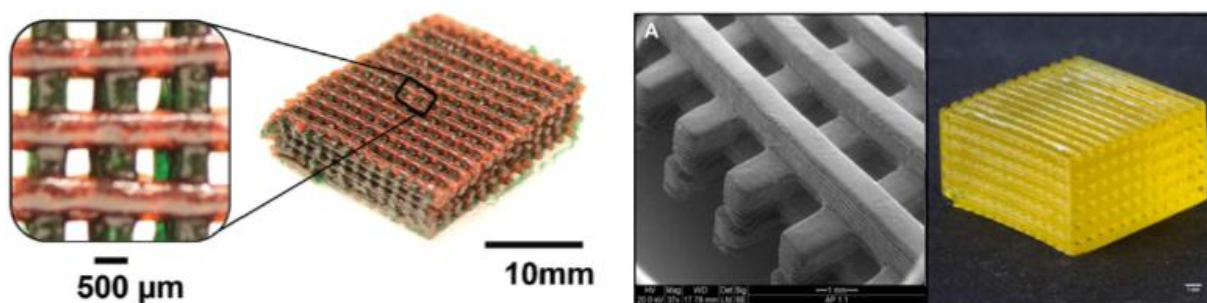


Figure 3-29 - Simple cubic lattices fabricated with extrusion printing (left) [149] and vat photopolymerization (right) [167].

Final remarks:

This chapter presented an overview of the different 3D printing techniques, remarking the main ink requirements for each method and the final results that can be achieved in terms of surface roughness, resolution, and fabrication speed. However, from the analysis of the different self-healable ink systems, it was possible to observe that the two main methods used so far to achieve 3D printing are extrusion-based 3D printing and stereolithography. Extrusion-based 3D printing has been so far more used thanks to the possibility to easily modify polymer chains with functionalities that allow the material to show the shear thinning behavior. By contrast, stereolithography-based 3D printing permits a more rapid process endowing in more precisely printed constructs. However, the major limitation of such systems is the availability of monomers with photopolymerizable acrylate or thiol-ene functionalities. Overall, almost all the self-healing chemistries have been exploited to produce self-healing ink, getting good results in terms of healing efficiency and printability. However, it is challenging to compare the different performances of inks due to the different geometries of final printed structures and different tests adopted to assess self-healing. Nevertheless, further research in this field is still ongoing, and it will most likely provide new strategies with higher performance for large-scale applications.

4. Experimental part

As previously mentioned in the introduction, the thorough investigation in the previous chapter on the different 3D printed systems showed that no hydrogels with self-healing ability had been printed via vat photopolymerization so far. Thus, the work presented in this thesis aimed to obtain a self-healing hydrogel printable via vat photopolymerization 3D printing, using a commercial DLP apparatus. DLP was selected because of its high fabrication speed and high precision achieved in the final constructs, characterized by complex geometries and smooth surfaces. In the following sections, there will be a description of the path followed to achieve a successful 3D printing of our self-healing hydrogel based on commercially available compounds such as polyvinyl alcohol (PVA), and photocurable species like acrylic acid (AAc), and poly (ethylene glycol) diacrylate (PEGDA).

4.1. Self-healing requirements vs. DLP requirements

The assessment of the feasibility of printing a self-supporting hydrogel with self-healing ability via DLP relies on the knowledge of the materials requirements to guarantee the self-healing behavior after processing the material via DLP.

Self-healing has been exhaustively discussed in the first chapter, and now we can summarize the key aspects. Two main approaches to achieve self-healing are available: via dynamic covalent bonds or non-covalent interactions. These two strategies are based on the same principle, forming reversible bonds (more or less strong) which can be broken and reformed. However, covalent reactions used in hydrogel self-healing often require the application of an external stimulus (e.g., pH, alternating current (AC), or UV light). By contrast, autonomous self-healing hydrogels are typically based on non-covalent interactions, used alone or even combined. Besides, the presence of moieties with sufficient mobility facilitate the interdiffusion between the two damaged surfaces leading to higher self-healing efficiencies. In particular, a loose network may enable enough chain mobility within the hydrogel, providing the damaged surfaces of many functionalities, resulting in a fast and successful healing process. Additionally, long chains can facilitate the repair by interdiffusion between the two separated surfaces through a bridging effect (figure 4.1) [7].

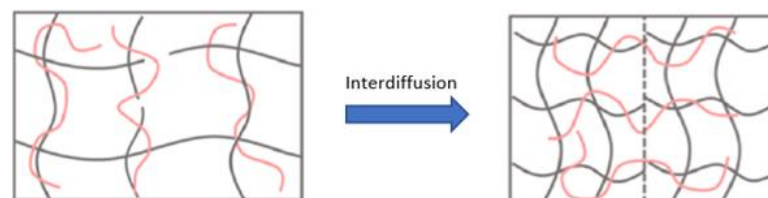


Figure 4-1 - Chains interdiffusion, enabling repair [168].

On the other hand, hydrogels processable via vat photopolymerization must fulfill completely different requirements. First, viscosities suitable for vat photopolymerization are in the range 0.25-10 Pa·s, since resins

must have a good spreading onto the building platform. Higher viscosity resins would require a longer time to re-coat and self-level, increasing the production time and eventually leading to defects due to absence of resin. All the polymers and monomers utilized require a photoactive functionality, such as acrylate/methacrylate, epoxides, or electron-deficient alkene for [2+2] cycloaddition (e.g., thiol-ene reactions). Multifunctional monomers (i.e. with a number of functional groups ≥ 2) are necessary to form a tight network through crosslinking. Crosslinking is necessary to obtain insoluble structures; furthermore, low crosslinking may lead to poor mechanical properties, and consequently, the material may not be able to self-support. Given the considerations above, the generated network would possess short network chains, limiting the interdiffusion between the damaged surfaces. In addition, the three-dimensional networks are based on non-reversible strong interactions such as covalent bonds. Thus, upon bond rupture, the system usually is not able to restore the initial network structure or at least fully or partially recover its initial properties [169].

A comparison of the requirements for obtaining efficient self-healing materials and 3D printable materials via vat polymerization is reported in Table 4.

Table 4 - Comparison between self-healing requirements and vat-photopolymerization requirements [7] [169].

Requirements for self-healing	Requirements for vat photopolymerization
Monofunctional monomers (higher mobility)	Multifunctional monomers (faster gelification)
Loose network	Tight network
Long network chains enabling interdiffusion	Short network chains limiting interdiffusion
Reversible interactions:	Strong interactions:
➤ Supramolecular interactions	➤ Covalent bonds
➤ Dynamic covalent bonds	➤ Dynamic covalent bonds
Autonomous restoration of bonds	Irreversible bond rupture

Therefore, to develop a self-healing hydrogel processable via vat photopolymerization (DLP), we needed to find a way to match these requirements in a unique material. This could be achieved by forming interpenetrating polymer networks (IPN), constituted by two or more interlaced networks with no covalent bonds between the two networks. One network can be exploited in the 3D printing process, endowing the formation of a covalently cross-linked hydrogel network, whereas the second network present within the 3D structure will be exploited to achieve the self-healing behavior, either via entanglement effect or via reversible bonds rupture and reformation [7]. In the next section, there will be a description of how we selected a determinate chemical structure for the covalent network and the reversible interaction, respectively.

4.2. Materials screening

To achieve good results in the final printed part, all the different chemical elements present in the formulation were deeply analyzed.

As previously mentioned, the 3D printed networks are usually dense covalently cross-linked networks; thus, it was necessary to introduce a second polymer with long chains, called the mending agent, into the cross-

linked matrix obtained via UV curing. By a screening action of literature, three possible candidates as mending agent were selected: Poly (acrylic acid) (PAAc), Poly (ethylene glycol) (PEG), and Poly (vinyl alcohol) (PVA), as they are water-soluble polymers available in various molecular weight. The PAAc was tested both as acid and as sodium salt, but it was discarded since it may show self-healing only in presence of Fe^{3+} ions to form metallo-supramolecular complexes. In fact, weak bonds among carboxyl acids alone were not strong enough to induce self-healing because the acid dissociates in presence of water, thus bearing a negative charge and inducing electrostatic repulsion. Furthermore, autonomous self-healing was not possible because repair occurred only upon soaking the cut surfaces in a solution containing Fe^{3+} ions, which act as crosslinking points between different AAc chains. At last, this option is undesired because the presence of the ions adds a further level of complexity in the photocurable formulation. As for what concern the use of PEG as mending agent, although it is one of the few water-soluble polymers with a low glass transition temperature, thus resulting in high chain mobility even at room temperature, it was not considered because it was already tested in a system obtained via photopolymerization, even if it was not employed in vat-based AM [168]. After these considerations, the selected mending agent was the polyvinyl alcohol (PVA) since it is capable to establish strong reversible interactions through hydrogen bonds among hydroxyl groups within the covalently cross-linked structure.

After the selection of the proper mending agent was done, several monomers were considered to form the chemically cross-linked network: acrylic acid (AAc), methacrylic acid (MAAc), hydroxyethyl methacrylate (HEMA), poly (ethylene glycol methyl ether methacrylate) (PEGMEMA-500 and PEGMEMA-950). As cross-linker of monomers, the alternatives were poly (ethylene glycol) diacrylate (PEGDA-250), PEGDA-575, PEGDA-700, or ethoxylated trimethylolpropane triacrylate (SR-9035). Among all the possible combinations, AAc and PEGDA-700 were used as the monomer and cross-linker, respectively, because they can guarantee a suitable kinetic for 3D printing, reacting rapidly and therefore reducing the irradiation time required to polymerize each layer. Finally, to trigger the photo-induced radical photopolymerization, a proper water-soluble photoinitiator was used, based on nanoparticles containing diphenyl (2,4,6-trimethylbenzoyl) phosphine oxide (TPO). This photoinitiator was selected because it is commercially available and can effectively absorb in the wavelengths of interest (385 and 405 nm), providing a sufficient yield of initiation.

Then, the focus of the work was directed towards the study of the PVA as mending agent of this formulation. The first tests were carried out by performing UV photopolymerization of samples produced by casting different formulations into molds. Several different factors have been considered:

- Amount of water → it determines the mobility and reactivity of the active species. Increasing the amount of water within the hydrogel enhances the chain mobility, but at the same time, has a detrimental effect on the mechanical properties of the hydrogel. However, a high amount of water keeps the chain distant, lowering the ability to form hydrogen bonds, thus reducing self-healing ability.
- Monomer concentration → it determines the length of the chains between two consecutive chemical cross-links. Increasing the monomer concentration leads to the formation of a denser cross-linked structure, limiting the interdiffusion of the chains, thus limiting the formation of H-bonds across the

damaged surfaces in the self-healing process. However, higher cross-link density leads to a more robust structure with higher mechanical properties [170].

- PVA concentration → it influences the viscosity and the self-healing ability of the system. Increasing the PVA concentration resulted in higher self-healing ability (figure 4.3), but 3D printing of the formulation was not feasible above the ratio of PVA/AAC of 0.8 wt/wt because of the high viscosity of the system (figure 4.2). Since this work aimed to achieve the highest self-healing ability possible, preserving the printability of the system at the same time, for the next steps, the ratio of 0.8 wt/wt was adopted.

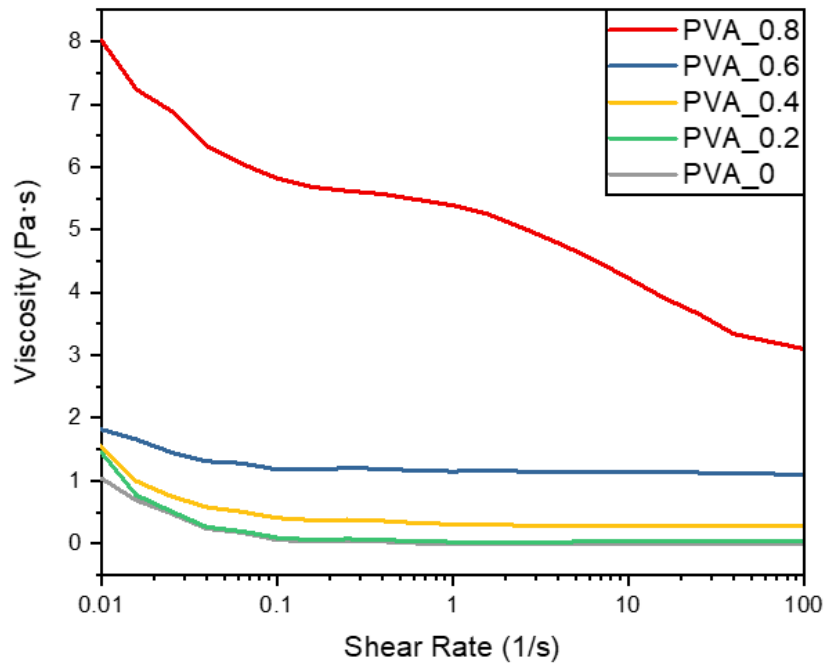


Figure 4-2 - Viscosity of the formulation with a different ratio of PVA/AAC wt/wt.

- PVA molecular weight → it influences the viscosity and the mobility of polymer chains. The PVA molecular weight covers a crucial role in both the requirements to achieve an optimal self-healing efficiency, the number of reversible interactions, and the interdiffusion of chains, respectively. If the molecular weight is too low, the short chains can move easily and rapidly within the hydrogel, but the number of interactions among different PVA chains would not be enough to result in high strength of the healed part. By contrast, a high PVA molecular weight limits the mobility of the chains, thus the system cannot show self-healing. This can be seen in figure 4.3, where the self-healing efficiency of samples with different PVA molecular weights (13-23k, 70-100k, 89-98k, 85-124k, 146-184k), and different PVA concentration have been tested. As can be seen from the graph, the best results in terms of self-healing ability and printability were obtained with an intermediate PVA molecular weight with low dispersity, in the range 89-98k.
- cross-linker concentration → determines the network density and indirectly the mobility.
- Photoinitiator concentration → determines the printability and species reactivity

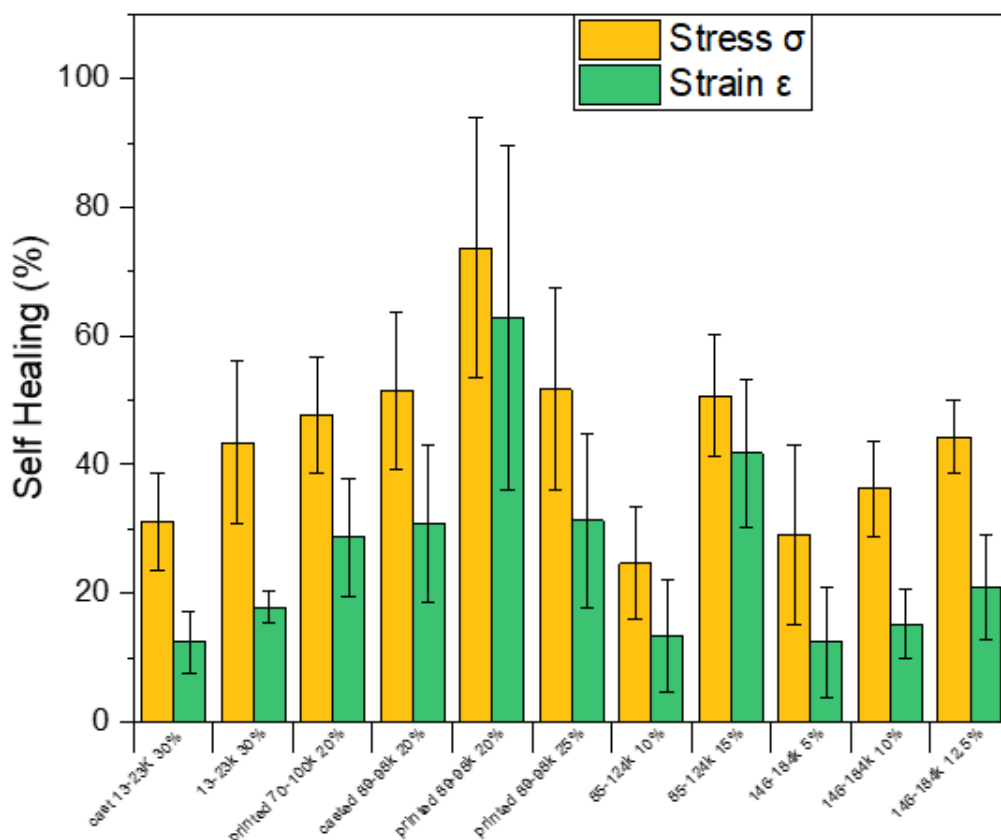


Figure 4-3 - Self-healing efficiency of samples fabricated varying the percentage of PVA (wt% in water) and the PVA molecular weight.

4.3. 3D printed hydrogel with complex shape via DLP

To characterize our system, we mostly focused on the effect of the variation of the concentration and molecular weight of PVA on the rheological properties of the hydrogel ink. The results have been shown in the previous section. In a following set of experiments, we have evaluated the effect of the presence of a dye in the formulation. Two different dyes were used, methyl red (MR) and brilliant green (BG). First, we demonstrated

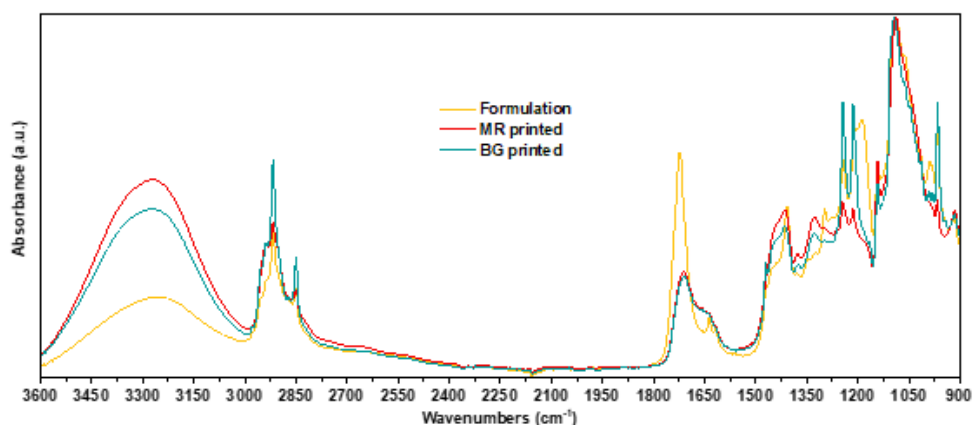


Figure 4-4 - FTIR spectrum of the formulation before being printed and after being printed (with the two different dyes, methyl red and brilliant green).

the conversion of the double bonds by Fourier-transform infrared spectroscopy (FTIR) analysis. Spectra showed that the peak corresponding to the double bond C=C (1633 cm^{-1}) strongly decreases, proving the conversion of the monomers (figure 4.4).

Furthermore, the presence of dyes in the formulation enabled to print structures with a better resolution by limiting the polymerization process in the x-y plane and lowering the light penetration depth. Three different cuboid structures ($25\text{ mm} \times 10\text{ mm} \times 5\text{ mm}$) were printed with formulations containing the two dyes and one with no added dye to demonstrate this effect. As can be seen in the figure, structures printed with no dye showed over-curing, and the shape differed completely from the ones printed with the presence of dyes, which showed good shape fidelity and sharp edges (figure 4.5).



Figure 4-5 - Cubic samples printed with formulations containing methyl red (left), no dye (center), and brilliant green (right). Ref bar: 10 mm

Finally, with these two different formulations, self-supporting structures with complex shapes were printed (figure 4.6). This demonstrated that the hydrogel could be printed in several complex shapes such as hollow structures, and overhanging features, with sharp edges, which are not achievable with extrusion printing techniques.

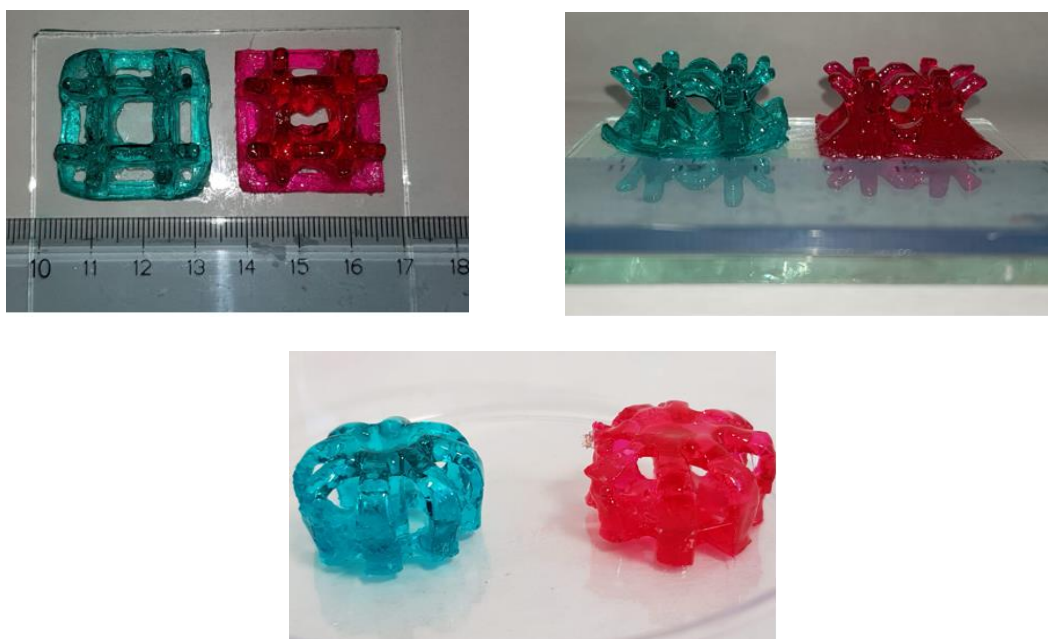


Figure 4-6 - 3D printed complex structures via Digital Light Processing (DLP).

The study of the self-healing ability of the hydrogel was showed with printed cuboid samples. After having cut the samples in half, the two cut surfaces were brought back in contact, and the samples were kept in a sealed closed vessel with a humid environment to limit the water evaporation. Healing could be observed within the first two hours, but the maximum repair was achieved after 12 hours of contact. Healed samples were pulled to show that the two parts were effectively merged and could withstand tensile stress (figure 4.7). Printed dumbbell-shaped samples showed an average of 72% of recovery in tensile strength after 12 hours.

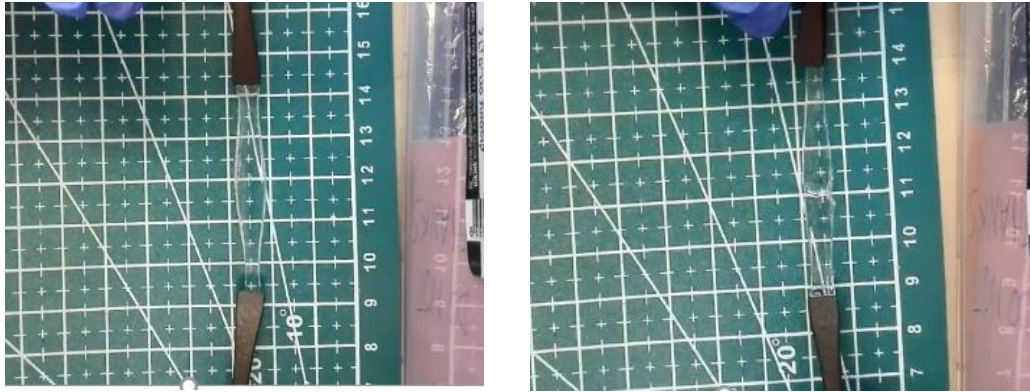


Figure 4-7 - Tensile test on the virgin sample (left) and the healed sample after healing for 12 hours (right).

5. Conclusions

With this thesis, we highlighted the advantages of self-healing materials over conventional materials because of the extended lifetimes and mechanical performance because of the absence of irreversible damage. We started with a deep insight into the different ways to achieve self-healing in materials, pointing out the advantages and disadvantages of extrinsic and intrinsic systems, respectively. Different chemistries are exploited in both categories, resulting in either autonomously self-healable materials or externally triggered self-healing. When moving towards the shaping of self-healing materials via 3D printing, different challenges arise, either if we are dealing with extrusion-based 3D printing or vat photopolymerization. In this work we listed many different formulations, developed especially to be suitable with extrusion-based techniques. However, vat photopolymerization 3D printing methods are growing because they enable higher resolutions (both in the X-Y plane and Z-axis), smoother surfaces, and higher production rates. In particular, DLP offers more significant results than SLA, and for this reason, it was selected as the processing technique for our work.

In our work, we managed to print a self-healing hydrogel with self-supporting ability via DLP, the first hydrogel system printed via vat photopolymerization, to the best of our knowledge. Issues related to the low mechanical properties of hydrogels have been overcome with the design of a hydrogel based on interpenetrating polymer networks (IPN). The robustness and printability of the system were guaranteed by the presence of a cross-linked network fabricated via photopolymerization, which enabled the 3D printability process. The second network, induced by the addition of PVA into the hydrogel, enabled self-healing to occur thanks to hydrogen bonds forming among PVA chains. Furthermore, the multiple induced hydrogen bonds resulted stable even with a large amount of water within the hydrogel (64% in our hydrogel), demonstrated by the successful self-repair achieved in the tested samples. Finally, as shown, it is possible to print 3D complex structures with high shape-fidelity and resolution. Thus, our printed system could be a promising candidate for application in biomedicine, wearable sensors, and soft robotics.

This work has the purpose of posing as starting point for future research in “3D printing of self-healing materials”, containing a critical review of the state-of-art of 3D printed self-healing materials. Future research might be directed towards developing new printable hydrogel systems based on IPN, exploiting different self-healing mechanisms than hydrogen bonds, among the available that have been described in the previous chapters.

Bibliography

- [1] B. J. e. a. Blaiszik, "Self-Healing Polymers and Composites," *Annual Review of Materials Research*, vol. 40, pp. 179-211, 2010.
- [2] Y. & U. ., M. W. Yang, "Self-healing polymeric materials," *Chemical Society Reviews*, vol. 42, pp. 7446-7467, 2013.
- [3] S. Y. A. e. a. An, "Recent strategies to develop self-healable crosslinked polymeric networks," *Chemical Communications* , vol. 51, pp. 13058-13070, 2015.
- [4] E. B. & W. F. Murphy, "The world of smart healable materials," *Progress in Polymer Science*, vol. 35, pp. 223-251, 2010.
- [5] S. H. e. a. Billiet, "Chemistry of crosslinking processes for self-healing polymers," *Macromolecular Rapid Communications*, vol. 34, pp. 290-309, 2013.
- [6] J. Z. e. a. Dahlke, "How to Design a Self-Healing Polymer: General Concepts of Dynamic Covalent Bonds and Their Application for Intrinsic Healable Materials.," *Advanced Materials Interfaces*, vol. 5, pp. 1-14, 2018.
- [7] D. L. & i. h. P. M. Taylor, "Self-healing Hydrogels," *Advanced Materials* , vol. 28, pp. 9060-9093, 2016.
- [8] I. P. S. S. a. a. Qamar, "Grand challenges in the design and manufacture of vascular self-healing," *Multifunctional Materials* , pp. 1-46, 2020.
- [9] N. R. S. e. a. S. R. White, "Autonomic healing of polymer composites," *Nature*, vol. 409, pp. 794-7, 2001.
- [10] S. N. W. S. Brown EN, "Fracture testing of a self-healing polymer composite," *Exper Mech*, vol. 42, pp. 372-9, 2002.
- [11] C. S. e. a. M. Aldridge, "Catalyst Morphology and Dissolution Kinetics of Self-Healing Polymers," *Compositional Materials* , vol. 44, p. 2605, 2010.
- [12] R. J. M. J. S. N. W. S. Kamphaus JM, "A new self-healing epoxy with tungsten (VI) chloride catalyst," *J Roy Soc Interface*, vol. 5, pp. 95-103, 2008.
- [13] J. K. L. ., S. H. Y. ., M. R. K. ., J. A. X. Liu, "Characterization of diene monomers as healing agents for autonomic damage repair," *Applied Polymer Science*, vol. 101, pp. 1266-1272, 2006.
- [14] H. M. A. ., S. R. W. ., N. R. S. ., P. V. B. S. H. Cho, "Polydimethylsiloxane-Based Self-Healing Materials," *Advanced Materials*, vol. 18, pp. 997-1000, 2006.
- [15] A. C. M. ., N. R. S. ., S. R. W. C. L. Mangun, "Self-healing of a high temperature cured epoxy using poly(dimethylsiloxane) chemistry," *Polymer*, vol. 51, pp. 4063-4068, 2010.
- [16] S. R. W. ., N. R. S. M. W. Keller, "A Self-Healing Poly(Dimethyl Siloxane) Elastomer," *Advanced Functional Materials*, vol. 17, pp. 2399-2404, 2007.
- [17] M. Z. R. ., M. Q. Z. ., G. C. Y. T. Yin, "Self-healing epoxy composites – Preparation and effect of the healant consisting of microencapsulated epoxy and latent curing agent," *Composites Science and Technology*, vol. 67, pp. 201-212, 2007.
- [18] Y. C. Y. ., M. Z. R. ., M. Q. Z. D. S. Xiao, "A Facile Strategy for Preparing Self-Healing Polymer Composites by Incorporation of Cationic Catalyst-Loaded Vegetable Fibers," *Advanced Functional Materials*, vol. 19, pp. 2289-2296, 2009.

- [19] M. Z. R. , M. Q. Z. Y. C. Yuan, "Preparation and characterization of microencapsulated polythiol," *Polymer*, vol. 49, pp. 2531-2541, 2008.
- [20] E. T. A. v. d. Dungen, "Self-healing coatings based on thiol- ene chemistry," PhD Thesis (Department of Chemistry and Polymer Science, University of Stellenbosch), Stellenbosch, 2009.
- [21] W. V. C. , X. K. D. H. , H. R. , F. E. D. P. S. Billiet, "Development of optimized autonomous self-healing systems for epoxy materials based on maleimide chemistry," *Polymer*, vol. 53, pp. 2320-2326, 2012.
- [22] M. S. , W. H. B. M. Gragert, "Azide/Alkyne-"Click"-Reactions of Encapsulated Reagents: Toward Self-Healing Materials," *Macromolecular Rapid Communications*, vol. 32, pp. 419-425, 2011.
- [23] C. Dry, "Procedures developed for self-repair of polymer matrix composite materials," *Composite structures*, vol. 35, pp. 263-269, 1996.
- [24] R. S. T. , I. P. B. H. R. Williams, "Self-healing sandwich panels: Restoration of compressive strength after impact," *Composites Science and Technology*, vol. 68, no. 15-16, pp. 3171-3177, 2008.
- [25] S. N. , J. C. M. , D. J. M. , D. V. , I. S. J. G. Kirk, "Self-healing epoxy composites based on the use of nanoporous silica capsules," *International Journal of Fracture*, vol. 159, pp. 101-102, 2009.
- [26] D. A. D. , V. H. , N. R. S. , J. S. M. , S. R. W. M. M. Caruso, "Solvent-Promoted Self-Healing Epoxy Materials," *Macromolecules*, vol. 40, pp. 8830-2, 2007.
- [27] Y. C. Y. , M. Z. R. , M. Q. Z. L. M. Meng, "A dual mechanism single-component self-healing strategy for polymers," *Journal of Materials Chemistry*, vol. 20, pp. 6030-8, 2010.
- [28] N. T. M. Zako, "Intelligent Material Systems Using Epoxy Particles to Repair Microcracks and Delamination Damage in GFRP," *Journal of Intelligent Material Systems and Structures*, vol. 10, no. 10, pp. 836-841, 1999.
- [29] J. Y. , J. M. Huang, "Facile microencapsulation of HDI for self-healing anticorrosion coatings," *Journal of Materials Chemistry*, vol. 21, pp. 11123-11130, 2011.
- [30] K. M. M. J. W. S. S. N. Yang J, "Microencapsulation of isocyanates for self-healing polymers," *Macromolecules*, vol. 41, pp. 9650-5, 2008.
- [31] U. K. V. , G. M. J. M. Motuku, "Parametric studies on self-repairing approaches for resin infused composites subjected to low velocity impact," *Smart Materials and Structures*, vol. 8, pp. 623-638, 1999.
- [32] K. e. a. Urdl, "Self-healing of densely crosslinked thermoset polymers—a critical review.," *Progress in Organic Coatings* , vol. 104, pp. 232-249, 2017.
- [33] Y. & Yang and M. W. Urban, "Self-Healing of Polymers via Supramolecular Chemistry," *Advanced Materials Interfaces*, vol. 5, p. 1800384, 2018.
- [34] A. D. D. & Campanella and W. H. Binder, "Self-Healing in Supramolecular Polymers," *Macromolecular Rapid Communications*, vol. 39, p. 1700739, 2018.
- [35] Z. e. a. Wei, "Self-healing gels based on constitutional dynamic chemistry and their potential," *Chem Soc Rev*, vol. 43, pp. 8114-8131, 2014.
- [36] F. T. M. H. J.-L. C. L. L. J. D. Montarnal, "Versatile one-pot synthesis of supramolecular plastics and self-healing rubbers," *J Am Chem Soc*, vol. 23, pp. 7966-7, 2009.

- [37] X. B. L. S. J. G. P. H. X. F. Z. Y. Y. W. S. Chen, "Poly (sebacoyl diglyceride) cross-linked by dynamic hydrogen bonds: a self-healing and functionalizable thermoplastic bioelastomer," *ACS applied materials & interfaces*, vol. 8, no. 32, pp. 20591-20599, 2016.
- [38] Y. H. G. S. Y. B. X. Y. T. D. P. P. R. Chang, "Alternating poly(lactic acid)/poly(ethylene-co-butylene) supramolecular multiblock copolymers with tunable shape memory and self-healing properties," *Polymer Chemistry*, vol. 6, no. 32, pp. 5899-5910, 2015.
- [39] H. E. N. Y. S. Yoshida, "Tough Elastomers with Superior Self-Recoverability Induced by Bioinspired Multiphase Design," *Advanced Functional Materials*, vol. 27, no. 30, p. 1701670, 2017.
- [40] F.-C. C. J.-K. C. T.-Y. W. D.-J. L. C.-C. Cheng, "High-efficiency self-healing materials based on supramolecular polymer network," *RSC Advances*, vol. 5, no. 122, pp. 101148-101154, 2015.
- [41] Y.-h. Q. Z.-p. Z. Y. Zhang, "The influence of 2,4-toluene diisocyanate content on the intrinsic self-healing performance of polyurethane at room-temperature," *Journal of Polymer Research*, vol. 22, p. 94, 2015.
- [42] C. P. L. Z. B. G. L. Liu, "A Novel and Non-Cytotoxic Self-Healing Supramolecular Elastomer Synthesized with Small Molecular Biological Acids," *Macromolecular Rapid Communications*, vol. 37, no. 19, pp. 1603-1610, 2016.
- [43] A. D. C. J. Cui, "Multivalent H-bonds for self-healing hydrogels," *Chemical Communications*, vol. 48, no. 74, pp. 9302-4, 2012.
- [44] G. L. Y. Lin, "An intermolecular quadruple hydrogen-bonding strategy to fabricate self-healing and highly deformable polyurethane hydrogels," *Journal of Materials Chemistry B*, vol. 2, pp. 6878-6885, 2014.
- [45] P. X. M. L. Saunders, "Self-Healing Supramolecular Hydrogels for Tissue Engineering Applications," *Macromolecular Bioscience*, vol. 19, no. 1, p. 1800313, 2018.
- [46] X. W. ., S. P. ., X. J. ., P. X. M. S. Hou, "Rapid Self-Integrating, Injectable Hydrogel for Tissue Complex Regeneration," *Adv Healthc Mater*, vol. 4, pp. 1491-5, 2015.
- [47] H. X. a. Y. Z. H. Zhang, "Poly(vinyl alcohol) Hydrogel Can Autonomously Self-Heal," *ACS Macro Lett.*, vol. 11, pp. 1233-6, 2012.
- [48] J. R. P. R. J. V. S. J. Kalista, "Effect of ionic content on ballistic self-healing in EMAA copolymers and ionomers," *Polymer Chemistry*, vol. 4, no. 18, pp. 4910-4926, 2013.
- [49] S. S. a. S. v. d. Z. R. J. Varley, "The effect of cluster plasticisation on the self healing behaviour of ionomers," *Polymer*, vol. 51, p. 679-686, 2010.
- [50] E. R. T. P. C. A. C. O. F. B. P. L. J. B. S. B. F. P. S. A. Reisch, "On the benefits of rubbing salt in the cut: self-healing of saloplastic PAA/PAH compact polyelectrolyte complexes," *Advanced Materials*, vol. 16, pp. 2547-51, 2014.
- [51] P. G. L. ., Y. L. Y. Huang, "Self-Assembly of Stiff, Adhesive and Self-Healing Gels from Common Polyelectrolytes," *Langmuir*, vol. 30, pp. 7771-7, 2014.
- [52] S. S. A. d. I. S. P. J. M. D. W. G. C. R.-E. N. Y. Kostina, "Novel antifouling self-healing poly(carboxybetaine methacrylamide-co-HEMA) nanocomposite hydrogels with superior mechanical properties," *Journal of Materials Chemistry B*, vol. 1, no. 41, pp. 5644-5650, 2013.
- [53] S. L. ., F. S. ., A. S. ., L. Z. ., Q. S. ., S. T. Bai, "Zwitterionic fusion in hydrogels and spontaneous and time-independent self-healing under physiological conditions," *Biomaterials*, vol. 35, pp. 3926-33, 2014.

- [54] H. M. C. B. W. G. W. H. S. Burattini, "A novel self-healing supramolecular polymer system," *Faraday discussions*, vol. 143, pp. 251-264, 2009.
- [55] B. W. G. W. H. M. E. M. S. J. R. H. M. C. S. Burattini, "A supramolecular polymer based on tweezer-type π - π stacking interactions: molecular design for healability and enhanced toughness," *Chemistry of Materials*, vol. 23, pp. 6-8, 2011.
- [56] J. H. H. N. A. N. J. L. H. B. W. G. M. E. M. H. M. C. W. H. L. R. Hart, "Multivalency in healable supramolecular polymers: the effect of supramolecular cross-link density on the mechanical properties and healing of non-covalent polymer networks," *Polymer Chemistry*, vol. 5, pp. 3680-8, 2014.
- [57] X.-Y. J. J.-C. L. Y. S. C.-H. L. J.-H. W. Y. C. X.-Z. Y. Z. B. J.-F. Mei, "A Highly Stretchable and Autonomous Self-Healing Polymer Based on Combination of Pt \cdots Pt and π - π Interactions," *Macromolecular Rapid Communications*, vol. 37, pp. 1667-75, 2016.
- [58] B. Á. S. A. S. B. Gyarmati, "Reversible interactions in self-healing and shape memory hydrogels," *European Polymer Journal journal*, pp. 642-669, 2017.
- [59] L. e. a. Shi, "Self-Healing Polymeric Hydrogel Formed by Metal-Ligand Coordination Assembly.," *Macromolecular Rapid Communications*, vol. 40, p. 1800837, 2019.
- [60] H. D. J. Q. J. Y. Z. L. W. Y. S. Q. Z. S. Y. Zheng, "Metal-Coordination Complexes Mediated Physical Hydrogels with High Toughness, Stick-Slip Tearing Behavior, and Good Processability," *Macromolecules*, vol. 49, pp. 9637-46, 2016.
- [61] M. J. H. H. B. B. P. L. P. B. M. K. Y. L. J. H. W. N. Holten-Andersen, "pH-induced metal-ligand cross-links inspired by mussel yield self-healing polymer networks with near-covalent elastic moduli," *Proc Natl Acad Sci U S A*, vol. 108, pp. 2651-5, 2011.
- [62] P. X. M. S. Hou, "Stimuli-Responsive Supramolecular Hydrogels with High Extensibility and Fast Self-Healing via Precoordinated Mussel-Inspired Chemistry," *Chemistry of Materials*, vol. 27, pp. 7627-35, 2015.
- [63] L. H. D. G. B. W. R. B. P. B. M. D. E. Fullenkamp, "Mussel-inspired histidine-based transient network metal coordination hydrogels," *Macromolecules*, vol. 46, no. 3, pp. 1167-74, 2013.
- [64] T. Z. H.-N. L. H.-P. C. M. A. S.-H. Y. H. Qin, "Dynamic Au-Thiolate Interaction Induced Rapid Self-Healing Nanocomposite Hydrogels with Remarkable Mechanical Behaviors," *Chem*, vol. 3, no. 4, pp. 691-705, 2017.
- [65] J. H. T. L. H. O. J. A. Z. T. C. W. Z. N. Z. Wei, "Autonomous self-healing of poly(acrylic acid) hydrogels induced by the migration of ferric ions," *Polymer Chemistry*, vol. 4, no. 17, pp. 4601-5, 2013.
- [66] Y. Z. X. Ma, "Biomedical Applications of Supramolecular Systems Based on Host-," *Chemical Reviews*, vol. 115, pp. 7794-7839, 2014.
- [67] J. e. a. Jin, "Progress in self-healing hydrogels assembled by host-guest interactions: preparation," *Journal of Materials Chemistry B*, vol. 7, pp. 1637-51, 2018.
- [68] C. B. M. J. E. & Rodell and J. A. Burdick, "Supramolecular Guest-Host Interactions for the," *Bioconjugate Chemistry*, vol. 26, pp. 2279-89, 2015.
- [69] Y. T. M. N. M. O. H. Y. a. A. H. T. Kakuta, "Preorganized Hydrogel: Self-Healing Properties of Supramolecular Hydrogels Formed by Polymerization of Host-Guest-Monomers that Contain Cyclodextrins and Hydrophobic Guest Groups," *Advanced Materials*, vol. 25, no. 20, pp. 2849-53, 2013.
- [70] S. J. H. T. W. W. X. S. a. Z. T. T. T. Cai, "Progress in self-healing hydrogels assembled by host-guest interactions: preparation and biomedical applications," *Journal of Materials Chemistry B*, vol. 7, no. 10, pp. 1637-51, 2019.

- [71] Y. T. H. Y. A. H. M. Nakahata, "Redox-responsive self-healing materials formed from host-guest polymers," *Nat. Commun.*, vol. 2, p. 511, 2011.
- [72] E. A. J. S. E. K. O. S. O. I. J.R. McKee, "Healable, stable and stiff hydrogels: combining conflicting properties using dynamic and selective three-component recognition with reinforcing cellulose nanorods," *Advanced Functional Materials*, vol. 24, pp. 2706-13, 2014.
- [73] F. B. U. R. S. T. J. J. M. Z. a. O. A. S. E. A. Appel, "Supramolecular Cross-Linked Networks via Host-Guest Complexation with Cucurbit[8]uril," *J. Am. Chem. Soc.*, vol. 132, pp. 14251-60, 2010.
- [74] J. W. M. J. S. M. D. R. J. W. L. L. W. Y. J. W. a. J. A. B. C. B. Rodell, "Shear-Thinning Supramolecular Hydrogels with Secondary Autonomous Covalent Crosslinking to Modulate Viscoelastic Properties In Vivo," *Advanced Functional Materials*, vol. 25, pp. 636-644, 2015.
- [75] S. L. F. P. N. C. a. R. A. O. T. Miao, "Self-Healing and Thermoresponsive Dual-Cross-Linked Alginate Hydrogels Based on Supramolecular Inclusion Complexes," *Biomacromolecules*, vol. 16, pp. 3740-50, 2015.
- [76] F. C. J. S. A. Hill, "Properties of hydrophobically associating polyacrylamides: influence of the method of synthesis," *Macromolecules*, vol. 26, pp. 4521-32, 1993.
- [77] C. L. X. L. G. Z. M. Y. F. L. G. Jiang, "Construction and properties of hydrophobic association hydrogels with high mechanical strength and reforming capability," *Macromol. Mater. Eng.*, vol. 294, pp. 815-20, 2009.
- [78] M. S. , A. A. , W. O. , O. O. D. C. Tuncaboylu, "Dynamics and Large Strain Behavior of Self-Healing Hydrogels with and without Surfactants," *Macromolecules*, vol. 45, pp. 1991-2000, 2012.
- [79] S. C. G. C. J. S. J. S. S.J. Rowan, "Dynamic covalent chemistry," *Angew. Chemie Int*, vol. 41, pp. 898-952, 2002.
- [80] N. B. B. & Roy and J.-M. Lehn, "DYNAMERS: dynamic polymers as self-healing materials," *Chem. Soc. Rev.*, vol. 44, pp. 3786-3807, 2015.
- [81] Z. e. a. Wei, "Self-healing gels based on constitutional dynamic chemistry and their potential," *Chem. Soc. Rev.*, vol. 43, pp. 8114-8131, 2014.
- [82] C. T. F. L. H. J. Y. C. G. Deng, "Covalent Cross-Linked Polymer Gels with Reversible Sol-Gel Transition and Self-Healing Properties," *Macromolecules*, vol. 43, pp. 1191-4, 2010.
- [83] S. B. R. K. B. J. V. A. S. S. H. S. J. G. S. S. S. v. d. Z. M. D. H. U. S. S. N. Kuhl, "Acylhydrazones as Reversible Covalent Crosslinkers for Self-Healing Polymers," *Advanced Functional Materials* , vol. 25, no. 22, pp. 3295-3301, 2015.
- [84] M. K. e. a. McBride, "Enabling Applications of Covalent Adaptable Networks.," *Annu. Rev. Chem. Biomol. Eng.* , vol. 10, pp. 1-24, 2019.
- [85] D. F. J. R. P. M. L. He, "PH responsive self-healing hydrogels formed by boronate-catechol complexation," *Chem. Commun.*, vol. 47, pp. 7497-99, 2011.
- [86] J. M. Craven, "Cross-linked thermally reversible polymers produced from condensation polymers with pendant furan groups cross-linked with maleimides," *US Pat.*, p. 3435003, 1969.
- [87] W. McElhanon, "Thermally responsive dendrons and dendrimers based on reversible furan-maleimide Diels-Alder adducts," *Organic Letters*, vol. 3, pp. 2681-3, 2001.
- [88] L. F. e. al., "Self-healing behavior of polyurethanes based on dual actions of thermo-reversible Diels-Alder reaction and thermal movement of molecular chains," *Polymer*, vol. 124, pp. 48-59, 2017.

- [89] P. R. J.-M. L. P. J. Boul, "Reversible Diels-Alder reactions for the generation of dynamic combinatorial libraries," *Org. Lett.*, vol. 7, pp. 15-18, 2005.
- [90] P. J. B. J.-M. L. P. Reutenauer, "Room Temperature Dynamic Polymers Based on Diels-Alder Chemistry," *Eur. J. Org. Chem.*, pp. 1691-97, 2009.
- [91] M. L. N. Roy, "Dynamic Covalent Chemistry: A Facile Room-Temperature, Reversible, Diels-Alder Reaction between Anthracene Derivatives and N-Phenyltriazolinedione," *Chem. Asian J.*, vol. 6, pp. 2419-25, 2011.
- [92] M. Z. R. M. Q. Z. J. Ling, "Photo-stimulated self-healing polyurethane containing dihydroxyl coumarin derivatives," *Polymer*, vol. 53, no. 13, pp. 2691-8, 2012.
- [93] R. G. R. K. B. S. B. B. D. M. S. J. P. S. J. G. S. v. d. Z. U. S. S. M. D. H. N. Kuhl, "Self-Healing Polymer Networks Based on Reversible Michael Addition Reactions," *Macrom. Chem. Phys.*, vol. 217, pp. 2541-50, 2016.
- [94] M. N. T. K. Y. A. A. T. H. O. K. Imato, "K. Imato, M. Nishihara, T. Kanehara, Y. Amamoto, A. Takahara, H. Otsuka, *Angew. Chem., Int. Ed. Engl.* 2012, 51, 1138," *Angew. Chem. Int. Ed. Engl.*, vol. 51, pp. 1138-42, 2012.
- [95] F. D. e. al., "A dynamic and self-crosslinked polysaccharide hydrogel with autonomous self-healing ability," *Soft Matter*, vol. 11, pp. 3971-76, 2015.
- [96] N. K. e. al., "Oxime crosslinked polymer networks: Is every reversible covalent bond suitable to create self-healing polymers?," *J. Appl. Polym. Sci.*, vol. 133, p. 44168, 2016.
- [97] S. M. e. al., "Self-healing hydrogels containing reversible oxime crosslinks," *Soft Matter*, vol. 11, pp. 6152-61, 2015.
- [98] J. C. e. al., "Self-Healing Materials Based on Disulfide Links," *Macromolecules*, vol. 44, pp. 2536-41, 2011.
- [99] J. A. Y. e. al., "Self-Healing Polymer Films Based on Thiol-Disulfide Exchange Reactions and Self-Healing Kinetics Measured Using Atomic Force Microscopy," *Macromolecules*, vol. 45, pp. 142-9, 2011.
- [100] K. C. e. al., "A transparent, highly stretchable, self-healing polyurethane based on disulfide bonds," *European Polymer Journal*, vol. 112, pp. 822-31, 2019.
- [101] C. Y. e. al., "Self-Healing of Polymers via Synchronous Covalent Bond Fission/Radical Recombination," *Chemistry of Materials*, vol. 23, pp. 5076-81, 2011.
- [102] C. Y. e. al., "Self-healing polyurethane elastomer with thermally reversible alkoxyamines as crosslinkages," *Polymer*, vol. 55, no. 7, pp. 1782-91, 2014.
- [103] C. Y. e. al., "Application of alkoxyamine in self-healing of epoxy," *Journal of Materials Chemistry A*, vol. 2, no. 18, pp. 6558-66, 2014.
- [104] Y.-X. a. Z. Guan, "Olefin Metathesis for Effective Polymer Healing via Dynamic Exchange of Strong Carbon-Carbon Double Bonds," *J. Am. Chem. Soc.*, vol. 134, pp. 14226-31, 2012.
- [105] S. M. e. al., "Polyethylene-co-methacrylic acid healing agents for mendable epoxy resins," *Acta Materialia*, vol. 57, no. 14, pp. 4312-20, 2009.
- [106] M. Y. e. al., "Self-repairing property of polymer network with dangling chains," *Materials Letters*, vol. 61, no. 6, pp. 1396-99, 2007.
- [107] S. C. Ligon, "Polymers for 3D Printing and Customized Additive Manufacturing," *Chemical Reviews*, vol. 117, no. 15, pp. 10212-90, 2017.

- [108] S. W. Y. K. L. D. X. Z. S. M. Y. L. Yuting Dong, "4D Printed Hydrogels: Fabrication, Materials, and Applications," *Advanced Materials Technologies*, vol. 5, no. 6, p. 2000034, 2020.
- [109] G. A. Appuhamillage, "3D printed remendable polylactic acid blends with uniform mechanical strength enabled by a dynamic Diels–Alder reaction," *Polymer Chemistry*, vol. 8, no. 13, pp. 2087-92, 2017.
- [110] V. G. Rocha, "Direct ink writing advances in multi-material structures for a sustainable future," *Journal of Materials Chemistry A*, vol. 8, no. 31, pp. 15646-57, 2020.
- [111] P. Heidarian, "Dynamic Hydrogels and Polymers as Inks for Three-Dimensional Printing," *ACS Biomaterials Science & Engineering*, vol. 5, no. 6, pp. 2688-2707, 2019.
- [112] H. C. W., "Apparatus for Production of Three-Dimensional Objects by Stereolithograph," *United States Patent*, p. 638905, 1984.
- [113] R. J. K. A. W. C. B. V. S. S. & L. T. E. Mondschein, "Polymer structure-property requirements for stereolithographic 3D printing of soft tissue engineering scaffolds.," *Biomaterials*, vol. 140, p. 170–188, 2017.
- [114] I. J. M. L. M. Z. Y.-W. C. K.-X. A. L. W. Y. Y. a. Y.-F. S. ei Long Ng6 6 6, "at polymerization-based bioprinting—process, materials, applications and regulatory challenges," *Biofabrication*, vol. 12, 2020.
- [115] J. & G. M. Tao, "Digital light processing based three-dimensional printing for medical applications.," *Int. J. Bioprinting*, vol. 6, p. 12–27, 2020.
- [116] S. Zakeri, "A comprehensive review of the photopolymerization of ceramic resins used in stereolithography," *Additive Manufacturing*, vol. 35, p. 101177, 2020.
- [117] W. Zhu, "3D printing of functional biomaterials for tissue engineering," *Current Opinion in Biotechnology*, vol. 40, pp. 103-112, 2016.
- [118] J. M. & Y. W. Y. Lee, "Design and Printing Strategies in 3D Bioprinting of Cell-Hydrogels: A Review.," *Adv. Healthc. Mater.*, vol. 5, pp. 2856-65, 2016.
- [119] P. C. M. E. W. M. H. & R. D. H. Ahangar, "Current Biomedical Application of 3D Printing and Additive Manufacturing," *Appl. Sci.*, vol. 9, p. 1713, 2019.
- [120] E. L. P. R. F. J. & M. D. George, "Measuring and establishing the accuracy and reproducibility of 3D printed medical models," *Radiographics*, vol. 37, pp. 1424-50, 2017.
- [121] J. H. Q. W. S. T. J. & G. M. Zhang, "Digital light processing based three-dimensional printing for medical applications," *Int. J. Bioprinting*, vol. 6, pp. 12-27, 2020.
- [122] L. e. a. Moroni, "Biofabrication: A Guide to Technology and Terminology," *Trends Biotechnol.*, vol. 36, pp. 384-402, 2018.
- [123] K. S. T. e. al., "Self-healing materials with microvascular networks," *Let.*, vol. 6, pp. 581-5, 2007.
- [124] K. Y. X. K. X. M. C. K. D. M. L. D. T. W. a. H. J. Q. Qian Shi, "Recyclable 3D printing of vitrimer epoxy," *Mterial Horizons*, vol. 4, pp. 598-607, 2017.
- [125] E. G. a. B. C. Tongfei Wu, "A self-healing, adaptive and conductive polymer composite ink for 3D printing of gas sensors," *J. Mat. Chem.*, vol. 6, pp. 6200-7, 2018.
- [126] A. Biswas, "Arylboronate esters mediated self-healable and biocompatible dynamic G-quadruplex hydrogels as promising 3D-bioinks," *Chemical Communications*, vol. 54, no. 14, pp. 1778-81, 2018.

- [127] K. Yang, "Diels-Alder Reversible Thermoset 3D Printing: Isotropic Thermoset Polymers via Fused Filament Fabrication," *Advanced Functional Materials*, vol. 27, no. 24, p. 1700318, 2017.
- [128] Q. Wei, "Dynamic hydrogels produced via monoamine oxidase B-catalyzed deamination and aldimine crosslinking for 3D printing," *Journal of Materials Chemistry B*, vol. 5, no. 26, pp. 5092-95, 2017.
- [129] M. Nadgorny, "2D and 3D-printing of self-healing gels: design and extrusion of self-rolling objects," *Molecular Systems Design & Engineering*, vol. 2, no. 3, pp. 283-292, 2017.
- [130] M. Nadgorny, "3D-printing of dynamic self-healing cryogels with tuneable properties," *Polymer Chemistry*, vol. 9, no. 13, pp. 1684-92, 2018.
- [131] H. Wang, "A High Strength Self-Healable Antibacterial and Anti-Inflammatory Supramolecular Polymer Hydrogel," *Macromolecular Rapid Communications*, vol. 38, no. 9, p. 1600695, 2017.
- [132] S. W. Kim, "Three-Dimensional Bioprinting of Cell-Laden Constructs Using Polysaccharide-Based Self-Healing Hydrogels," *Biomacromolecules*, vol. 20, no. 5, pp. 1860-6, 2019.
- [133] C. P. Kabb, "Photoreversible Covalent Hydrogels for Soft-Matter Additive Manufacturing," *ACS Applied Materials and Interfaces*, vol. 10, no. 19, pp. 16793-16801, 2018.
- [134] C. B. Highley, "Direct 3D Printing of Shear-Thinning Hydrogels into Self-Healing Hydrogels," *Advanced Materials*, vol. 27, no. 34, pp. 5075-79, 2015.
- [135] L. Ouyang, "3D Printing of Shear-Thinning Hyaluronic Acid Hydrogels with Secondary Cross-Linking," *ACS Biomaterials Science & Engineering*, vol. 2, no. 10, pp. 1743-51, 2016.
- [136] K. H. Song, "Complex 3D-Printed Microchannels within Cell-Degradable Hydrogels," *Advanced Functional Materials*, vol. 28, no. 31, p. 1801331, 2018.
- [137] Z. Wang, "3D-printable self-healing and mechanically reinforced hydrogels with host-guest non-covalent interactions integrated into covalently linked networks," *Materials Horizons*, vol. 6, no. 4, pp. 733-742, 2019.
- [138] J. H. Shim, "Three-dimensional bioprinting of multilayered constructs containing human mesenchymal stromal cells for osteochondral tissue regeneration in the rabbit knee joint," *Biofabrication*, vol. 8, no. 1, p. 14102, 2016.
- [139] H. Wang, "A High Strength Self-Healable Antibacterial and Anti-Inflammatory Supramolecular Polymer Hydrogel," *Macromolecular Rapid Communications*, vol. 38, no. 9, p. 1600695, 2017.
- [140] Q. Wu, "A robust, highly stretchable supramolecular polymer conductive hydrogel with self-healability and thermo-processability," *Scientific Reports*, vol. 7, pp. 1-11, 2017.
- [141] H. Zhang, "Direct 3D Printed Biomimetic Scaffolds Based on Hydrogel Microparticles for Cell Spheroid Growth," *Advanced Functional Materials*, vol. 30, no. 13, p. 1910573, 2020.
- [142] F. Zhu, "3D Printing of Ultratough Polyion Complex Hydrogels," *ACS Applied Materials & Interfaces*, vol. 8, no. 45, pp. 31304-10, 2016.
- [143] Q. Liu, "Preparation and properties of 3D printed alginate-chitosan polyion complex hydrogels for tissue engineering," *Polymers*, vol. 10, no. 6, p. 664, 2018.
- [144] Q. Chang, "Hydrogels from natural egg white with extraordinary stretchability, direct-writing 3D printability and self-healing for fabrication of electronic sensors and actuators," *Journal of Materials Chemistry A*, vol. 7, no. 42, pp. 24626-40, 2019.

- [145] S. Liu, "Ultrastretchable and Self-Healing Double-Network Hydrogel for 3D Printing and Strain Sensor," *ACS Applied Materials and Interfaces*, vol. 9, no. 31, pp. 26429-26437, 2017.
- [146] S. A. Wilson, "Shear-Thinning and Thermo-Reversible Nanoengineered Inks for 3D Bioprinting," *ACS Applied Materials & Interfaces*, vol. 9, no. 50, pp. 43449-58, 2017.
- [147] L. Shi, "Dynamic Coordination Chemistry Enables Free Directional Printing of Biopolymer Hydrogel," *Chemistry of Materials*, vol. 29, no. 14, pp. 5816-23, 2017.
- [148] X. Li, "Dual Ionically Cross-linked Double-Network Hydrogels with High Strength, Toughness, Swelling Resistance, and Improved 3D Printing Processability," *ACS Applied Materials & Interfaces*, vol. 10, no. 37, pp. 31198-31207, 2018.
- [149] S. Hong, "3D Printing of Highly Stretchable and Tough Hydrogels into Complex, Cellularized Structures," *Advanced Materials*, vol. 27, no. 27, pp. 4035-40, 2015.
- [150] S. Y. Zheng, "Metal-Coordination Complexes Mediated Physical Hydrogels with High Toughness, Stick-Slip Tearing Behavior, and Good Processability," *Macromolecules*, vol. 49, no. 24, pp. 9637-46, 2016.
- [151] M. A. Darabi, "Skin-Inspired Multifunctional Autonomic-Intrinsic Conductive Self-Healing Hydrogels with Pressure Sensitivity, Stretchability, and 3D Printability," *Advanced Materials*, vol. 30, no. 4, p. 1705922, 2018.
- [152] S. Park, "Three-Dimensional Self-Healable Touch Sensing Artificial Skin Device," *ACS Applied Materials & Interfaces*, vol. 12, no. 3, pp. 3953-60, 2020.
- [153] J.-C. Lai, "A rigid and healable polymer cross-linked by weak but abundant Zn(II)-carboxylate interactions," *Nature Communications*, vol. 9, no. 1, p. 2725, 2018.
- [154] X. Kuang, "3D Printing of Highly Stretchable, Shape-Memory, and Self-Healing Elastomer toward Novel 4D Printing," *ACS Applied Materials & Interfaces*, vol. 10, no. 8, pp. 7381-8, 2018.
- [155] S. Qi, "Versatile magnetorheological elastomer with 3D printability, switchable mechanics, shape memory, and self-healing capacity," *Composites Science and Technology*, vol. 183, p. 107817, 2019.
- [156] T. J. Wallin, "Click chemistry stereolithography for soft robots that self-heal," *Journal of Materials Chemistry B*, vol. 5, no. 31, pp. 6249-55, 2017.
- [157] P. Sanders, "Stereolithographic 3D printing of extrinsically self-healing composites," *Scientific Reports*, vol. 9, no. 1, p. 388, 2019.
- [158] X. Li, "Self-Healing Polyurethane Elastomers Based on a Disulfide Bond by Digital Light Processing 3D Printing," *ACS Macro Letters*, vol. 8, no. 11, pp. 1511-1516, 2019.
- [159] K. Yu, "Healable, memorizable, and transformable lattice structures made of stiff polymers," *NPG Asia Materials*, vol. 12, p. 26, 2020.
- [160] K. Yu, "Additive manufacturing of self-healing elastomers," *NPG Asia Materials*, vol. 11, no. 1, 2019.
- [161] B. Zhang, "Reprocessable thermosets for sustainable three-dimensional printing," *Nature Communications*, vol. 9, no. 1, p. 1831, 2018.
- [162] M. Invernizzi, "4D printed thermally activated self-healing and shape memory polycaprolactone-based polymers," *European Polymer Journal*, vol. 101, pp. 169-176, 2018.
- [163] T. M. Valentin, "3D printed self-adhesive PEGDA-PAA hydrogels as modular components for soft actuators and microfluidics," *Polymer Chemistry*, vol. 10, no. 16, pp. 2015-28, 2019.

- [164] Z. Liu, "Self-healing, reprocessing and 3D printing of transparent and hydrolysis-resistant silicone elastomers," *Chemical Engineering Journal*, p. 124142, 2020.
- [165] B. Zhang, "Self-Healing Four-Dimensional Printing with an Ultraviolet Curable Double-Network Shape Memory Polymer System," *ACS Applied Materials & Interfaces*, vol. 11, no. 10, pp. 10328-36, 2019.
- [166] I. K. A. F. A. T. A. A. P. P. L. O. B. & S. M. Liraz Larush, "3D printing of responsive hydrogel for drug delivery systems," *JOURNAL OF 3D PRINTING IN MEDICINE*, vol. 1, 2017.
- [167] G. S. I. C. L. L. J. A. J. S. R. T. N.-J. C. S. M. Amol A. Pawar, "High-performance 3D printing of hydrogels by water-dispersible photoinitiator nanoparticles," *Applied Science and Engineering*, vol. 2, p. 1501381, 2016.
- [168] Y. F. Y. Z. L. Y. X. H. F. S. Z. D. A. Z. Z. Y. L. Y. W. J. W. P. J. T. C. a. H. W. Kaiwen Chen, "Entanglement-Driven Adhesion, Self-Healing, and High Stretchability of Double-Network PEG-Based Hydrogels," *Applied Materials & Interfaces*, vol. 11, pp. 36458-68, 2019.
- [169] A. K. C. B. W. S. S. V. T. E. L. Ryan J. Mondschein, "Polymer structure-property requirements for stereolithographic 3D printing of soft tissue engineering scaffolds," *Biomaterials*, vol. 140, pp. 170-188, 2017.
- [170] H. Z. D. F. H. X. a. Y. Z. Guo Li, "Poly(vinyl alcohol)-Poly(ethylene glycol) Double-Network Hydrogel: A General Approach to Shape Memory and Self-Healing Functionalities," *Langmuir*, vol. 31, pp. 11709-16, 2015.

Acknowledgements

I would like to express my deep gratitude to Professor Marco Sangermano to give me the possibility to work on this subject and Dr. Ignazio Roppolo for his patient guidance, enthusiastic encouragement and useful critiques of this research work. I would also like to thank the Ph.D. student Matteo Caprioli for his advices and assistance during my writing of the thesis.

Finally, I wish to thank my family for their support and encouragement throughout my study.